BUREAU OF RECLAMATION

Final Report No. ST-2025-19105

Fish Passage at River Diversion Junction: A Science-Based Approach

Research and Development Office

Science and Technology

Research Program

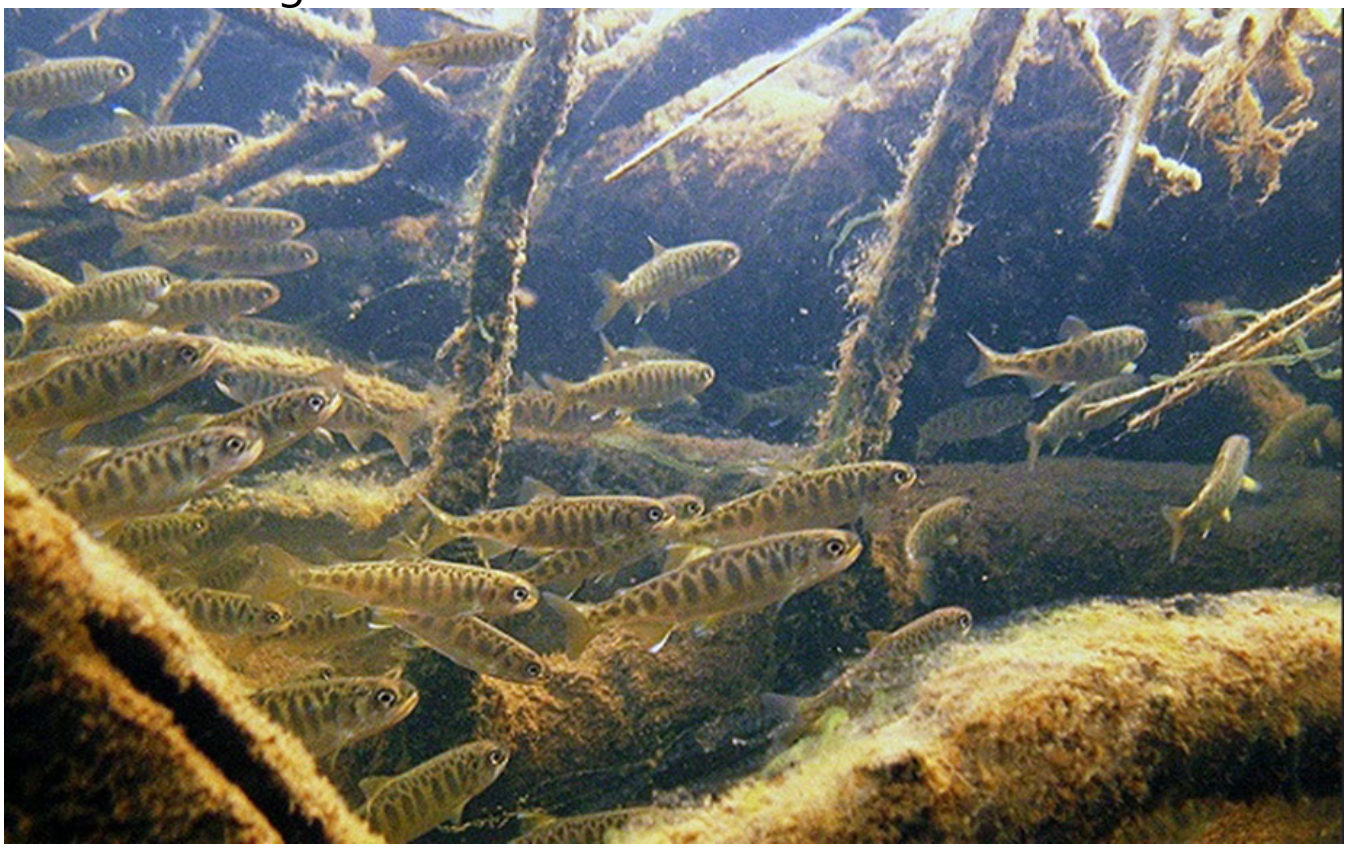

U.S. Department of the Interior

September 2025

REPORT DOCUMENTATION PAGE

Form Approved
OMB No. 0704-0188

1. REPORT DATE (DD-MM-YYYY)	2. REPORT TYPE	3. DATES COVERED *(From - To)*
30-09-2025	Research	2019-2025

4. TITLE AND SUBTITLE
Fish Passage at River Diversion Junction: A Science-Based Approach

5a. CONTRACT NUMBER
XXXR4524KS-RR4888FARD1903301/F018A

5b. GRANT NUMBER

5c. PROGRAM ELEMENT NUMBER
1541 (S&T)

6. AUTHOR(S)
Yong Lai, Ph.D., Hydraulic Engineer

5d. PROJECT ID NUMBER
Final Report ST-2025-19105

5e. TASK NUMBER

5f. WORK UNIT NUMBER

7. PERFORMING ORGANIZATION NAME(S) AND ADDRESS(ES)
Sedimentation and River Hydraulics Group
Technical Service Center
Bureau of Reclamation
U.S. Department of the Interior
Denver Federal Center
PO Box 25007, Denver, CO 80225-0007

8. PERFORMING ORGANIZATION REPORT NUMBER

9. SPONSORING/MONITORING AGENCY NAME(S) AND ADDRESS(ES)
Science and Technology Program
Research and Development Office
Bureau of Reclamation
U.S. Department of the Interior
Denver Federal Center
PO Box 25007, Denver, CO 80225-0007

10. SPONSOR/MONITOR'S ACRONYM(S)
Reclamation

11. SPONSOR/MONITOR'S REPORT NUMBER(S) (if applicable)

12. DISTRIBUTION/AVAILABILITY STATEMENT
Final Report may be downloaded from https://www.usbr.gov/research/projects/index.html

13. SUPPLEMENTARY NOTES

14. ABSTRACT

This research aims to develop a science-based, numerical approach for fish passage to assist the design and evaluation of ways to reduce juvenile salmonid entrainment into or enhance passage through diversion channels at river junctures. Three current state-of-the-art are adopted: (a) multi-dimensional flow models; (b) fish track models; and (c) knowledge of fish behaviors in response to flow features. Two flow models are updated to provide the flow variables to which juvenile fish respond: 2-D hydraulic model SRH-2D and a 3-D computational fluid dynamics (CFD) model. Two fish track tools, one in the Eulerian framework and the other in the Lagrangian framework, are developed so that fish entrainment at diversion channel junctures may be evaluated. A third sophisticated tool ELAM, a fish track model developed by Army Corps of Engineers (USACE), is further adopted through a collaboration with USACE. These flow and fish track tools have been applied to several diversion junctures, including Reclamation projects; valuable knowledge has been gained in understanding the ways to alter the flow features to increase or decrease fish entrainment. The research has led to the following outcomes: (a) a science-based, defensible approach for fish passage evaluation; (b) development and/or extensions of modeling tools that are linked for fish entrainment modeling studies; (c) guidelines for conducting fish passage simulations; and (d) knowledge about geometric and flow features of a diversion channel that are important for attraction or rejection of migrating Juvenile salmon passage.

15. SUBJECT TERMS
Fish passage; fish track model; CFD model; fish entrainment; junction flows

16. SECURITY CLASSIFICATION OF:			17. LIMITATION OF ABSTRACT	18. NUMBER OF PAGES	19a. NAME OF RESPONSIBLE PERSON
a. REPORT	b. ABSTRACT	c. THIS PAGE			Yong Lai
U	U	U		138	19b. TELEPHONE NUMBER *(Include area code)* 303-445-2560

Mission Statements

The U.S. Department of the Interior protects and manages the Nation's natural resources and cultural heritage; provides scientific and other information about those resources; honors its trust responsibilities or special commitments to American Indians, Alaska Natives, Native Hawaiians, and affiliated Island Communities.

The mission of the Bureau of Reclamation is to manage, develop, and protect water and related resources in an environmentally and economically sound manner in the interest of the American public.

Disclaimer

Information in this report may not be used for advertising or promotional purchases. The data and findings should not be construed as an endorsement of any product or firm by the Bureau of Reclamation, Department of Interior, or Federal Government. The products evaluated in the report were evaluated for purposes specific to the Bureau of Reclamation mission. Reclamation gives no warranties or guarantees, expressed or implied, for the products evaluated in this report, including merchantability or fitness for a particular purpose

Acknowledgements

The Science and Technology Program, Bureau of Reclamation, sponsored this research. Steve Hollenback, a physical scientist formerly worked at the Technical Service Center, provided an initial literature review with fish passage studies (see Appendix A).

Cover Image – A photo of juvenile salmons in a stream (USFWS/Togiak National Wildlife Refuge).

Fish Passage at River Diversion Junction: A Science-Based Approach

Final Report No. ST-2025-19105

Prepared by:

Bureau of Reclamation
Technical Service Center
Yong Lai, Ph.D., Hydraulic Engineer

Peer Review

Bureau of Reclamation
Research and Development Office
Science and Technology
Research Program

Final Report ST-2025-19105

Fish Passage at River Diversion Junction: A Science-Based Approach

YONG LAI Digitally signed by YONG LAI
Date: 2025.09.29 11:25:03 -06'00'

Prepared by: Yong Lai, Ph.D.
Hydraulic Engineer, Sedimentation and River Hydraulics, Technical Service Center

BENJAMIN ABBAN Digitally signed by BENJAMIN ABBAN
Date: 2025.09.29 14:32:04 -06'00'

Peer review by: Ben Abban, Ph.D.
Hydraulic Engineer, Sedimentation and River Hydraulics, Technical Service Center

This document has been reviewed under the Research and Development Office Discretionary peer review process, consistent with Reclamation Policy CMP P14. It does not represent and should not be construed to represent the Bureau of Reclamation's determination, concurrence, or policy.

Contents

Tables

Figures

Appendices

Executive Summary

Fish passage is one of the most important environmental and ecological issues for waterways in the country. At Reclamation, facilities and projects must take fish passage into consideration for the operation and improvement of facilities due to regulations at Federal, State and local levels. Despite significant amount of effort devoted to the topic, the current practice of fish passage design relies mostly on empirical and exploratory approaches. The need for the development of a science-based approach has been emphasized in the last decade and championed by scientists in the fish passage community–but such an approach has not been available at Reclamation.

The goal of this Science and Technology research is to develop a science-based, numerical approach for fish passage to assist the design and evaluation of ways to reduce juvenile salmonid entrainment into or enhance passage through diversion channels at river junctures. The proposed approach builds on the premise that fish movement is affected by local flow hydrodynamics, which has been proven in many field-based studies. Three elements of current state-of-the-art fish modeling technology are adopted: (a) multi-dimensional flow models; (b) fish track models; and (c) increased knowledge of fish behaviors in response to flow features. Two flow models are updated to provide the needed flow variables to which juvenile fish respond: the in-house depth-averaged 2-D (two-dimensional) hydraulic model SRH-2D and a 3-D (three-dimensional) computational fluid dynamics model originally developed at the University of Iowa. In this research, a 3-D mesh generation tool is developed for use by the 3-D CFD model so that 3-D modeling can be carried out in relative ease. Two fish track tools, one in the Eulerian framework and the another in the Lagrangian framework, are developed in this research so that fish entrainment at diversion channel juncture may be studied with ease. In addition, the ELAM fish track model, developed by Army Corps of Engineers (USACE), is further adopted through a collaboration with USACE for the purpose of more advanced fish tracking modeling. These flow and fish track tools have been applied to several diversion junctures, including Reclamation projects and valuable knowledge has been gained in understanding ways to alter the flow features to increase or decrease fish entrainment.

The research has led to the following outcomes: (a) a science-based, defensible approach for fish passage study; (b) development and/or extensions of modeling tools that may be used for future fish entrainment studies; (c) guidelines for conducting fish passage studies; and (d) knowledge about geometric and flow features of a diversion channel that are important for attraction or rejection of migrating Juvenile salmon passage.

In this report, a literature review of the current state-of-the-art in fish responses to flow hydrodynamics is first described (chapter 2 and appendix A). The numerical methods/modeling tools are presented in chapter 3, including 2-D and 3-D flow models, Eulerian and Lagrangian particle track models, and the USACE ELAM model. In chapter 4, both laboratory and field cases of diversion junctures are selected and simulated; the flow model results are validated between the model and measured results. The flow modelling study confirmed the complexity of the flow features at the juncture of diversion channels and verified that the 3-D model is adequate for such a study. Chapter 5 reports the fish entrainment results using the modeling tools. The laboratory-scale diversion cases are used to investigate various entrainment features

such as the entrainment rate with a straight channel, the effect of the secondary flows produced by a bend, and impact of the local instream structures. In chapter 7, field applications of the modeling tools are documented and discussed: one at the Georgiana-Slough and another at the Fremont Weir section of the Sacramento River.

In summary, the science-based approach developed in this research is now available for use in future for evaluating alternatives that could enhance fish entrainment or reduce fish passage through a diversion channel at a river juncture. The study focused primarily on the downstream migrating juvenile salmonids.

1.0 Introduction

Water delivery is a primary mission of Reclamation in the western states of the United States. However, it is impacted by the need to meet regulations for fish passage. Annually, a large amount of Reclamation resources is devoted to addressing fish passage. Despite efforts devoted to the topic and increased knowledge about fish passage, the current practice of fish passage design has mostly been exploratory, empirical, and *ad hoc*. There is a need for the development of *a science-based approach*; a need that has been emphasized by scientists in the fish passage community for years. This study represents such an effort in that the current state-of-the-art in numerical modeling is proposed as a science-based approach.

The focus of this research is entrainment of downstream migrating juvenile salmonids at river bifurcation junctions. However, the modeling approach developed is likely applicable to other fish passage applications such as upstream fish migration. Fish entrainment at junctions is a prominent issue at many locations of the river systems in the nation. For example, on the west coast, juvenile anadromous salmonids often travel great distances from spawning habitat in freshwater rivers to the ocean, sometimes located hundreds of kilometers away. As juveniles migrate downstream from natal streams to the ocean, they encounter a variety of different migration pathways and rearing habitats. Some of these pathways may be advantageous, such as productive floodplains and side channels that may enhance growth (Sommer et al. 2001; Jeffres et al. 2008; Bellmore et al. 2013). Others may lead to habitats with greater risks of mortality such as agricultural diversions, turbines, industrial cooling systems, or habitats with high predator abundance (Roberts and Rahel 2008; Buchanan et al. 2013). Although patterns of habitat use have been relatively well studied and reported (Brandes and McLain 2001), it has been difficult to estimate the proportion of a population that is exposed to entrainment into alternative routes (Post et al. 2006; Carlson and Rahel 2007).

A good example is the Chinook salmon migration in the Sacramento - San Joaquin River Delta (called the Delta in this report). A key life stage is the outmigration period from natural tributaries to the ocean. During the migration run, juveniles have the option of moving along several routes through the Delta as shown in Figure 1 (Perry et al. 2010). The routes consist of a complex network of natural and artificial tidal channels and have been highly altered to convey water for domestic and agricultural uses (Nichols et al. 1986). Depending on the route selected, their survival chances vary. Four routes were discussed by Perry (2010) for the Delta and two leading to the interior Delta were found to exhibit the lowest survival rates (Perry et al. 2010, 2013, 2014). The low survival was the result of high predation rates, longer migration times, and potential entrainment into the water pumping stations (Brandes and Mclain 2001; Newman and Brandes 2010). Being able to understand the factors controlling the migration route selection is the first step to developing the strategies to recover endangered salmon populations in the Delta. The two migration routes in the Sacramento River that lead to the interior Delta are through the Delta Cross Channel (DCC) and Georgiana Slough (GEO) (see Figure 1). The GEO is a natural connection between the upper and the interior Delta; while DCC is a 1.1 km-long artificial channel used to divert water from the Sacramento River into the interior Delta through a system of moveable gates with control of salinity levels at the pumping stations.

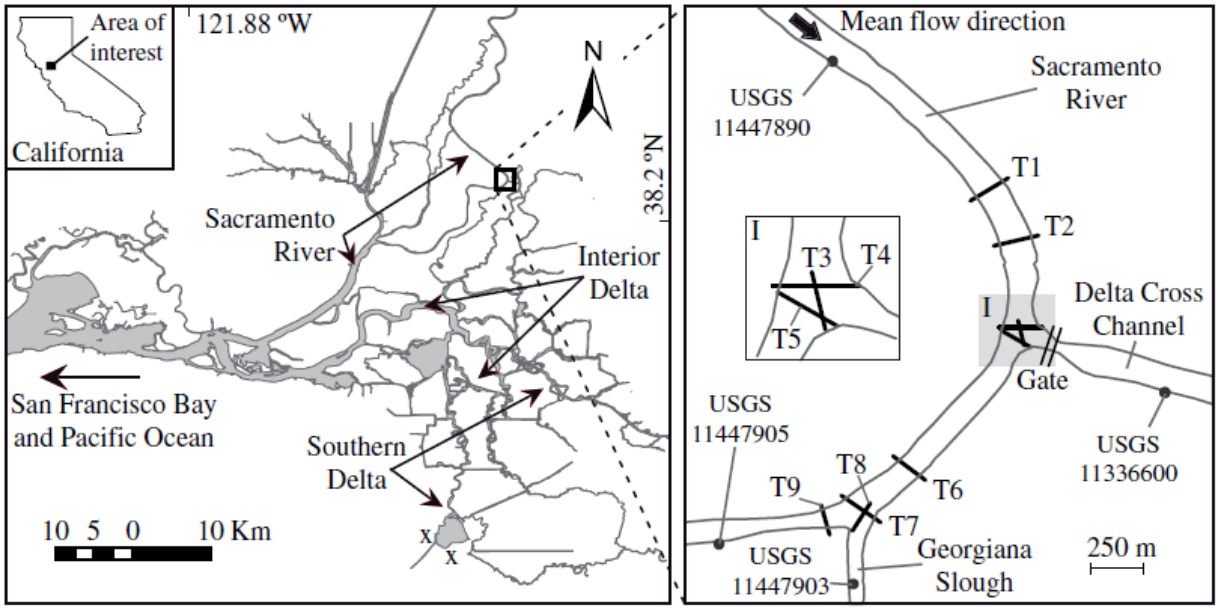

Figure 1.—Sacramento - San Joaquin River Delta (left) and the area of DCC and GEO (figure source: Ramon et al. 2018).

Migrating fish route selection has been found complex; it has been particularly difficult to estimate the proportion of a fish population entrained into alternative routes (Post et al. 2006; Carlson and Rahel 2007). Few methods are available to devise remedies, e.g., by altering the local terrain or using instream structures, so that fish attraction into or rejection from a side channel may be achieved. Lack of science-based approaches motivated this present research.

A science-based approach is proposed herein, based on the improvement and development of a suite of numerical tools. The tools build on the premise that local flow hydrodynamics is a dominant factor affecting fish migration selection, among many other variables. Use of numerical models for fish passage evaluation is an emerging field. Early work was mostly on juvenile salmonid migration through hydropower dams. Such studies were reported, e.g., by Goodwin (2004), Goodwin et al. (2006; 2014), and Smith et al. (2010), and has been shown effective and useful. The success of the modeling approach for downstream migration fish passages at reservoirs, however, has not been transferable to downstream migrating fish passage in streams or for upstream fish migration. Two obstacles were reported: (a) inability of the existing models in predicting the complex flow hydrodynamics experienced by fish in streams, and (b) lack of understanding of fish responses to local flow features in the riverine environment. For issue (a), three-dimensional (3-D) computational fluid dynamics (CFD) models have been matured at present, and it is not an obstacle anymore. For example, the 3-D CFD model developed by Lai et al. (2003a; b) has been improved and applied to several locations along the Sacramento River. Good agreements were obtained in comparison with ADCP velocity data.

For obstacle (b), recent-year studies have increased our understanding about fish behaviors in response to local flow features induced by terrains or instream structures in the riverine environment. Recent relevant studies include, e.g., McNamara et al. (2013), Goodwin et al. (2014), Dabiri (2017), Oteiza et al. (2017), Bever and MacWilliams (2015), Ramon et al. (2018), and Goodwin et al. (2018), among others. The time is ripe to develop a new numerical-based approach towards the understanding and assessment of fish entrainment dynamics at a flow junction.

In this study, new model tools are developed which combine a current 3-D CFD flow hydrodynamic model with different levels of fish tracking models. The new tools may be used for assessing entrainment characteristics at a river junction for downstream migrating juvenile salmonid. Increasing juvenile salmon survival during their downstream migration in regulated rivers is an important topic as survival of juvenile salmon in regulated rivers is often many-fold lower than a corresponding free-flowing river section. For example, survival of smolts was found to be six-fold lower within a river system with five hydropower dams than in a corresponding section of a free-flowing river (Huusko 2018). It has been recognized that initiatives to rebuild salmon stocks and safeguard downstream migration juveniles are equally important as the upstream migration of spawning salmon. However, downstream fish passage technologies are much less advanced than upstream fish passage. It is due to that the efforts to re-establish free movement of migrating fish has traditionally been on building the upstream passage facilities because facilities designed for downstream migration are much more difficult to develop (Larinier and Travade 2002). Fish entrainment occurs whenever water is diverted into a branch channel from the main channel. In this study, fish attraction refers to a junction where fish entrainment into the side channel is encouraged, while fish rejection refers to situation where fish entrainment is undesirable. Both attraction and rejection of juvenile salmon must be understood to effectively develop a migration pathway.

This report is organized as follows: a literature review is presented in chapter 2 on the fish entrainment issue, particularly at flow junctions, and fish passage behaviors in general. Chapter 3 documents the theoretical background of the numerical models used or developed to investigate the fish passage at typical flow diversion junctions in streams. Chapter 4 provides the CFD model validation study cases by comparing with available measured data at flow diversions and natural rivers. Chapter 5 presents model results to shed light on fish entrainment characteristics at a representative diversion junction. The objective is to show that: (a) fish distribution across the cross-section upstream of the junction has a significant impact on fish entrainment; (b) presence of a secondary flow upstream of the junction may redistribute fish before they enter the side channel and alter fish entrainment; and (c) local bathymetry features may be manipulated upstream of the diversion junction to increase or decrease fish entrainment. Chapter 6 presents fish entrainment results in the Field.

2.0 Literature Review

In this chapter, a literature review is presented, focusing on the current state-of-science in juvenile salmonid downstream migration. The methods or models used in the fish entrainment studies are reviewed along with specific flow variables as key stimuli. A general review has also been conducted separately and documented in appendix A.

2.1. Fish Entrainment Evaluation Tools

Methods and tools have been developed in the past and used to evaluate the entrainment effectiveness at river flow junctions. They are reviewed in this sub-section.

A method was developed by the California Department of Fish and Wildlife (CDFW) to evaluate the entrainment of juvenile Chinook Salmon onto the Yolo Bypass (Acierto et al. 2014). In this approach, historic flow data and Knights Landing rotary screw trap catch data of juvenile Chinook Salmon between 1997 and 2011 were used to compare existing conditions to a proposed notching of Fremont Weir. This was further developed into a spreadsheet tool, called the Juvenile Entrainment Evaluation Tool (JEET) (DWR 2017). The tool was designed to be an evaluation tool for juvenile salmon entrainment at the Fremont Weir junction with different fish runs and river stage levels. The tool uses the flow variables simulated by TUFLOW hydraulic model. The tool, however, assumed that the fish entrainment rate was equal to the water rate diverted into the side branch and based on the specific site-specific data. As a result, it was more suited to a site where the model had been calibrated, and less suitable for predicting the fish entrainment rate with altered conditions. The model cannot be used to evaluate the effects of changes of local terrain or diversion geometry; it cannot be used to predict fish distributions across the river.

Another analysis tool was reported by Blake and Horn (2004) and Perry et al. (2014) and had been successfully applied for fish entrainment studies. The method adopted the so-called critical streakline concept. A critical streakline is defined as a point (if 2-D) or a line (if 3-D) on river cross sections; it separates waters continuing downstream from those diverted to the side channel. If the critical streakline can be determined upstream of a junction, fish distributed on the side channel side of the streakline was assumed to enter into the side channel so that the fish entrainment potential can be determined. This method has been applied to analyze fish entrainment at several locations along the Fremont Weir section of the Sacramento River (Blake et al. 2017). In the studies, the in-stream flow information was from a set of field-measured data including the ADCP velocity and flow stage (Stumpner et al. 2017), while the cross-sectional fish distribution was estimated from the fish acoustic tag data (Blake et al. 2017). With the computed critical streaklines and fish cross-channel distribution, fish entrainment potential was computed and evaluated. It is commented that the velocity field may also be obtained from a 3-D CFD model and the critical streakline concept is equally appliable. The critical streakline approach is useful when measured fish distribution data are available; it is particularly applicable to the existing condition scenarios. The method relies on a number of assumptions. For example,

fish response is passive and measured fish distribution needs to be available. The method is not predictable; therefore, it may not be adequate for design alternatives which deviate from the existing conditions as future-condition scenarios are not measurable. As commented by Tompkins et al. (2017), "the model provides an initial evaluation of entrainment potential for each location while noting that actual entrainment would depend on specific characteristics of the notch, such as absolute dimension, relative position, and structural geometry."

Tompkins et al. (2017) provided a review of three methods that were used for the Fremont Weir notch selection study for diversion into the Yolo Bypass. They included the JEET, critical streakline, and ELAM method (ELAM will be reviewed below). Pros and cons of each were discussed in detail in the report. The study concluded that "All three predicted that more flow capacity results in more entrainment. JEET did not address notch location or configuration. Streakline characterized potential differences in entrainment in the Western section of the weir but did not address effects of configuration. ELAM addressed entrainment for all alternative locations and configurations. In addition, it explored configurations beyond those in the six alternatives. For determining the notch location, only the ELAM provides enough information to be useful for decision making in support of the EIR/EIS (environmental impact report/environmental impact statement). For evaluating the basic notch configuration, the ELAM model is most useful but a more complex form, including 3-D hydrodynamics and higher order fish responses, will be required for optimizing the design."

Other entrainment methods or models have also been proposed and applied. For example, statistical or linear regression models have been developed to investigate the fish entrainment rate into side channels (e.g., Perry et al. 2014; 2015; Cavallo et al. 2015). Based on the field data of tracked fish, a linear model was developed relating the fish entrainment rate to the fraction of water diverted into the side channel. Specific models have been developed for sites such as at the Georgiana Slough section of the Sacramento River (Perry et al. 2014) and the California Delta river network (Cavallo et al. 2015). Once the linear regression model is developed for a specific set of hydrology, it could be used other flow periods, using measured or simulated hydrology and hydraulics, to estimate the entrainment potential at the flow junction and/or study the impact of management measures. Such models are useful for planning purpose. For example, Perry et al. (2015) stated that, "Prior to this study, fisheries managers had little mechanistic information with which to guide water management actions for minimizing fish entrainment into the interior Delta. Uncertainty about the driving mechanisms has forced fisheries managers to act in a precautionary manner, implementing actions that are least likely to harm endangered populations but at the expense of consumptive water use." Cavallo et al. (2015) stated that "These results suggest that total flow proportion at each junction can be used in conjunction with the linear model to predict fish routing. This will be an effective tool for evaluating water management actions on fish routing; especially where little or no observed fish routing data are available." Note that these studies used the existing measured data for the analyses. Success of such linear regression models, however, hinges on the assumption that the percentage of flow diversion is the dominant metric determining the percentage of fish entrained. The model may also be limited to the specific site where the model was developed (i.e., not predictive). It shares similar limitations to the JEET method discussed above.

Entrainment zone concept has been proposed to examine the entrainment dynamics at a junction by Blake and Horn (2004) and applied to a section of the Sacramento River by Ramon et al. (2018). The entrainment zone is defined as a zone upstream of the junction where water velocities are sufficient to move juveniles into the downstream side channel which passive fish would enter the side channel. The concept is illustrated in Figure *2*, where the spatial divide between the entrainment zone and the zone with fish bypassing the junction is marked as red and was referred to as the critical stream surface. In general, the entrainment zone size is linearly proportional to the percentage of water entering the side channel (flow entrainment rate). Under the uniform flow conditions, the fraction of the cross section of the entrainment zone should be equal to the flow entrainment rate. The entrainment zone concept may be useful to examine the entrainment dynamics under an unsteady flow condition (e.g., the case studied by Ramon et al. 2018). It is more a qualitative way to examine the entrainment dynamics.

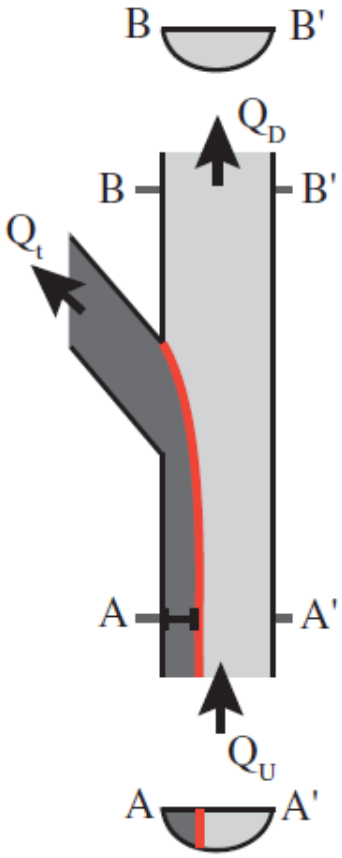

Figure 2.—A sketch showing the entrainment zone for fish entering the side channel (dark gray areas) demarcated with the critical stream surface (red line) (source: Ramon et al. 2018).

In another study, Hance et al. (2020) reported the use of a conceptual model to study entrainment rates based on combined concepts reviewed above - entrainment zone, critical streakline and cross-sectional fish distribution of fish. In this study, statistical models of the critical streakline, cross-sectional fish distribution, and entrainment probability were developed and used for fish entrainment prediction at the Georgiana Slough junction of the Sacramento River. Streakline and entrainment zone were based on the field measured ADCP velocity data while fish distribution and entrainment probability were derived from the fish telemetry data.

More sophisticated models have been developed based on numerical models of fish tracking. A noteworthy study was reported by Ramon et al. (2018) in which a 3-D hydro-static assumption flow model was adopted to obtain the flow information, while a 3-D Lagrangian particle-tracking model of Rueda et al. (2008) was used for fish tracking. The numerical model was demonstrated by applying to the diversion junctions on the Sacramento River. In this model, fish were simulated as neutrally-buoyant particles. Particle trajectories were assumed to mimic those of salmon individuals, i.e., their motion is largely passive. This assumption is consistent with the literature (Blake and Horn 2004; Perry et al. 2010) that fish behavior can be broadly explained in terms of water flowing speed as long as it is strong enough in comparison with the fish swimming capabilities. Typically, juvenile Chinook salmon can sustain approximately a flow speed of two body lengths per second (Nelson et al. 1994). For an average fish length of 100 mm (Brandes and Mclain 2001), the swimming capability is about 0.2 m/s. Sacramento River flow velocity is mostly higher than this threshold, suggesting that hydrodynamics is dominating over fish behavior and the passive approach is applicable.

The models described above were mostly based on the neutrally buoyant assumption (or passive movement). To take fish perception and response characteristics into account, more sophisticated track models are needed. A fish tracking numerical model was developed and demonstrated for effectively designing bypass systems at hydropower dams by Arenas et al. (2015). The fish tracking model was Lagrangian based and deviated from the assumption of passive fish movement. In this study, a 3-D CFD model was used to obtain the flow hydrodynamics, the probability distribution functions (PDF) describing the fish swimming behaviors were then derived using the acoustics tag data of fish tracks and the CFD results, and the PDFs were finally used to predict fish movement. The fish behaviors contained in the PDFs included fish swimming orientation and thrust in response to flow acceleration; and the model took into consideration of both fish drifting and active swimming. A key finding was that smolts tend to orient themselves against the flow and are less likely to drift when encountering increased acceleration. Juveniles showed the tendency to avoid flows with significant vertical accelerations though the behaviors varied among species. In particular, it was shown that the model performed better than the assumption of passive behaviors. It is noted that the model of Arenas et al. (2015) did not directly use the theory of fish behaviors in relation to hydrodynamic conditions, which are yet to become mature. Instead, the study adopted the inverse problem approach: using the measured fish track data to infer the relations (PDFs) between flow field variables (e.g., acceleration in the study) and smolt swimming behaviors.

A state-of-the-art fish perception-and-response model is the so-called Eulerian-Lagrangian Agent-based Model (ELAM) developed at U.S. Army Corps of Engineers (USACE) and has

been described in a series of publications (Goodwin 2004; Goodwin et al. 2006; Smith et al. 2010; Goodwin et al. 2014). Early studies were mostly for downstream migrating juvenile salmonid passage through hydropower dams in the Pacific Northwest. Studies have also been carried out in recent years for applications to the riverine environment – fish entrainment at the Georgiana Slough junction (Goodwin et al 2018) and the Yolo Bypass junction (Smith et al. 2017) of the Sacramento River. ELAM is a mechanistic representation of individual fish movement and simulates fish movement according to fish responses to variations in the flow field – a perception-and-response model. Changes in flow hydrodynamics are detected by a fish within a perception oval and changes in swimming behaviors are made in response to the flow changes. Fish perceptions of hydrodynamic conditions were modeled using a number of defined detection thresholds. Data from acoustically-tagged fish were used to calibrate the parameters of the model looking for qualitative resemblance between measured and simulated swim paths and similarity between model predictions and fish measured passage proportions through the bypass, spillway, and turbines. In a typical application, local flow features are normally computed by numerical flow models such as the depth-averaged 2-D models or the 3-D CFD models. ELAM is then calibrated using observations of fish movement at a specific study site if the field telemetry tracks are available. The individual tracks are not directly modeled. Rather, statistical properties of the measured tracks are used to guide the model coefficient development. The approach supports extension of empirical observations toward unmeasured environmental conditions.

2.2. Flow Variables Relevant to Fish Response

Fish movement is influenced by many environmental factors such as flow hydrodynamics, temperature, total dissolved gas (TDG), turbidity, light (e.g., day or night), cover, predation, and food web. Fish species and size also play important roles. However, it is generally accepted that near a dam or at a water diversion junction, fish mostly respond to local flow hydrodynamics (e.g., velocity, acceleration, vorticity and turbulence) in comparison with other stimuli (Popper and Carlson 1998). Literature review reveals that it is generally accepted that fish respond to flow hydrodynamics; the details of such responses, however, are yet to be fully understood. Such information nevertheless is important in the success of any numerical fish tracking models. A review of what has been known is provided in this sub-section.

2.2.1. Flow Velocity

Stream flow velocity is probably the dominant flow stimulus for fish movement decision. It is generally held that anadromous juvenile outmigrant salmon tend to follow the highest flow of water as they migrate to the ocean, or they tend to migrate downstream in the river thalweg (Whitney et al. 1997). This is probably why fish entrainment rate at a diversion junction is often proportional to the amount of water diverted into the side channel. In a flume, Kemp et al. (2005) analyzed the behavior of salmon smolts and observed that most selected a route in a ratio consistent with the flow proportion. In the field, such as at the Delta cross channel (DCC) and Georgiana Slough (GEO) junctions of the Sacramento River, studies showed that the proportion of fish entering any of the two routes, DCC or GEO, averaged over a tidal cycle, was largely

controlled by the fraction of flow moving into that route (Perry et al. 2010; Cavallo et al. 2015). Steel et al. (2013) analyzed Chinook salmon routing at the DCC junction of the Sacramento River. The ratio of mean velocity in the main stem and side was found to be a strong predictor for the portion of fish diverted. In a review by Perry et al. (2016), it was stated that "the working hypothesis was that migrating fish became entrained in side channels in direct proportion to the relative volume of water entering the side channel."

The above-described behavior of fish response to flow velocity can be explained by the concept of fish swimming speed capacity. If stream flow velocity is higher than a threshold – the swim speed capacity, fish do not alter their location and usually select a route and move with the flow. Below this value, however, fish may actively hold and mill and select a route to emigrate through. The fish speed capacity is about 2 body length of the juveniles per second (Romine et al. 2017) although it varies among species and sizes. In their study of fish entrainment on the Sacramento River, the swim capacity was assumed to be about 0.2 m/s when juvenile Chinook salmon of 100- 200mm (Romine et al. 2017) and it was assumed that "fish can do little to alter their location and actively select a route and are thus constrained by the parcel of water they are located and where it goes." In the study of Arenas et al. (2015), it was assumed that salmon smolts were prone to follow the flow under velocities greater than 0.9 m/s. For lower velocities they exhibited a less direct behavior. When stream velocity is mostly higher than the speed capacity, it is reasonable to assume fish move passively. It is also often assumed that fish entrainment rate at a flow junction is linearly correlated to the percentage of water diverted – an assumption adopted by most models reviewed above.

Larger juvenile salmon populations were observed to follow flow along the thalweg of the water control structure where water velocity magnitudes were greater than 3 ft/s by the time they had reached within 200 feet of the water control structure.

The velocity-driven fish movement assumption may break down under several scenarios. For example, diel light (day and night) may have an impact on how fish move in response to the same flow. Perry et al. (2015), for example, discussed that fish may choose to stay close to the banks during the day and move near the center of the channel at night. This preference is due to fish migrating mostly in the night. The diel migration pattern has been observed in many fish species (e.g., Reebs 2002). Water temperature may also play a role in the diel migration behavior. The above finding may hold when water temperature is relatively low. At higher water temperature, juvenile salmon in the California Delta migrate preferentially during the day (Wilder and Ingram 2006).

Note that downstream migration may be impacted by the tendency of fish to seek habitat areas which interrupts their migration downstream. This tendency seems to differ among juvenile sizes. In a review by Tompkin et al (2017), it was stated that smaller juveniles (30 to 70 mm) tend to seek and rear in shallow and low-velocity areas whereas larger smolts often move in higher velocities in the deep portion of the river and often actively migrate downstream. In a study of the lower Willamette River by Friesen et al. (2007), nearshore, shallow beaches were found to be an important habitat for small Chinook salmon, whereas larger ones (>100 mm) were distributed in the mid-channel area. In other studies, small juvenile Chinook salmon were often

found in the shallow, low-velocity areas such as inner side of the bends, rather than in the mid-channel or outside of the bends (Schroeder et al. 2013; 2016; van Remoortere 2014). This suggests that fish tracking models need to distinguish small Chinook salmon from the large smolts. Models developed for large ones may not be extendable to smaller fish. It has been discussed by Tompkin et al. (2017) that smaller Chinook fish downstream migration is important in the California Central Valley. In one study by Miller et al. (2010), for example, it was found that 20% of fall Chinook salmon migrated as fry (<55 mm), 48% as parr (56-75 mm), and 32% as smolts (>75 mm).

2.2.2. Fish Distribution

Despite the importance of flow velocity, fish entrainment rate can deviate from water diversion rate markedly, as discussed by Ramon et al. (2018) and reviewed by Hance et al. (2020). Field observations suggest that the mechanisms governing fish route selection are complex; in addition to the flow entrainment velocity other factors may play important roles in influencing fish entrainment rate. An important parameter is the spatial distribution of fish upstream of a flow junction which is influenced by local flow features (Perry et al. 2014; Ramon et al. 2018). Despite its importance and knowledge of its qualitative importance, quantitative study of its impact has not been carried out. Equally lacking is the study of ways by which local terrain or geometry features may be manipulated to increase or decrease fish entrainment at a junction.

Fish distribution is generally non-uniform in the vertical direction. Studies of fish vertical distribution, however, are few. Qualitative information is available. On the Sacramento River, for example, salmon was found to travel primarily within the top 4 meters of the surface water (Blake and Horn 2004). As a comparison, water depth at the Georgiana Slough junction of the Sacramento River averages about 7 meters in water depth with the maximum depth reaching 13 meters downstream of the Delta cross channel along the bend outside. In a different flow environment, salmonid juveniles, when approaching a dam, were found to follow the bulk flow but remained in the upper portion of the water column (Whitney et al., 1997; Buckley and Kynard, 1985; Faber et al., 2011).

Fish vertical movement features are important for simulating passage through structures: an important impact on the efficiency of fish entrainment or rejection at a flow junction. It is generally found that juvenile salmon migrating downstream exhibit diel vertical migration. The tendency is often for salmon to be more surface oriented at dusk (for food), may be deeper at night during the summer (temperature related), and deeper during the day due to predation. The results, however, were derived mostly from studies in lakes where flow velocity is small. In a stream environment, it is believed that fish are mostly in the upper surface during active migration due probably to high current flow. They move to deeper depths, even near stream bed or bank and in-stream structures, when looking for food or rest, or avoiding predation.
Lateral distribution of fish has not been studied systematically. Limited studies have shown that salmon tends to distribute towards the outer bank within a river bend. This was observed at a number of locations on the Sacramento River such as at the Delta cross channel (Blake and Horn 2004), Clarksburg (Blake et al. 2012), and Yolo Bypass (Steel et al. 2016). This was explained to be the result of the secondary flows present in the bend (Blake and Horn 2004; Blake et al.

2012). The observed behavior may also be attributed to the preference of migrating fish to stay within the thalweg as discussed before. It is cautioned that the above finding may not hold at every bend. For example, in a study of the fish entrainment at the Georgiana Slough junction of the Sacramento River, the peak of the fish distribution was found towards the inner side (Perry et al. 2014) despite the presence of a bend and secondary circulation at the site. The reason for this is unclear and may be influenced by the complex and unsteady flows created by the tidal flows and/or the fish size.

At present, no quantitative or systematic studies have been conducted on the impact of the non-uniform fish distribution, both vertically and laterally, on fish entrainment at a junction, although the importance of such non-uniform fish distribution was studied before. For example, Blake et al. (2017) conducted fish entrainment study at the Yolo Bypass junction at the Sacramento River when the measured fish distribution in a bend was used to estimate the best diversion location. Ramon et al. (2018) adopted a CFD model and a passive fish tracking model to study the fish entrainment characteristics at flow junctions. The impact of non-uniform fish distribution on fish entrainment, however, was indirectly studied by considering the effect of secondary circulation within a bend.

2.2.3. Other Flow Stimuli

In addition to flow velocity and fish distribution, changes in local terrain or presence of instream structures may play important roles in fish movement behaviors. In fact, non-uniform fish distribution can be partly due to fish responses to local flow changes. When downstream migrating salmon approach to a barrier such as a diversion junction or other instream structures, significant changes of local flow hydrodynamics occur which may increase the chance for fish searching or milling, leading to different fish entrainment behaviors. For example, at the Delta cross channel (DCC) and Georgiana Slough (GEO) junctions of the Sacramento River, the proportion of fish entering DCC and GEO varied in time and deviated markedly from the tidal-averaged flow entrainment rate (Perry et al. 2010; Cavallo et al. 2015). Impact of local flow hydrodynamics other than the velocity may play an important role.

Various flow parameters have been proposed to be important fish stimuli leading to fish to respond differently from cruising speed. As reviewed by Ramon et al. (2018), juvenile salmon was shown to respond to flow variables such as acceleration, turbulence and velocity gradients. Arenas et al. (2015) stated that flow acceleration or velocity gradients in general were identified as the flow field components that correlated better with fish swimming patterns. Previous studies have tried to parameterize the stream hydraulic complexity so that they alone are used to infer fish migration behaviors (e.g., Crowder and Diplas 2000; 2002; Gualtieri et al. 2017) or to link hydraulic complexity to actual salmon behavioral rules that may be adopted in fish tracking models (e.g., Goodwin et al. 2006; Nestler et al. 2008).

Fish are generally found to respond to velocity gradient. Flow acceleration has been adopted frequently by fish tracking models. In a flume experiment studying the behavior of salmon smolts by Kemp et al. (2005), it was observed that when flows were constricted within a channel, smolts were observed to be capable of detecting and avoiding accelerating flow.

In the study of Mulligan (2014), a design metric adopted was the creation of a high downstream acceleration upstream of the Fish Intake Guidance Structure (FIGS) that would improve guidance efficiencies because juveniles tend to avoid regions of high acceleration.

In the fish track modeling of Arenas et al. (2015), flow acceleration was also used as the dominant stimulus. When acceleration increases, the effort made by fish to resist the flow increases (i.e., fish swim away from the high acceleration zone). However, beyond a given threshold, the tendency of fish to swim against the flow decreased. In their study, the effort made by fish to swim against the flow peaked at a flow acceleration of approximately 0.3 m/s^2.

In the ELAM model of Goodwin et al. (2006; 2014), the theory of fish perception-and-reaction centers around the flow acceleration also. Fish behaviors in ELAM are represented by a set of rules that are implemented in the model to drive fish movement. Four potential fish response behaviors may be activated: [B1] for downstream fish drift with the flow; [B2] for response to moderate flow acceleration - fish swim across the streamlines into higher velocity area; [B3] for response to strong flow acceleration - fish swim upstream against the flow; and [B4] for response to vertical velocity changes - fish swim against changes in vertical velocity to maintain depth. Rules [B2] to [B4] are related to flow acceleration. These rules are based on the observation that juvenile salmonids tend to drift downstream and when encountering moderate flow acceleration, they swim across the streamlines into higher velocity areas. However, when fish encounter strong flow acceleration, they may swim upstream against the flow. They also tend to swim against changes in the vertical velocity in order to maintain depth (Tompkins et al. 2017). For example, Faber et al. (2001) showed that juvenile tended to move against or orthogonal to the current when water velocity was lower than 3 cfs. As a note, the recommended maximum velocity for an upstream fish passage designed for juvenile salmonids of 80 to 100 mm is 3 to 4.5 ft/s (NMFS 2011). These results may explain why fish distributed towards the outer bank when encountering secondary flows with a bend: surface-oriented fish drift towards the outer bank but do not circulate back towards the inner bend by the deeper secondary current.

Vorticity or circulation has also been proposed as a stimulus for fish response to flow changes. In one study, larval zebrafish performed rheotaxis - a behavior of fish that they orient and swim against incoming flows - by using flow velocity gradients as navigational cues to avoid getting dragged by flowing water (Oteiza et al. 2017). Specifically, the study showed that fish used their mechanosensory lateral line to sense the curl (or vorticity) of the local velocity vector field to detect the presence of flow changes and to measure its temporal change after swim bouts to deduce flow direction. It suggests the vorticity (or the relevant circulation) may be a flow stimulus to determine the fish response to flow changes. Since the scale of vorticities can vary widely in a flow, it is conjectured that fish size may be important in determining the important scales of vorticities. That is, the size of circulations larger than the fish size may have a higher probability to cause drastic fish response. Oteiza et al. (2017) postulated that vorticity was the key stimulus that the fish body surface is capable of measuring. In a follow-up study by Dabiri (2017), fish response to velocity gradient and vorticity was further described.

Navigation that is based on the lateral-line sensing of flow gradients enabled fish to swim at the center of the channel and to avoid the walls. It indicated that the vorticity generated near the banks kept fish away from them.

It is noted that the tendency of fish seeking habitat areas may break down the fish response behaviors discussed above. As reviewed in appendix A, habitat tendency is especially relevant for smaller fish (fry <70 mm) although it is less a concern for smolt (>100mm) when they are in active migration. Fry tends to seek habitat areas with shallow and small velocity areas near banks, inner bend, deep pool, and areas with large wood. Rearing habitat is related to foraging, cover, and resting areas for juvenile anadromous fish. It seems active migration occurs mostly at night, while fish use habitat areas more often during daylight, due possibly to predation pressure (appendix A).

2.3. Flow Models

Both 2-D and 3-D models have been developed to provide flow hydrodynamic data needed for fish tracking numerical modeling or for assisting fish passage design and evaluation.

2-D depth-averaged models have been widely used for fish habitat modeling as the water depth and flow velocity can be predicted well with such models. In recent years, 2-D hydraulic models have also been used for fish migration studies. 3-D flow models, however, have been recognized to be necessary for fish passage studies, in particular for fish passages at flow junctions or through instream structures.

2-D and 3-D hydraulic models have been well documented in the literature and not repeated here. A few relevant studies of fish tracking using the flow models have been reported in recent years. One such example is the fish tracking modeling by Ramon et al. (2018). In this study, a 3-D hydrostatic-assumption flow model, developed by Smith (2006), Rueda and Schladow (2003) and Acosta et al. (2010), was used to compute the flow hydrodynamics. The flow momentum equations are solved on a staggered Cartesian grid, using a second-order accurate, space-centered, semi-implicit, and three-level iterative leapfrog-trapezoidal finite difference scheme. A Laplacian operator with constant eddy viscosities is used to represent the horizontal turbulent mixing of momentum. Vertical eddy viscosities are calculated using a two-equation model. Ramon et al. (2018) argued that the nonhydrostatic pressure effect was not important based on the argument that the ratio of the scales for the vertical and horizontal variability of the flow was small. Although it is generally true, secondary flow computation, however, may need to be simulated using the non-hydrostatic pressure distribution. Such a need was shown by Lai (2020).

In general, non-hydrostatic 3-D flow models, called 3-D CFD models in this report, are needed for general fish track modeling. Such a method has been adopted widely (e.g., Arenas et al. 2015; Goodwin et al. 2006; 2014). For example, a combination of the 3-D CFD and fish tracking model ELAM has been adopted for fish tracking studies (Goodwin et al. 2018). The 3-D model was initially developed by Lai (2000), modified for river applications later by Lai (2003a; b).

The 3-D model has since been advanced to simulate flows with complex geometry. For example, the ability of the model to simulate complex flow through a large wood was documented by Lai and Bandrowski (2014) and Lai et al. (2017a) using the terrain-conforming method. The Terrain-embedding method was developed by Song et al. (2020) and a comparison between the terrain-conforming and terrain-embedding methods was reported by Lai (2020).

3.0 Numerical Methods and Models

This chapter documents the theoretical background of the models used to investigate the fish passage at typical flow diversion junctions in streams. The tools consist of SRH-2D and a 3-D CFD model for flow simulation, two fish tracking models developed in this study, and the ELAM fish track model developed by USACE. SRH-2D is well documented (e.g., Lai 2010) and its description is omitted; others are described below.

3.1. A 3-D CFD Model

In this study, the 3-D CFD model reported by Lai et al. (2003a; b) is adopted and extended for fish tracking study. The model belongs to the category of unsteady Reynolds-Averaged Navier-Stokes (URANS) solver which adopts the non-hydrostatic assumption. The governing equations are the standard Navier-Stokes equations and may be expressed for incompressible flows in tensor form as:

$$\frac{\partial U_j}{\partial x_j} = 0$$

$$\frac{\partial U_i}{\partial t} + \frac{\partial \left(U_j U_i\right)}{\partial x_j} = \frac{\partial}{\partial x_j}\left(\upsilon \frac{\partial U_i}{\partial x_j} + \tau_{ij}\right) - \frac{\partial P}{\rho \partial x_i} + g_i$$

In the above, t is time; x_j is j-th Cartesian coordinate; U_j is mean velocity component along coordinate x_j; $\tau_{ij} = -\overline{u_i u_j}$ is turbulence stress (u_j is j-th turbulent fluctuating velocity component); P is mean pressure; ρ is water density; υ is water kinematic viscosity; and g_i is i-th component of the acceleration due to gravity. Repeated subscript (e.g., j) means summation over the three Cartesian coordinates.

The turbulent stress τ_{ij} is related to the mean velocity strain rate using the Boussinesq approximation (Pope 2000) as:

$$\tau_{ij} = \upsilon_t \left(\frac{\partial U_i}{\partial x_j} + \frac{\partial U_j}{\partial x_i}\right) - \frac{2}{3} k \delta_{ij}$$

In the above, υ_t is the turbulence eddy viscosity to be computed with a turbulence model and δ_{ij} is the Kronecker delta (a unit tensor). In this study, the two-equation k-ε model of Launder and Spalding (1974) is adopted. That is, the eddy viscosity is computed by:

$$\upsilon_t = C_\mu \frac{k^2}{\varepsilon}$$

In the above, k is the turbulence kinetic energy and ε is the turbulence dissipation rate. Two transport equations for k and ε are solved to obtain the turbulent viscosity and expressed as:

$$\frac{\partial k}{\partial t} + \frac{\partial (U_j k)}{\partial x_j} = \frac{\partial}{\partial x_j}\left(\left(\upsilon + \frac{\upsilon_t}{\sigma_k}\right)\frac{\partial k}{\partial x_j}\right) + G - \varepsilon$$

$$\frac{\partial \varepsilon}{\partial t} + \frac{\partial (U_j \varepsilon)}{\partial x_j} = \frac{\partial}{\partial x_j}\left(\left(\upsilon + \frac{\upsilon_t}{\sigma_\varepsilon}\right)\frac{\partial \varepsilon}{\partial x_j}\right) + C_{\varepsilon 1}\frac{\varepsilon}{k}G - C_{\varepsilon 2}\frac{\varepsilon^2}{k}$$

where $G = \tau_{ij}\frac{\partial U_i}{\partial x_j}$ is the production rate of the turbulence kinetic energy. The standard turbulence model constants take the following values: $C_\mu = 0.09, C_{\varepsilon 1} = 1.44, C_{\varepsilon 2} = 1.92, \sigma_k = 1.0,\ \sigma_\varepsilon = 1.3$.

Numerical solution of the above governing equations is not trivial and has been subject to many years of research and development. Various methods and algorithms have been proposed and developed. The present model is based on the unstructured, arbitrarily shaped mesh cell method of Lai et al. (2003a). In essence, the CFD model developed in this study has the following features: finite-volume method for discretization, pressure as the primitive variable, implicit time marching scheme, collocated-mesh, cell-centered arrangement, and pressure-correction method for solving the continuity equation. Extensions to and improvements over the method of Lai et al. (2003a) have been carried out, they include: implicit unsteady term added and tested, mixed mesh cell shapes consisting of polyhedrons with an arbitrary number of cell faces, linkage to 3-D meshes generated by snappyHexMesh (a tool within the OpenFOAM), and near-wall log-law functions incorporating the bed roughness height. In addition, both sigma and Z meshes are built into the model so that only a 2-D mesh is needed as input for most stream simulation applications.

Once a 3-D mesh is available covering the model domain, the governing equations are discretized on the mesh according to the finite-volume method and cell-centered and collocated schemes. The extension to mixed cell shapes with an arbitrary number of cell faces means that the CFD solver is based on most general mesh types. In addition, the cell-centered and collocated schemes are selected so that that all flow variables are located at the centroid of a mesh cell. It is in contrast with the staggered scheme with which velocity and pressure are stored at difference locations. The collocated scheme greatly simplifies the CFD solver development.

The governing equations are discretized using the finite-volume method and the Gaussian integral. The procedure was discussed by Lai et al. (2003a); it is briefly presented focusing on the unsteady and implicit terms. As an illustration, consider the following general convection-diffusion equation for variable C in vector form which is a representative of all governing equations:

$$\frac{\partial C}{\partial t} + \nabla \cdot \left(\vec{V} C\right) = \nabla \cdot (\sigma \nabla C) + S_C^*$$

When all variables at time level (*k*-1) are given, the variables at the new time level *k* are solved from the following discretized equation derived by the Gaussian integration of the above equation over a polygon:

$$\frac{m_0 C^k + m_1 C^{k-1} + m_2 C^{k-2}}{\Delta t} \forall + \sum_f \left(V_f^k A\right) C_f^k = \sum_f \left(\sigma_f^k A \nabla C^k \cdot \vec{n}\right) + S_C^{*k} \forall$$

In the above, Δt is time step, C^k is the variable value at time level *k*, $V_f^k = \left(\vec{V} \cdot \vec{n}\right)_f$ is velocity component normal to the cell face which satisfies the mass conservation, A is cell face area, $\forall$ is cell volume, C_f^k is the face value of the dependent variable, $\vec{n}$ is the cell face unit normal vector, and σ_f^k is eddy viscosity at the cell face. Summation *f* is over all cell faces of a mesh cell.

The time derivative term has three parameters which determine the time discretization scheme applied. For example, $(m_0, m_1, m_2) = (1, -1, 0)$ corresponds to the first-order Euler scheme; and $(m_0, m_1, m_2) = (1.5, -2, 0.5)$ is the second-order backward differencing scheme. Note that all main variables are at time level *k* in (8) so that the implicit scheme is utilized to achieve model stability and robustness.

Detailed expressions for the discretized convective and diffusive terms in (8) were reported in Lai et al. (2003a). It is sufficient here to list the final discretized governing equation at a mesh cell (say, P); the equation is derived by linearization of the above equation and expressed in a linear equation form concisely as:

$$A_P C_P = \sum_{nb} A_{nb} C_{nb} + S_C$$

In the above, C_P and C_{nb} are values of *C* at cell *P* and "*nb"*, respectively, A_P and A_{nb} are the diagonal and off-diagonal matrix coefficients, respectively, and summation over "*nb*" refers to all neighboring cells connected to the nodes of cell *P*. For each discretized equation, the conjugate gradient squared (CGS) solver is used as the linear equation solver.

The pressure-correction scheme for the collocated cell-centered method is modified from Lat et al. (2003a) so that some terms are treated more accurately. First, a special procedure is adopted to compute the cell face normal velocity that is used to enforce mass conservation. Without a proper treatment, the well-known checkerboard instability, related to the velocity and pressure decoupling, may occur (Patankar 1980). In this study, the velocity-pressure coupling procedure is modified from the approach of Rhie and Chow (1983).

That is, the cell face velocity is computed by averaging the momentum equation from the two cells to the cell face, leading to the following expression:

$$V_f = \langle \vec{V} \rangle \cdot \overrightarrow{n_f} - \langle \frac{\forall}{A_P} \rangle (\nabla P)_f \cdot \overrightarrow{n_f} + \langle \frac{\forall}{A_P} \nabla P \rangle \cdot \overrightarrow{n_f}$$

In the above, "< >" is the averaging operator from two cell centers to cell face, and the time level index is dropped for notation simplification. When the averaging operator is applied to a vector, it implies application to each Cartesian component of the vector. In this study, the averaging is performed using a second-order method. The above equation shows that the mass-conserving face velocity is composed of two terms: a velocity term based on the arithmetic linear averaging, plus a correction term in the form of a 4th-order pressure damping. The pressure damping term serves to remove the spurious checkerboard instability and provides the velocity-pressure coupling.

The adopted version of the pressure-correction method is to derive the pressure-correction equation representing the mass conservation using the discretized equations. Three algorithms are available for the derivation: SIMPLE and SIMPLEC (Patankar 1980). They were originally developed for use with the staggered mesh models. In this study, SIMPLEC algorithm is adapted for the unstructured and collocated model and described below.

With a known pressure field P^o at time zero, a new velocity field may be predicted by solving the following discretized momentum equation (starred superscript denotes provisional predicted values at the new time):

$$A_P \vec{V}_P^* = H\left(\vec{V}_{nb}^*\right) - \forall \nabla P^0 + \vec{S}_V^0$$

where H stands for the linear operator $H(X) = \sum_{nb} A_{nb} X_{nb}$ and the pressure gradient term is separated out from the source term. The new predicted face velocity is then computed as:

$$V_f^* = \langle \overrightarrow{V^*} \rangle \cdot \overrightarrow{n_f} - \langle \frac{\forall}{A_P} \rangle (\nabla P^0)_f \cdot \overrightarrow{n_f} + \langle \frac{\forall}{A_P} \nabla P^0 \rangle \cdot \overrightarrow{n_f}$$

Next, a corrector step is performed to compute the new pressure and velocity fields P^* and $\vec{V}_P^{**}$ such that both the continuity and momentum equations are satisfied; that is:

$$\nabla \cdot \vec{V}_P^{**} = 0$$

$$A_P \vec{V}_P^{**} = H\left(\vec{V}_{nb}^*\right) - \forall \nabla P^* + \vec{S}_V^0$$

Substitution of the incremental momentum equation into the continuity equation and application of the SIMPLEC algorithm led to the following pressure correction equation:

$$\nabla \cdot \left(\frac{\forall}{A_p - \sum_{nb} A_{nb}} \nabla P' \right) = \nabla \cdot \vec{V}^*$$

In the above, $P' = P^* - P^0$ is the pressure correction and the pressure is the Poisson equation.

For an unstructured mixed polyhedral mesh, the data structure is important. In the model development, three whole-mesh operations are implemented. The most frequently used operation is a loop over all cells as the solver is cell centroid based. All main variables are stored at cells and the linear equation solver is cell based, so cell operation represents a major portion of the computing time. In addition, connectivity integer arrays are used to address mesh relations from a cell to its faces and neighboring cells. The second data structure is face based and created to compute the convective and diffusive fluxes. The face-based data structure requires the creation of connectivity arrays that specify the linkage from a face to its neighboring cells. The final and third is the node-based data structure which provides information from a mesh node to its neighboring cells. The nodal data structure is used to compute nodal values from known centroid vales of a variable as well as the non-orthogonal diffusion term.

All governing equations are solved in a sequential manner. First, the momentum equations are solved given the known pressure and turbulence viscosity. Such predicted velocity is used to compute the mass conservation term. The corrector step is applied by solving the pressure correction equation. A corrected velocity and pressure are thus obtained. Finally, scalar equations such as the turbulence model equations are solved using the corrected velocity. This completes one iteration of the solution cycle. Normally, a number of iterations are performed within a time step for an unsteady flow simulation. For steady flows, iterations are performed until a preset error or residual criterion is met. The residual of a governing equation is defined as the sum of the absolution errors over all mesh cells.

3.2. Eulerian Fish Track Model

As reviewed in chapter 2, several fish track models have been developed in the past, ranging from simple passive to complex perception-and-response models. In this study, we focus on the development and use of two fish track models: any Eulerian model and a Lagrangian particle track model, in addition to the use of USACE's ELAM model. Both Reclamation models are simple to operate and capable of answering some important fish entrainment study questions.

The Eulerian track model is described first below, which makes the following assumptions:

1. Fish distribution function (FDF) – FDF is used to represent the number of fish per unit volume and is assumed appropriate to represent fish distributions in a stream; FDF may be interpreted as the probability of a fish found at a point in the stream.

2. FDF is assumed a continuous function in space and time that is transported by the flowing water.

The above assumptions mean that the Eulerian model takes into accounts primarily the effects of water velocity and non-uniform fish distribution on fish movement – or a fish population is treated as passive particles transported by flows, without the fish perception-and-response features.

Note that the passive transport model is deemed valid if stream flow velocity is above the fish swim capacity or the cruising speed (Blake and Horn 2004; Perry et al. 2010) and has been utilized by previous studies (e.g., Ramon et al. 2018). The swim speed capacity for juvenile Chinook salmon is about two body lengths per second according to Nelson et al. (1994) although it may vary among species. For stream flows slower than the capacity or when fish perception-and-response is strong, the absolute entrainment rate computed by the model may not be accurate. Even under such circumstances, the relative comparative result is still regarded representative as far as fish indeed respond to flow velocities in the stream (Ramon et al. 2018). A passive track model is considered representing, to the first order, the movement behavior of salmon juveniles.

It is also noted that typical burst swimming speeds of smolts is about 10 body lengths per second (Goodwin et al. 2006). If flow velocity is larger than this, swimming speeds required not to follow the flow would be physically unattainable (Perry et al. 2014). So, the burst speed may be an upper limit of the validity of the passive model.

With the above assumptions, the transport equation of FDF may be written as:

$$\frac{\partial F_d}{\partial t} + \frac{\partial \left(U_j F_d\right)}{\partial x_j} = 0$$

where F_d is the fish distribution function in the number of fish per unit volume, t is time; x_j is j-th Cartesian coordinate; and U_j is mean velocity component along coordinate x_j. The equation states that FDF is advected by the flowing water, and the dispersion due to turbulence or other random features are ignored. Note that the diffusion term may be added to represent fish drift behavior in future, though not explored in this study. Horizontal and vertical diffusion coefficients may be distinguished. In addition, source terms may be added to take into accounts of secondary flows and fish tendency to stay away from high shear area like near a bank (not explored further in this study).

The numerical solution of F_d follows the same approach as described above for the flow model. Given an initial distribution at an upstream, say an inlet, location, unsteady transport of F_d may be numerical simulated in a stream, providing information on how fish may be entrained into the side channel of a junction given a particular location

3.3. Lagrangian Fish Track Model

A Lagrangian fish track model (LFTM) has also been developed in this study and is discussed below. Note that a general LFTM has been traditionally developed to simulate and understand the behavior of sediment particles in particle-laden flows, e.g. for understanding sediment transport patterns in river restoration and sedimentation studies. It has also been used to predict fish movement patterns, and, in some cases, to effectively visualize the flow field and movement of individual fluid particles.

LFTM development, however, is not trivial. Sophisticated particle track models have been developed in the literature to take into accounts of various interacting forces exerted on particles. These forces have created complex time scales. For example, Dutta (2017) developed a semi-implicit scheme to track sediment particles in order to address the disparate time scales.

In the present study, however, the Lagrangian track model is based on the assumption that fish are passive in movement; that is, fish are transported by the flowing water only, without the fish perception-and-response features and complex time scales associated with particles. With the above assumptions, the Lagrangian fish track model is based on the following equations for the fish position:

$$\frac{dx_i}{dt} = v_i$$

where x_i is the particle position, v_i is the fish velocity, i is the i^{th} space coordinate (i = 1, 2, 3), and t is the time coordinate. It is assumed that there is no feedback of fish swim on the flow. The fish movement equation is solved using the first-order Euler time discretization. That is, the discretized form is expressed in vector form as:

$$\frac{d\tilde{\boldsymbol{x}}}{d\tilde{t}} = \tilde{\boldsymbol{v}}$$

$$\tilde{\boldsymbol{x}}^{\boldsymbol{n}} = [\tilde{\boldsymbol{x}}^{\boldsymbol{n-1}} + \Delta\tilde{t}\tilde{\boldsymbol{v}}^{\boldsymbol{n}}]$$

The complexity of developing a Lagrangian particle track model includes: (a) how to determine the fish velocity, (b) how to move particles through a space represented by a discrete set of points (called mesh); and (c) what to do when particles hit boundaries or move out of the model domain. They are described below.

3.4. USACE ELAM Model

ELAM is a state-of-the-art fish track model developed by USACE and the developer of ELAM is a partner of this research. ELAM has been initially documented by Goodwin (2006) and Goodwin et al. (2014).

For the most recent information of ELAM, refer to the documentation by Goodwin et al. (2023) in which the PI of this research, Dr. Lai, is a co-author. A summary description is provided below.

ELAM considers the fish perception-and-response features in addition to water flow and fish drift. It is based on the combined Eulerian and Lagrangian approach. Hydrodynamic information is from a CFD model and stored at discrete points in a Eulerian mesh. Individual fish movement is simulated in a Lagrangian framework allowing the generation of directional sensory inputs and movements in a reference framework like that perceived by real fish. A sensory oval is defined, and flow variables are interpolated to the fish location. Movement is treated as a two-step process: first, the fish evaluates agent attributes within the detection range of its sensory system and, second, it executes a response to an agent by moving. The volume from which a fish acquires decision-making information is represented as a sensory ovoid. A virtual fish's sense of direction at each time increment is based on its orientation at the beginning of the time increment. Directional sensory inputs are tracked relative to the horizontal orientation of the fish because fish response to laterally-located versus frontally-located stimuli can be different. The sensory ovoid has a vertical reference because fish detect accelerations and gravitation through the otolith of its inner ear. It also senses three-dimensional information on motion. Fish is assumed to respond to a number of flow variables, including flow strength (velocity) and direction, whole body acceleration, spatial velocity gradients, and pressure.

4.0 CFD Model Validation

In this chapter, the 3-D CFD model is validated using the available measured data at flow diversions and natural rivers. The validation studies are needed to lend credence to the flow model used for fish entrainment and rejection studies. SRH-2D has been well validated and documented (e.g., Lai 2008; 2010), so 2-D model validation is not reported herein.

4.1. Introduction

Flow structures at the junction of a diversion are complex as shown in Figure 3 and has been discussed by Neary and Odgaard (1993). Two secondary flows are usually generated due to the interaction between longitudinal pressure gradient, shear forces, and centrifugal forces. One clockwise secondary flow is formed along the right wall of the side channel and the other is the counterclockwise secondary flow along the left wall of the main channel. Further, a strong flow recirculation or flow separation usually occurs near the entrance on the left side of the side channel (zone A in Figure 3). There is also a potential flow separation zone on the left side of the main channel just downstream of the junction (zone B in Figure 3). These secondary flows and recirculation zones have an important impact on the decision of fish movement resulting in altered fish entrainment rate. That is, the relation between the fish entrainment rate versus the diverted flow rate is not linear.

The relative strengths of the secondary flows, recirculation zones, and turbulence are dictated by a number of flow factors such as the main channel flow velocity, flow diversion ratio, and local geometric features of the junction (e.g., side channel cross section shape and angle, width ratio). These flow characteristics are changing constantly in natural environment due to the unsteady flow nature. The computational model is probably the only alternative to studying these flow features and make informed decision for fish entrainment study.

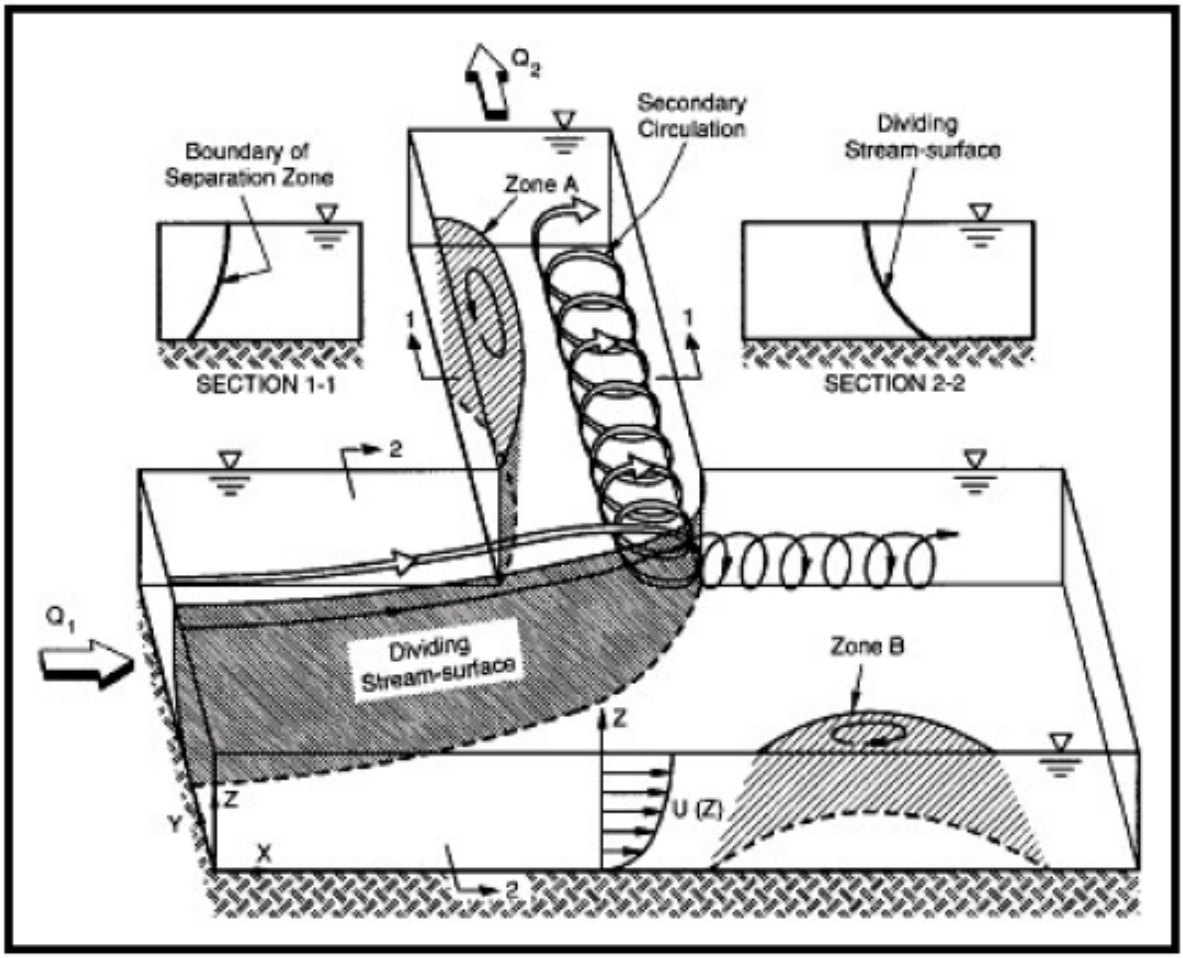

Figure 3.—Flow characteristics at a junction of the flow diversion (Neary and Odgaard, 1993).

Fish modeling at flow junctions has not been studied comprehensively. At a junction, a guidance system may be designed and used to attract migrating fish toward favorable locations or repel them from dangerous ones (Coutant 2001a; b). Physical barriers such as screens and louver systems are measures commonly used to prevent fish from entering irrigation diversions or turbine intakes (Odeh 1999; 2000). Although effective, these types of engineering solutions are costly and may also cause mortality when fish become impinged on these structures.

Non-physical, behavioral barriers are an attractive alternative to physical barriers because they can deter fish without injury and without altering water flow (Noatch and Suski, 2012). In this study, we focus on a diversion junction without the guidance systems.

When fish come to a flow diversion junction, there are three factors that may determine the fish entrainment rate. The first is the percentage of flow diverted into the side channel (called flow entrainment ratio in this report) into which passive fish would swim. The second is the fish distribution on a cross section upstream of the diversion. The third is the local flow structures and/or turbulence at the junction that might alter fish perception and response. All three have been reviewed in chapter 2.

It is noted that local flow structures at a junction would impact the fish swim decision; however, specific rules are still lacking in carrying out a reliable fish tracking modeling. We know that the flow is accelerated into the side channel due to the recirculation zone present at the corner of the left side channel; but the flow is decelerated along the main channel. If the experience of fish responses to flow acceleration is applicable, we expect that the acceleration factor alone may favor a higher percentage of fish rejected by the side channel if other factors are the same.

4.2. Flow Diversion at a 90-degree Juncture

Background

Early studies of such flow junctures are primarily of experimental or analytical nature. Taylor (1944) was one of the first to conduct a detailed experiment. Using the results, a graphical solution was proposed. Grace and Priest (1958) reported experimental results of flow division with varying channel width ratio and side channel angle. Two flow regimes were identified: with and without the standing waves near the side channel entrance. The two were distinguished primarily by the Froude number. Analytical methods were developed by, e.g., Tanaka (957), Murota (1958), Law and Reynolds (1966), Hager (1984), using simplifying assumptions.

More extensive laboratory investigations have been carried out since early studies. For example, Neary and Odgaard (1993) focused on 3-D flow structures at the juncture and detailed velocity-vector and particle-trace plots were reported in the separation zone.

Ramamurthy et al. (2007) reported an experimental study focusing on the measurement of 3-D mean velocity components and water surface profiles in a 90°, sharp-edged, rectangular open-channel junction formed by channels of equal width.

Gohari (2012) reported an experimental study to examine the flow separation line at the junction entrance and how it is related the sediment movement. In particular, the effect of spur dike structures and vanes was examined to alter the flow separation line to control the sediment entrance into the side channel. Results demonstrated that vanes could alter the local flow separation due to the creation of a counter-balancing secondary flow.

Numerical models have also been developed or applied to study the flow characteristics at the flow juncture. Early numerical modeling was limited to two-dimensional (e.g., Liepsch et al. 1982, Shettar and Murthy1996, Vasquez 2005), or laminar flows (e.g., Neary and Sotiropoulos 1996).

Issa and Oliveira (1994) are among the first to investigate the flow characteristics at a junction using a 3-D turbulent flow model. Similarly, Neary et al. (1999) reported the use of a 3-D Reynolds-Averaged-Navier-Stokes (RANS) to study flow phenomena at a flow juncture. Heer and Mosselman (2004) used 3-D model and simulated Bulle experiment. Ramamurthy et al. (2007) developed a 3-D RANS model to simulate the diversion flow they measured and reported good results. Babagoli Sefidkoohi et al. (2017) reported the numerical results of the flow patterns at the diversion junction using the commercial CFD model FLOW-3D. Flow separation zone was investigated at the entrance of a 90-degree junction with various flow depth, diversion ratio and turbulence models. It was found that the Reynolds Normal Group model (RNG) performed the best.

Case Description

The experimental case of Ramamurthy et al. (2007) is selected for the CFD model validation in this study to show that the 3-D RANS model used in this research has the capability to reproduce the observed flow characteristics at a flow diversion juncture.

The model domain is show in Figure 4. Both the main and side channels have the rectangular cross sections with a width (b) of 0.61 m and height (H) of 0.305 m. The upstream section of the main channel is 6.1 m (10B), while the downstream section of the main channel and the side channel is 2.44 m (4B).

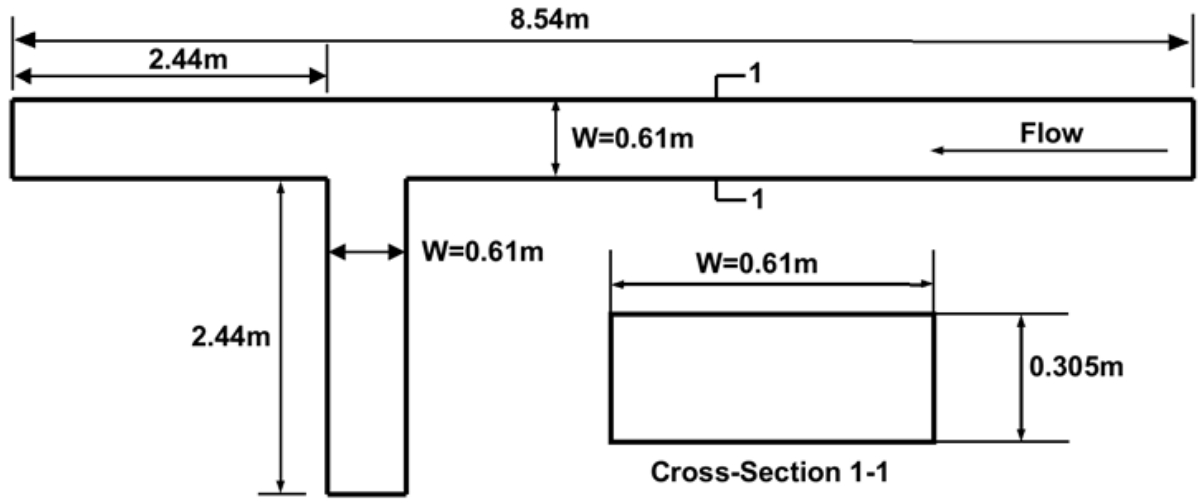

Figure 4.—Model domain and geometric dimensions of the diversion flow case of Ramamurthy et al. (2007).

The baseline model of the present study uses the same domain as shown in Figure 4 with a 3-D mesh shown in Figure 5. The mesh has a total of 576,000 mesh cells, with 30 cells uniformly distributed in the vertical direction, and 19,200 cells in the horizontal plane distributed non-uniformly and clustered at the juncture area (40 cells across each channel). This mesh is similar but finer than the mesh adopted by Ramamurthy et al. (2007). A mesh sensitivity has been carried out in this study, one is to extend the model domain from (10W, 4W, 4W) to (15W, 8W, 8W) in terms of the channel length of the upstream main channel, downstream main channel, and side channel. The other is to refine the baseline model mesh described above to 1,728,000 cells. Results in predicted velocities do not deviate from the baseline by more than a few percentages.

The flow conditions follow an experiment run in which the total discharge in the main channel is 0.046 m^3/s and the side channel flow is 0.038 m^3/s. The ratio of the side channel to main channel flows is 0.838. This represented the most severe diversion case with 83.8% of the total flow is diverted into the side channel. Both flow discharges are imposed as the inlet and outlet boundary conditions. At the outlet of the main channel, the known water elevation is imposed. In the simulation, the free surface is not flat and determined based on the depth-averaged governing equations. It is found that the use of a flat free surface condition produced similar solutions, so the use of free surface algorithm is not important.

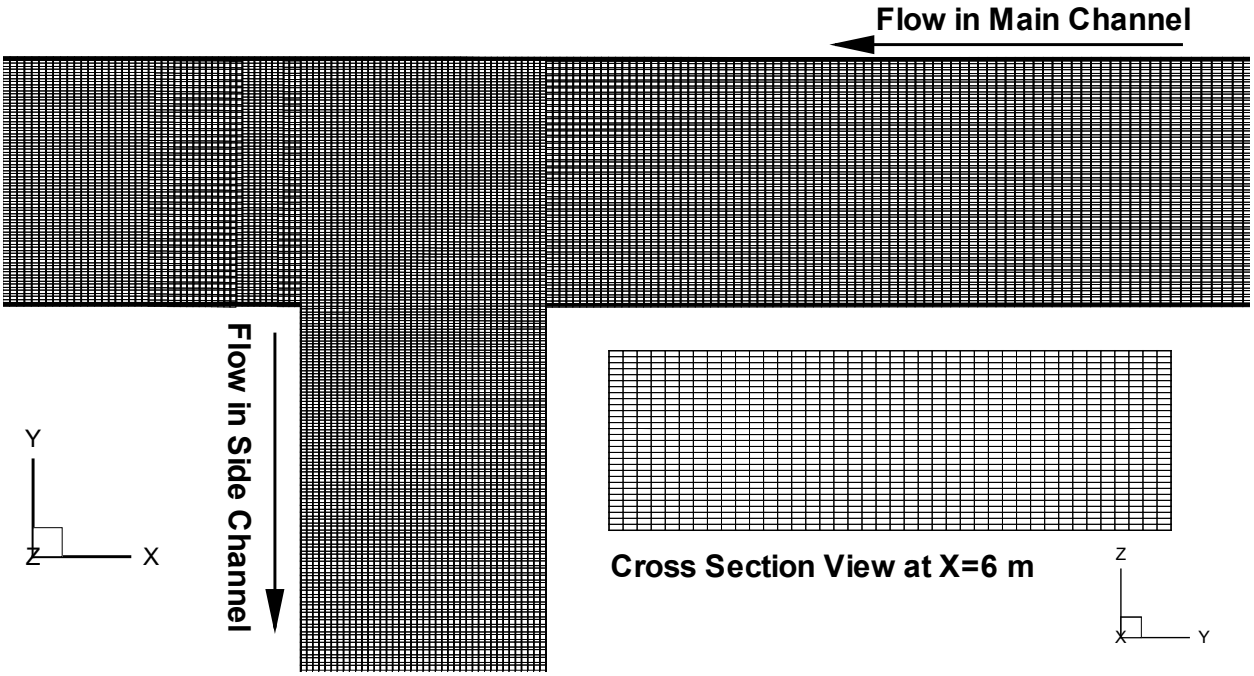

Figure 5.—Mesh of the baseline model: a zoom-in horizontal (xy) view and a cross section (yz) view of the mesh.

Comparison with Laboratory Data

The CFD results are compared with the laboratory data of Ramamurthy et al. (2007) to validate the model.

First, the CFD predicted free surface pressure distribution near the juncture is shown in Figure 6; the CFD predicted pressure is equivalent to the water surface elevation distribution as the two are linearly correlated. It is seen that the water surface level in the side channel is lower than that in the main channel. All major flow zones are predicted. The stagnation zone has the highest pressure (elevation) with a steep gradient, in agreement with the experiment observation. The lowest pressure is located within the separation zone in the side channel, which is the driver for creating the flow reversal on the left side of the side channel near the entrance. The large lateral pressure difference across the side channel width and the large pressure gradient towards the side channel in the entrance zone are the result of flow diversion into the side channel. The CFD predicted and the measured water surface elevation are further compared in Figure 7 along three longitudinal lines (y direction) within the side channel, as it is inside the side channel that the water elevation (pressure) changes the most. It is seen that the agreement is good.

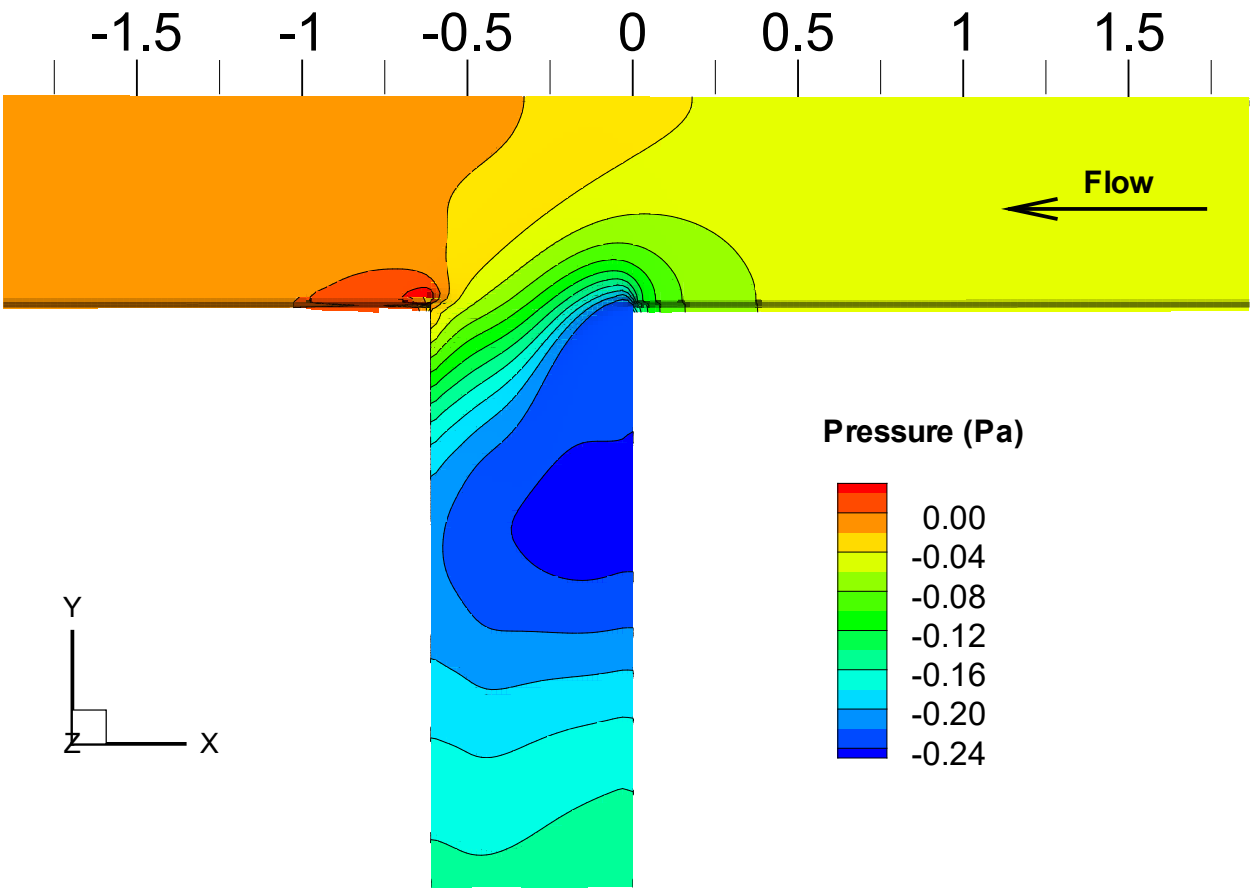

Figure 6.—CFD simulated surface water pressure (equivalent to water surface elevation) distribution at the free surface near the juncture.

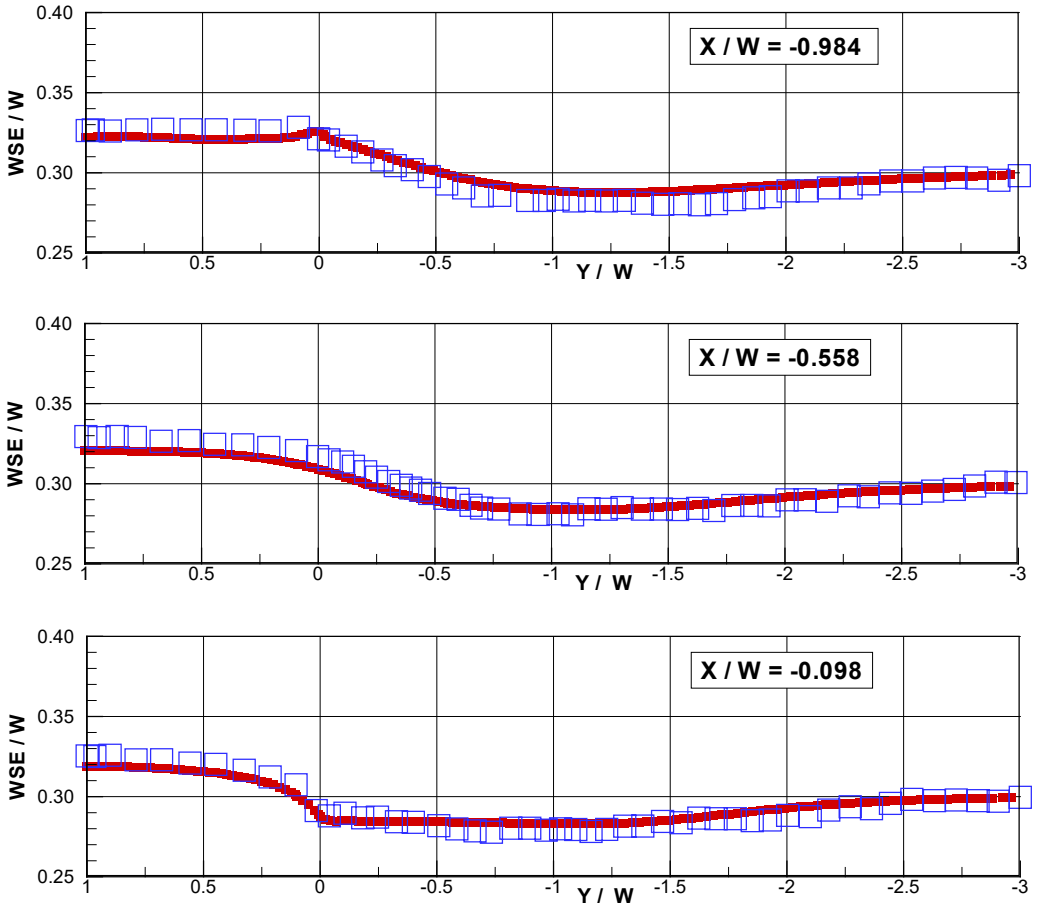

Figure 7.—Comparison of CFD predicted water surface elevation (WSE) and the measured data along three longitudinal lines in the side channel. The coordinates and water surface elevation are normalized by the channel width W.

Next, the flow velocity field is examined and compared. The contours of the velocity component in the y direction (v) are compared with the measured data at the z/W=0.27 plane (near the free surface) in Figure 8. The horizontal velocity vector on the same plane is compared in Figure 9. Both the CFD and experimental results show the existence of the separation zone in the side channel and the flow contraction zone between y/W= -1.0 and -2.0. Overall, model results agree with the measured data reasonably except that the model predicts a longer separation zone. The separation zone size mismatch may be attributed to several factors: (a) the short side channel length used by the experiment; (2) the highly unsteady nature of the recirculation zone; and (3) the turbulence model. The use of the RNG-based turbulence model did not improve the results (not reported herein). The results point to the existence of another separation zone in the main channel downstream of the juncture. The highest velocity occurs at the upstream corner of the juncture.

Further, Figure 10 shows the comparison of the v velocity contours between the CFD result and the measured data at the y/W=−1.0 cutting place within the side channel. On the same plane, the u-w velocity comparison is made in Figure 11 so that the secondary flow entering the side channel is compared (the view is for an observer looking toward the positive y direction). It is seen that a strong secondary flow is developed for the flow entering the side channel and the CFD model result replicates that observed in the experiment.

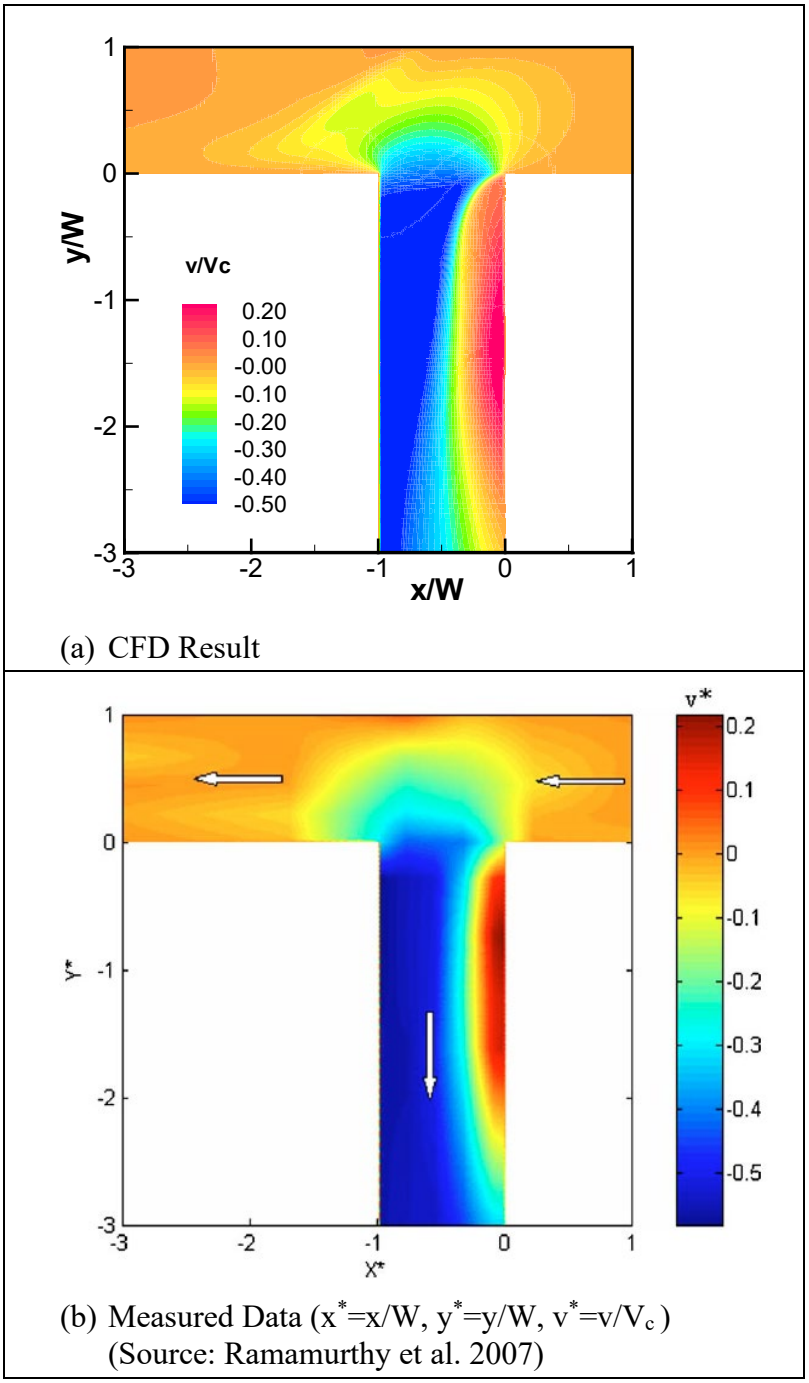

(a) CFD Result

(b) Measured Data ($x^*=x/W$, $y^*=y/W$, $v^*=v/V_c$)
(Source: Ramamurthy et al. 2007)

Figure 8.—Comparison of velocity component along y-axis (v) between CFD and measured data at a z/W = 0.27 horizontal plane.

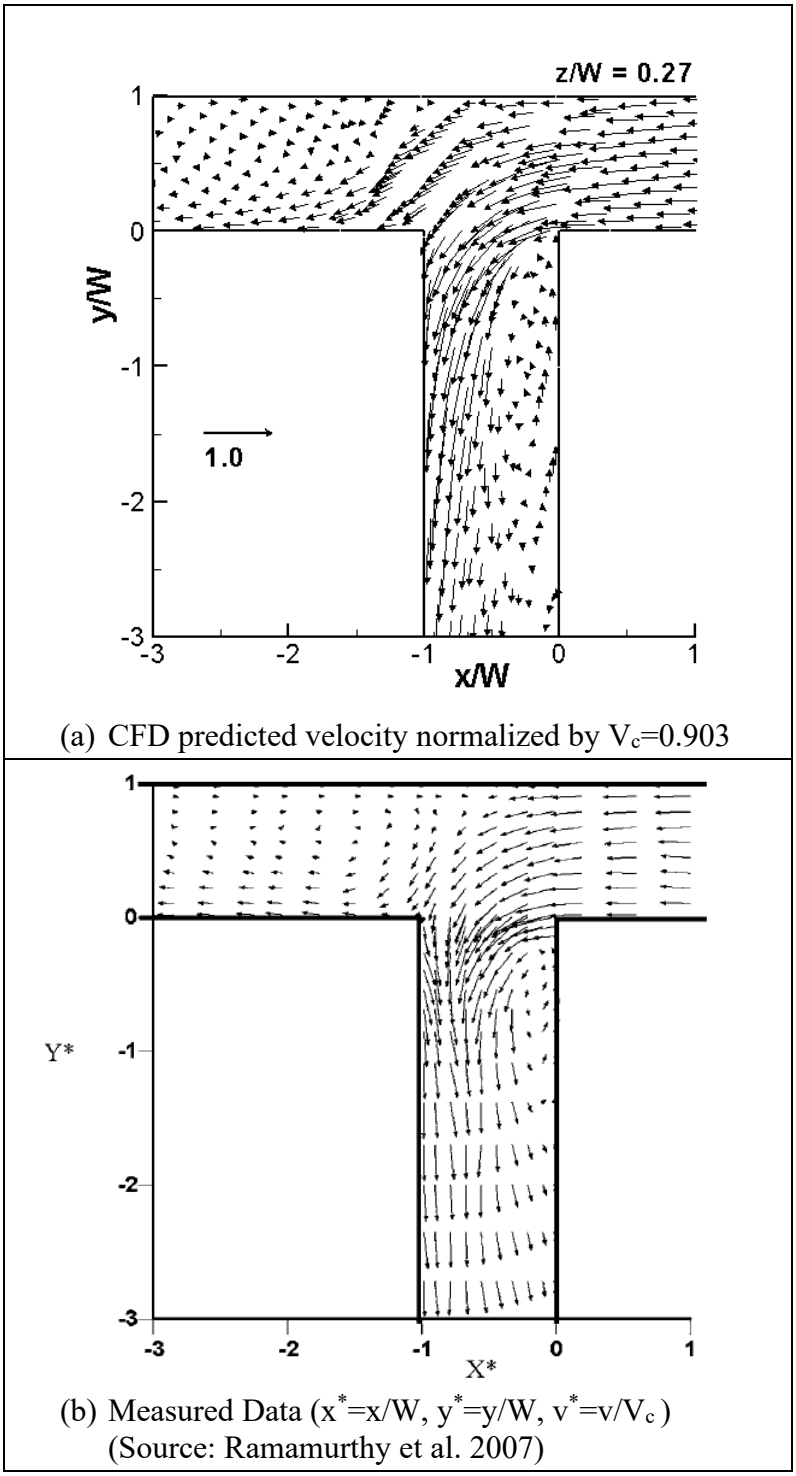

(a) CFD predicted velocity normalized by V_c=0.903

(b) Measured Data (x^*=x/W, y^*=y/W, v^*=v/V_c)
(Source: Ramamurthy et al. 2007)

Figure 9.—Comparison of horizontal velocity vector between CFD and measured data at the z/W = 0.27 horizontal plane.

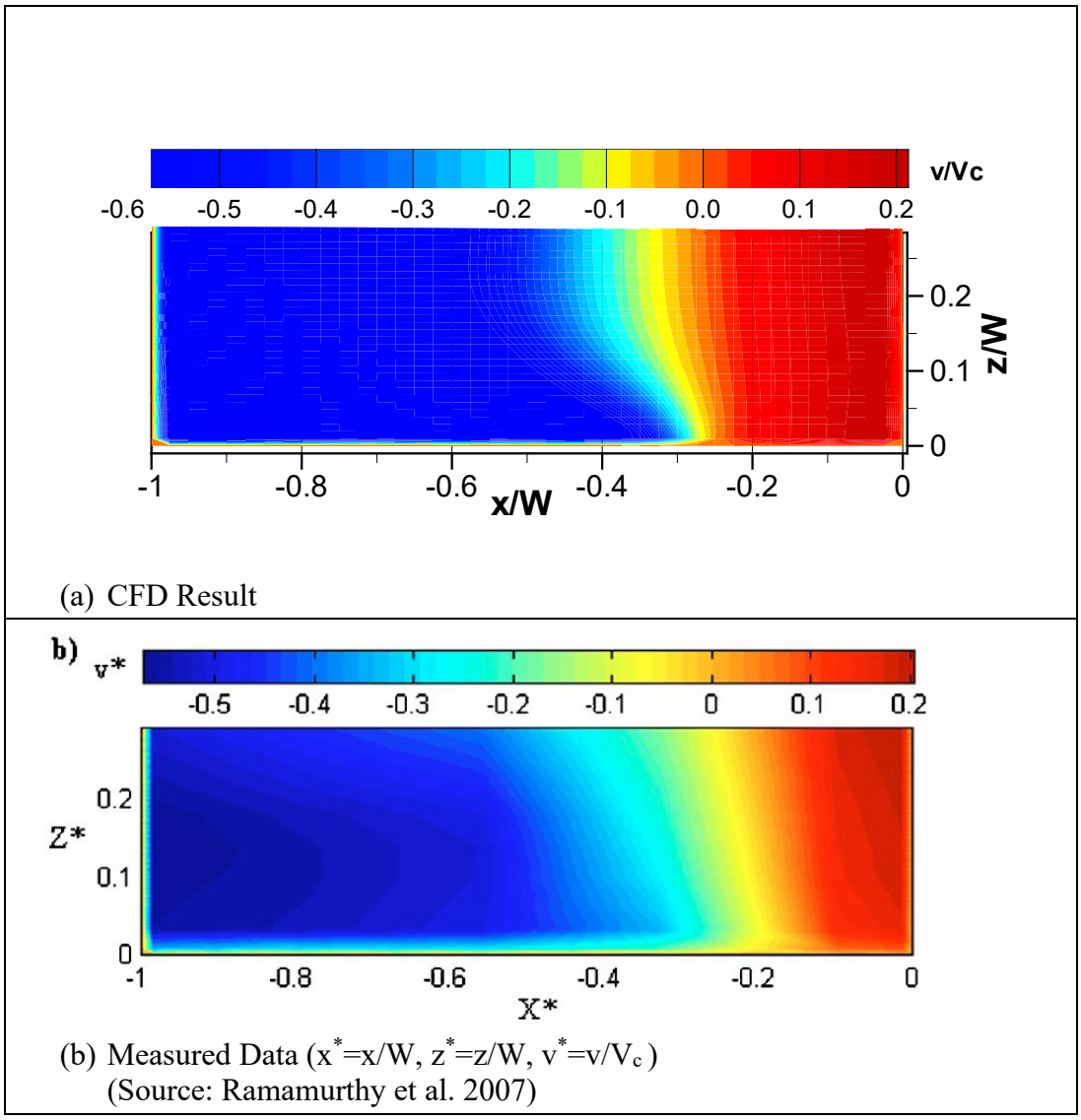

Figure 10.—Comparison of v velocity component between CFD and measured data at a y/W = -1.0 within the side channel (looking at the positive y-axis or upstream direction).

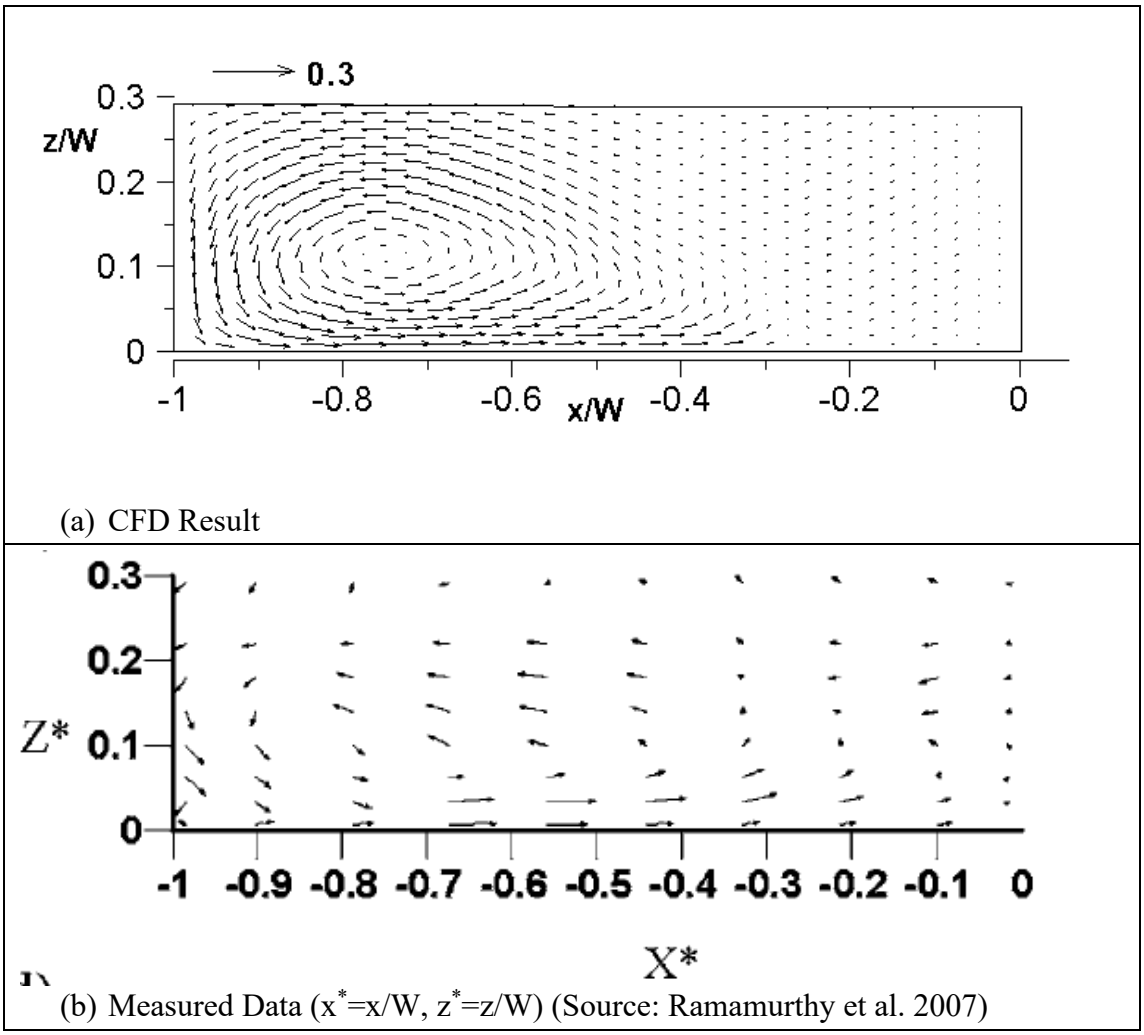

(a) CFD Result

(b) Measured Data (x^*=x/W, z^*=z/W) (Source: Ramamurthy et al. 2007)

Figure 11.—Comparison of u-w velocity vector between CFD and measured data at a y/W = -1.0 in the side channel (looking at the positive y-axis or upstream direction). U and w velocity components are normalized by Vc=0.903 m/s.

Finally, a detailed velocity profile comparison is made. Figure 12 shows the comparison of the vertical distribution of the v-velocity component at a number of horizontal (x y) points in the side channel. Note that the modelling study was also reported by Qu (2005) whose results are also plotted as a comparison. Overall, comparison is good at some locations while discrepancy is noticeable at others. Figure 13 compares the predicted and measured vertical distribution of u velocity in the main channel at selected horizontal points. The agreement is reasonable overall.

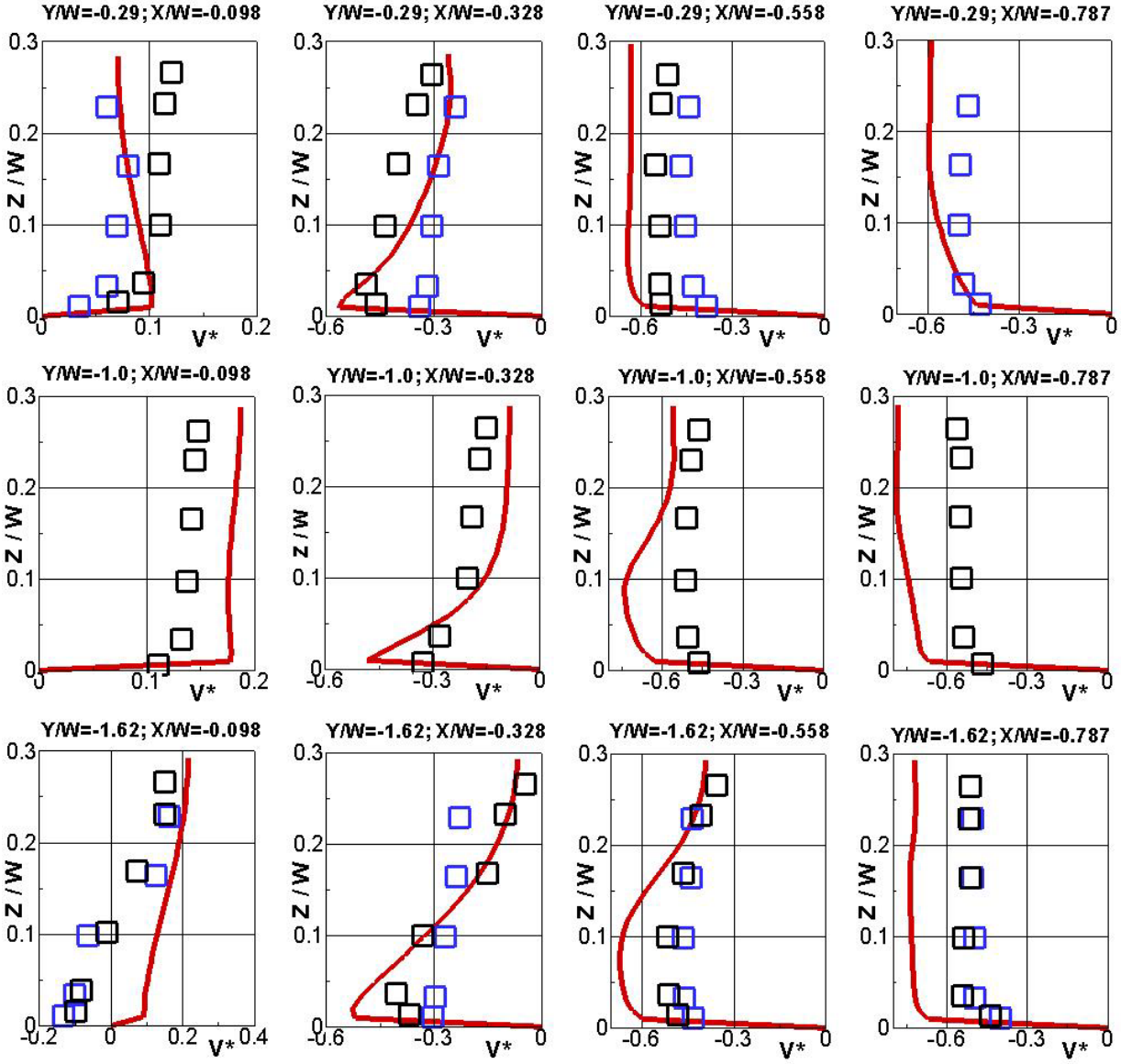

Figure 12.—Comparisons of v velocity vertical profiles in the side channel between CFD and measured data at selected x and y points. Black symbols are from Ramamurthy et al. (2007) while blue symbols are from Qu (2005).

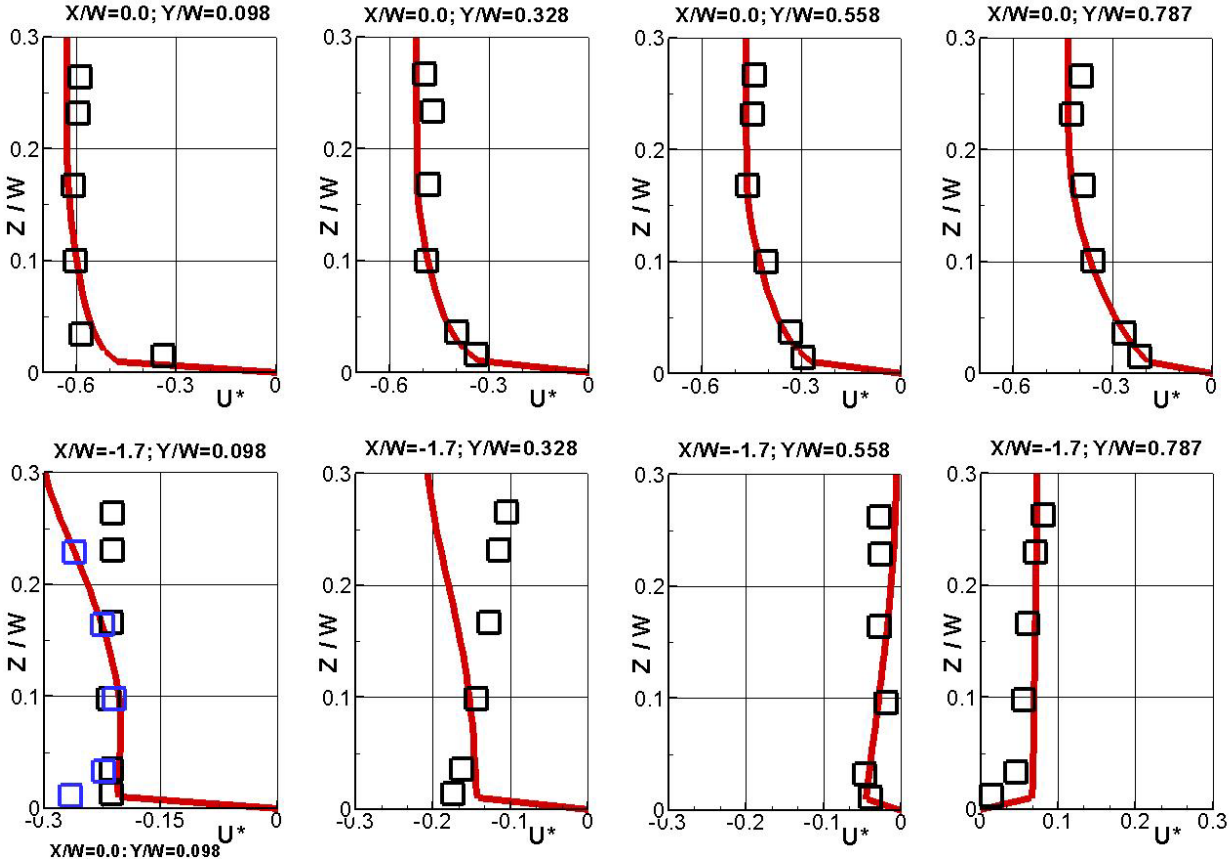

Figure 13.—Comparisons of u velocity vertical profiles in the main channel between CFD and measured data at selected x and y points. Black symbols are from Ramamurthy et al. (2007) while blue symbols are from Qu (2005).

Discussion of Flow Characteristics

Flow characteristics at the 90^0 junction is discussed, now that the numerical model is validated. Figure 14 and Figure 15 show the velocity characteristics on two horizontal planes: one is near the bed (z/W=0.04) and the other is near the free surface (z/W=0.27). Distinct features in the flow patterns include the following:

1. The dividing streamline in the main channel changes drastically over the water depth – the line moves toward the right bank of the main channel with increasing depth. This suggests more flow is entrained into the side channel with decreased depth.
2. The CFD model predicts the existence of the two separation zones, one in the side channel near the juncture and the other in the main channel downstream of the juncture. The side-channel flow reversal is much stronger than the main channel. In the side channel, the recirculation zone is larger near the free surface than that near the bed.

3. Near the bed, streamlines are observed to emanate from the stagnation zone into both the side and main channels. It points to a strong downward fluid flow, from free surface towards the bed, which is set up by the two counter rotating vortices.
4. It is apparent that the flow near the bed is predominantly into the side channel, implying that majority of the bedload sediment, if not all, would move into the side channel. This is consistent with the Bulle Effect with which more than 90% the bedload was found to move into the side channel although only about 50% of the flow was entrained (Bulle1926).

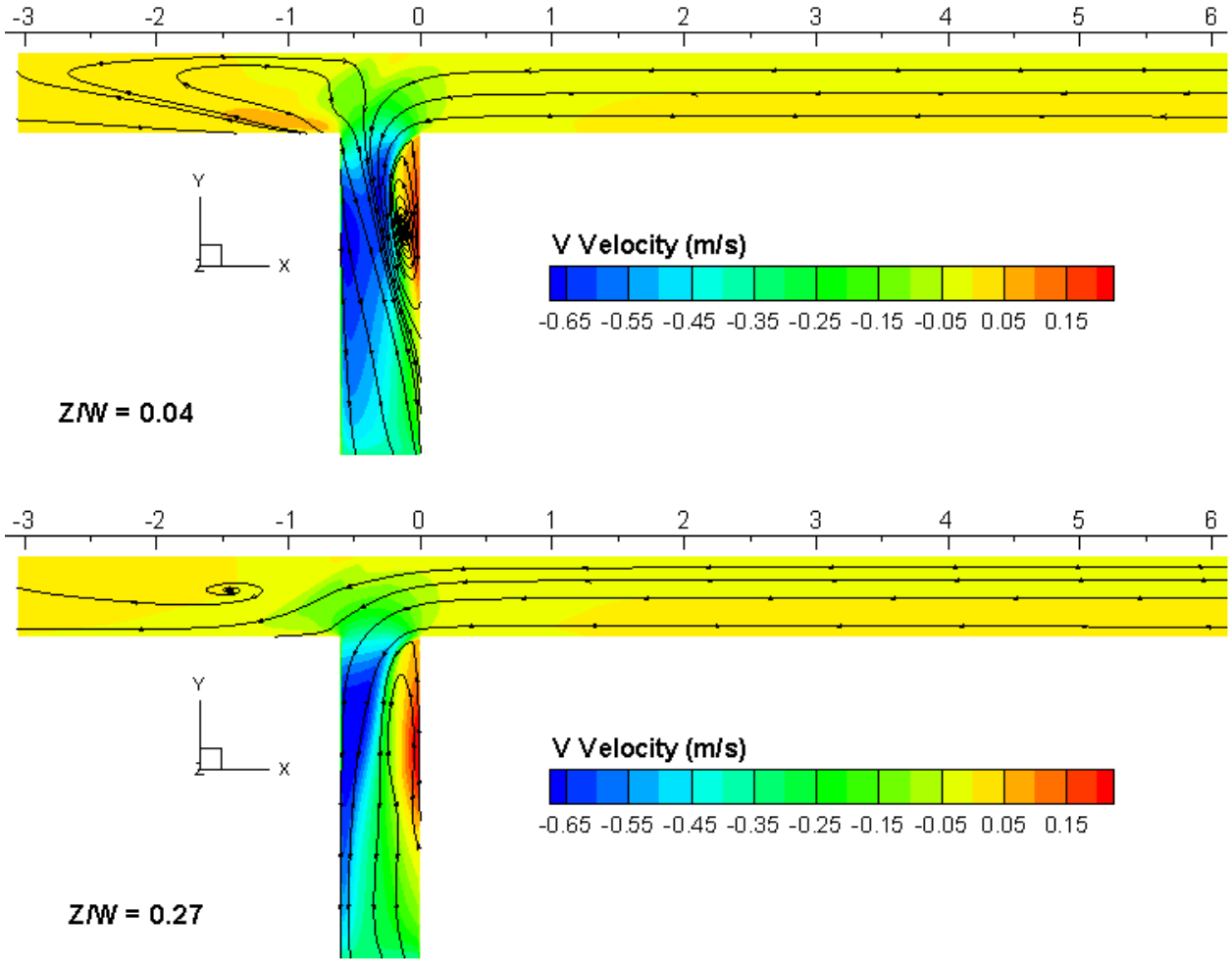

Figure 14.—Simulated V velocity component contours at two vertical cutting planes. The top is near the bed while the bottom is near the free surface.

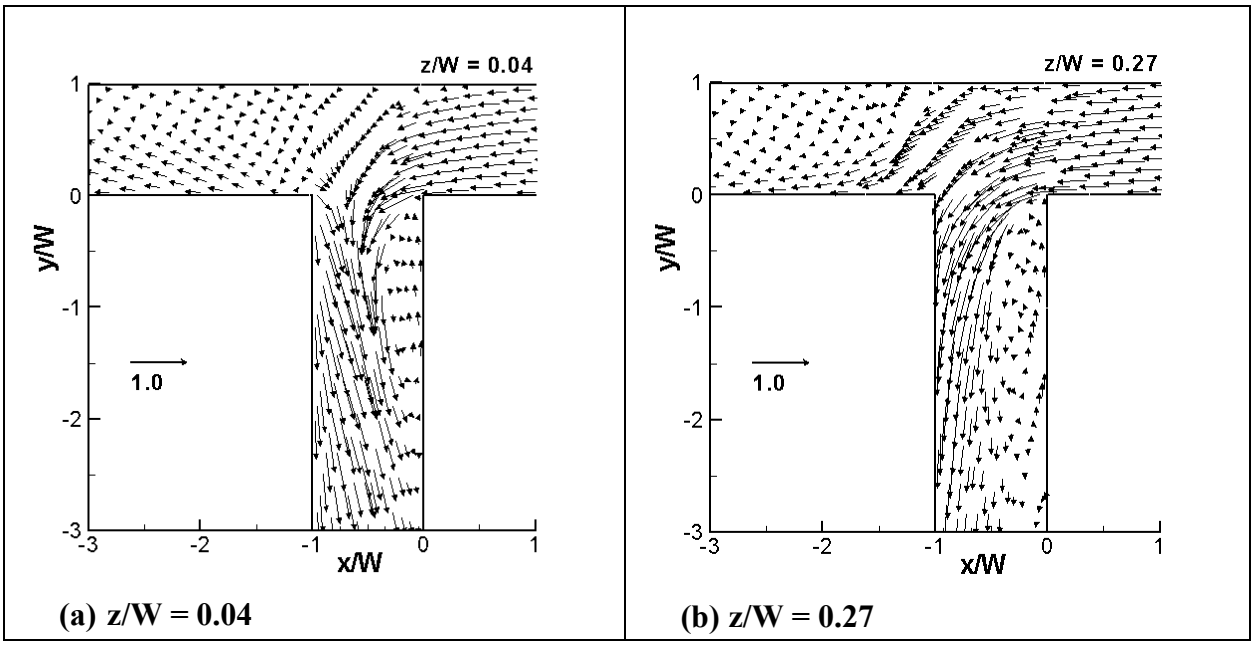

Figure 15.—Velocity vector comparison at two horizontal cutting planes: (a) near the bed at z/W=0.04; (b) near the free surface at z/W=0.27.

4.3. A Flow Diversion Field Case

The 3-D CFD model has also been applied to simulate the flow hydrodynamics along a reach of the Sacramento River along the Fremont Weir section – the objective is verify that the CFD model is also applicable to simulate complex natural rivers.

Background

Increased inundation within the Yolo Bypass is deemed necessary to improve rearing habitat for listed juvenile salmonids. It is being achieved by constructing a notch in the vicinity of Fremont Weir on the Sacramento River. A critical component of the notch is the approach channel that will be necessary to direct fish from the Sacramento River to the notch and the Yolo Bypass. The project success hinges on a better understanding of how juvenile salmonids are distributed across the river section when local river bathymetry and terrain are complex. Field telemetry fish tracking, flow modeling, and ELAM fish track modelling can be used conjunctively to gain the fish entrainment knowledge at the project site. Complex flow hydrodynamics is the necessary input to any fish track models; such results can also inform agencies to choose an appropriate location, as well a design, that is likely to achieve best entrainment into the bypass.

Both SRH-2D and 3-D CFD simulations have been carried out along the Fremont Weir section of the Sacramento River. However, various questions are raised in carrying out 2-D and 3-D flow modeling of practical rivers: e.g., the appropriate domain size and mesh resolution, and the accuracy of the model. In the following, the results obtained, and experience gained in applying

both 2-D and 3-D flow models are documented at the Fremont Weir section of the Sacramento River. The results shed light on the differences of two 2-D models, the ability of 2-D models in predicting velocity field in rivers with sharp bends, the difference of 2-D and 3-D models, and the model performance in comparison with the field data.

Model Results

Two model domains are developed for the study: low-resolution and high-resolution. They are shown in Figure 16.

The low-resolution domain covers about 115 km (69 miles) of the Sacramento River (Figure 16a). It starts at Freeport (river mile 47.6) at the downstream and ends at Wilkins Slough (river mile 117) at the upstream. The low-resolution model covers the river section through the city of Sacramento, along the Fremont Weir, past Knights Landing, and towards Wilkin Slough just downstream of the Tisdale Weir; it includes several tributaries: the Feather River and the American River. Laterally, the model domain covers both the main channel and the overbank area between the levees.

The high-resolution domain is a small subsection of the low-resolution model and has about 18 km (10.8 miles) in river length as shown in Figure 16b. It starts from Knight Landing at the upstream and ends at Verona station at the downstream.

(a) Low Resolution Domain

(b) High Resolution Domain

Figure 16.—Numerical model domains; map (a) is adapted from Dynamics Solutions (2011).

Low-Resolution Model Results

SRH-2D is used for the simulation with a low-resolution mesh. The study used the same model domain and the triangular mesh as that by Dynamic Solutions (2011) and Hammack et al. (2013a). The 2-D mesh was generated using the Surface-water Modeling System (SMS) software as detailed by the two previous studies. The 2-D mesh consisted of a total of 64,577 purely triangular cells. The bathymetry and terrain data were collected between 1997 and 2000. Changes of the Sacramento River in planform and bed elevation were relatively small, so the model was deemed adequate in simulating flows in future years. The selection of the domain was such that all open boundaries were located at or near gauge stations so recorded data are available as boundary conditions.

Two simulations are carried out: the period of December 8, 2010 - March 1, 2011 and the period of December 1, 2014 - March 31, 2015. The first is a repeat of the Hammack et al. (2013a) study. This simulation allows us to compare SRH-2D with ADH obtained by Hammack et al (2013a). The second simulation serves two purposes: model verification and boundary condition setup for the fine-resolution model.

The Manning's coefficient (n) is a key model input and the primary calibration parameter for SRH-2D. The model domain was partitioned into 18 zones and the Manning's coefficient in each zone was then calibrated using the discharge and stage at several gauges. In this study, the same 18-zone partition of the ADH model is used; but the Manning's coefficient is determined through a separate calibration. Initially, the calibration starts with the Manning's coefficients of Hammack et al. (2013a). Several model runs are then performed using the same percentage of increase or reduction in all zones. The final calibrated Manning's roughness coefficients used by SRH-2D are 10% higher than those used by ADH. The higher Manning's coefficients are due to the differences of the two 2-D models in applying the turbulent viscosities, numerical discretization, integration algorithms, etc.

There are a total of eight open boundaries – seven discharge boundaries and one stage boundary (see Figure 16a. The discharge and stage data are obtained mostly from nearby gauge records but a few are estimated. Hourly discharge hydrographs at seven open boundaries used are shown in Figure 17 and the stage at the downstream boundary is in Figure 18 for both simulation periods. They are used as the boundary conditions to the model.

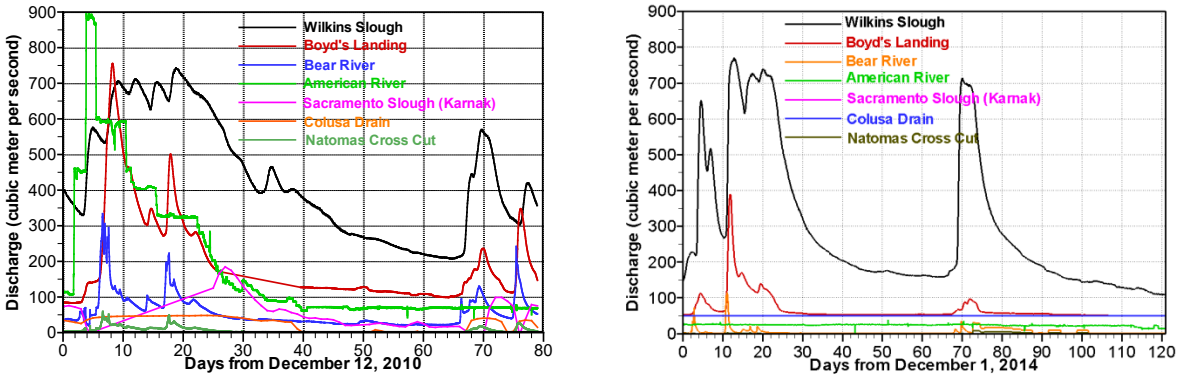

(a) December 2010 – March 2011 (b) December 2014 – March 2015

Figure 17.—Flow hydrographs at seven inflow boundaries of the model.

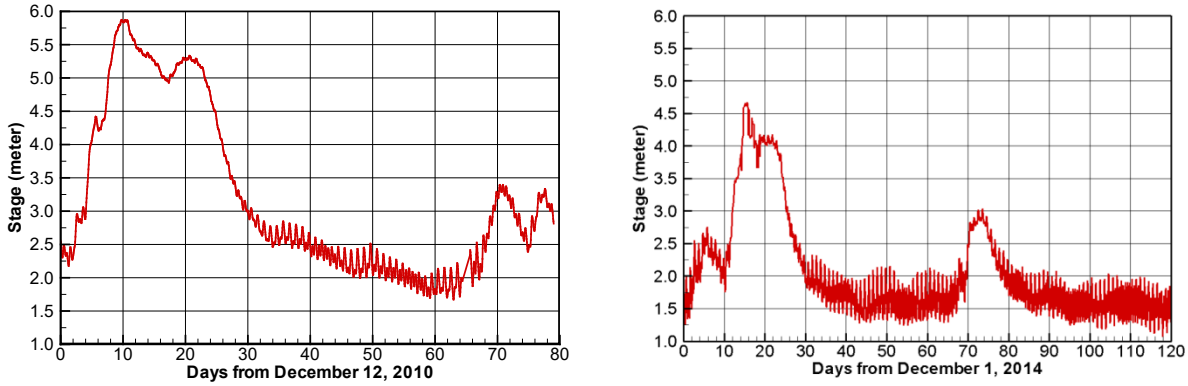

(a) December 2010 – March 2011 (b) December 2014 – March 2015

Figure 18.—Stage recorded at Freeport, the most downstream of the model.

For the 2010-2011 period, model predicted stages are compared with gauge data in Figure 19; predicted discharges are compared in Figure 20. The model results compare well with the recorded river stages and discharges most of the time except for high flows. At the highest flow stage, the models underpredict the stage by up to 1.5 m and discharge by up to 280 cms. The large discrepancy at high flow is attributed to either the high uncertainty of the discharge data or to unaccounted in- and out-flows through the model domain. The latter is more probable.

It is shown that SRH-2D model results match very well with ADH results of Hammack et al. (2013a) study (so the two curves collapse into almost one in the plots). This is important since both models claimed to have been well verified and have been used widely for numerous project applications. SRH-2D and ADH solve the same governing partial differential equations (PDEs)

but use quite different numerical discretization schemes and solution algorithms. The comparison offers an additional test case verifying that both models meet the "consistency" criterion that their discretized equations recover to the PDEs they intend to solve.

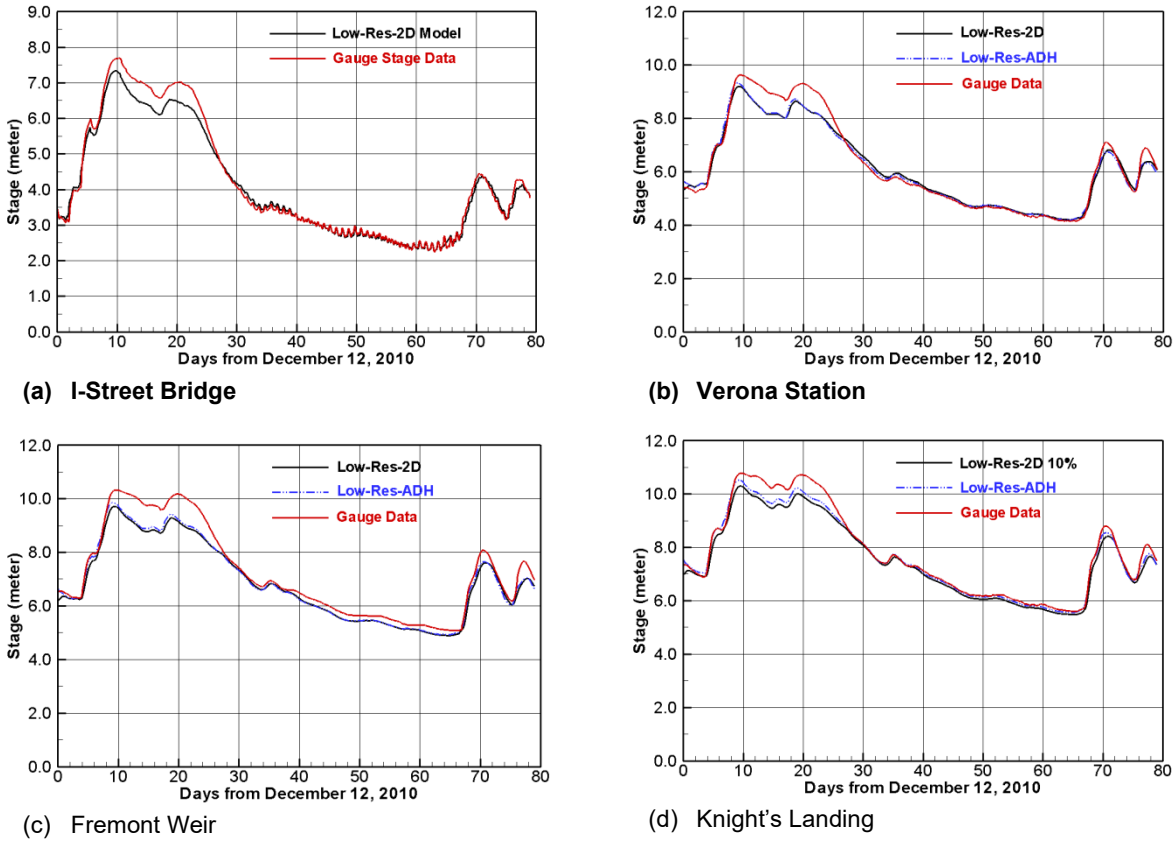

Figure 19.—Comparison of simulated and recorded stage at four gauge stations between December 12, 2010 and March 1, 2011.

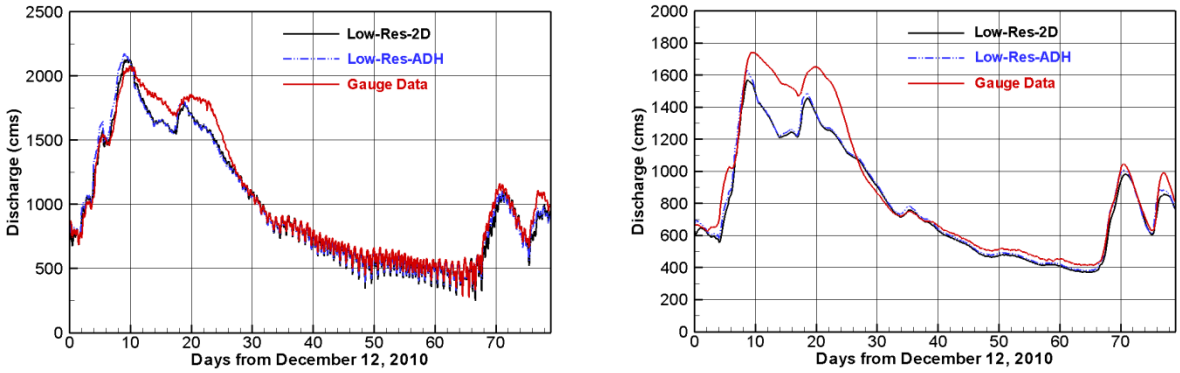

Figure 20.—Comparison of simulated and recorded discharges at two gauge stations between December 12, 2010 and March 1, 2011.

2-D model predicted depth-averaged velocities are compared with the ADCP data collected between January 31 and February 2, 2011, at 42 transects between river miles (RM) 80 and 87. A total of 634 depth-averaged velocity points, located on the 42 transects, were available for comparison. The depth-averaged velocity comparison is shown in Figure 21 for transects 5 to 24 including sharp bends. The SRH-2D predicted velocity is in general agreement with the ADCP data at most transects, even at sharp bends. In general, velocity comparison is much harder than the stage and discharge as velocity is a local flow variable and is influenced significantly by the local bathymetric features. Any bathymetric features not represented well by the model terrain can alter the local velocity prediction. The overall good comparison of the predicted and ADCP velocities is very encouraging considering that a very coarse mesh has been used. This point has been discussed in detail by Hammock et al. (2013b) who showed that a much refined mesh for the ADCP reach does not improve the model results. Therefore, a coarse mesh 2-D model is sufficient for flow predictions and it is often true at other streams.

The same low-resolution model is also applied to simulate another time period between December 2014 and March 2015 without any changes to the model. Since the model is not recalibrated, the 2-D model now is used as a predictive tool. With the field data available for the 2014-2015 period, a comparison of the predicted and measured results has been made. It is found that the model performs similarly to the 2010-2011 period.

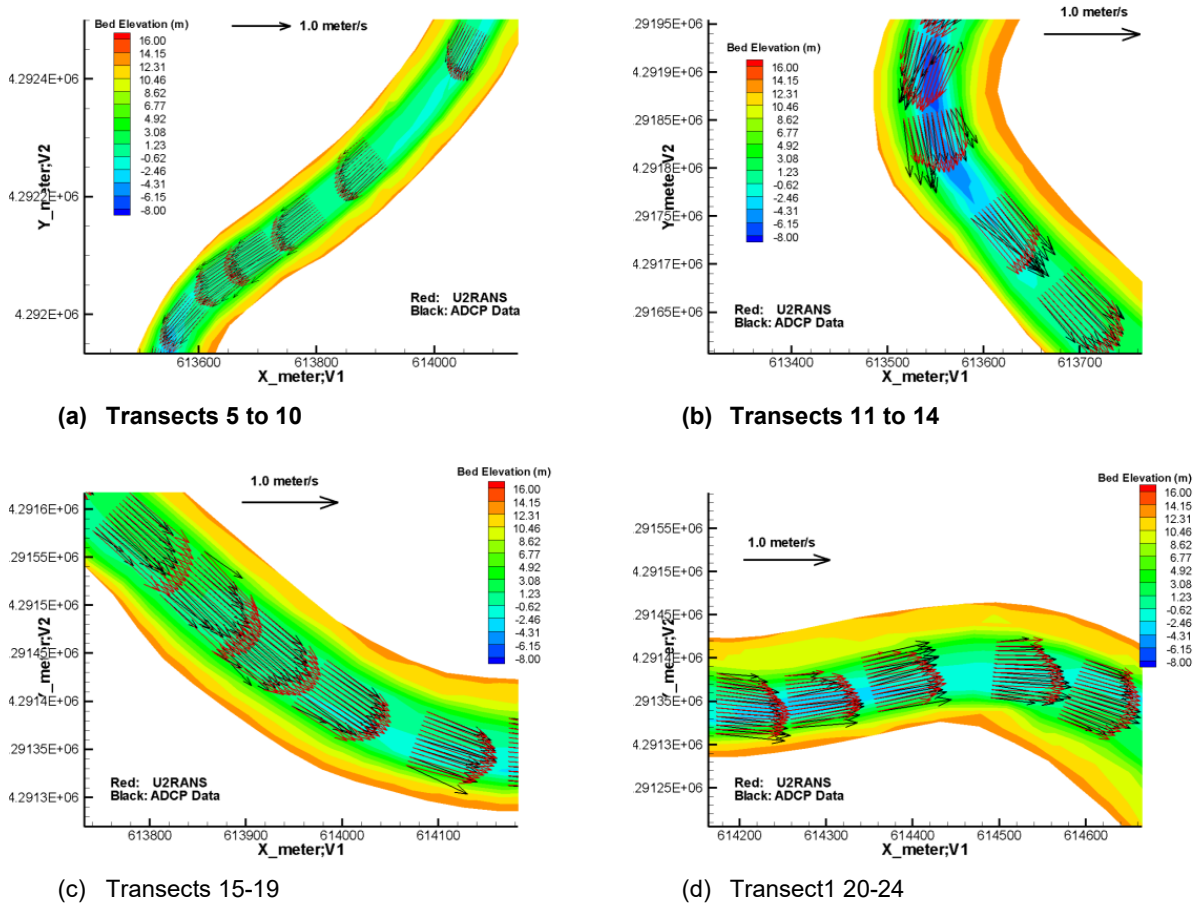

Figure 21.—Depth-averaged velocity comparison between model and ADCP data.

High-Resolution Model Results

The model domain and the mesh for the high-resolution model are shown in Figure 22a while the terrain, surveyed in 2015 by USGS, is displayed in Figure 22b. The domain is along the Fremont Weir section of the Sacramento River and is a subsection of the low-resolution model. The 2-D horizontal mesh is obtained using SMS which consists of 35,701 mesh cells of mixed quadrilaterals and triangles. The mesh is used first by SRH-2D to provide the initial condition for 3-D CFD modeling. The 3-D mesh is then developed using the sigma-mesh approach and a total of 20 vertical cells. The resultant 3-D mesh has a total of 714,020 cells comprising both hexahedrons and prisms.

There are five open boundaries that need boundary conditions (see Figure 22a). Discharges from Karnak and Natomas are small and estimated to be similar to the low-resolution model (see Figure 17b). Hourly discharges at Knights Landing and Feather River and the stage at Verona are plotted in Figure 23 for the period of December 1, 2014 to March 31, 2015; these are used as the boundary conditions to the 2-D and 3-D fine resolution models.

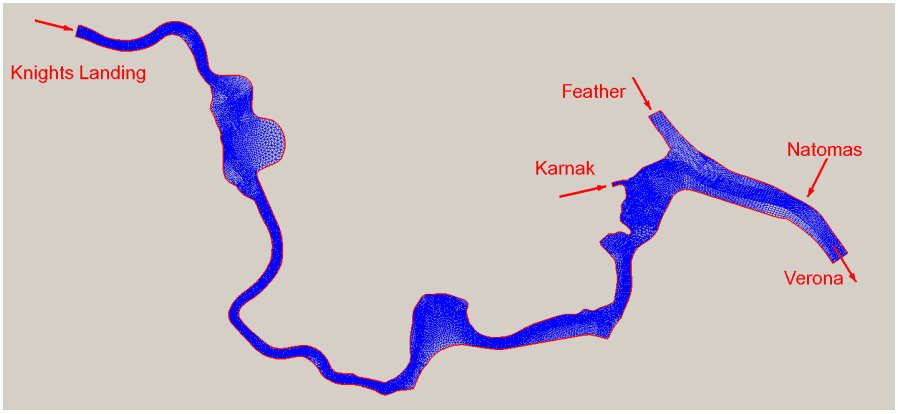

(a) Model domain and 2-D horizontal mesh

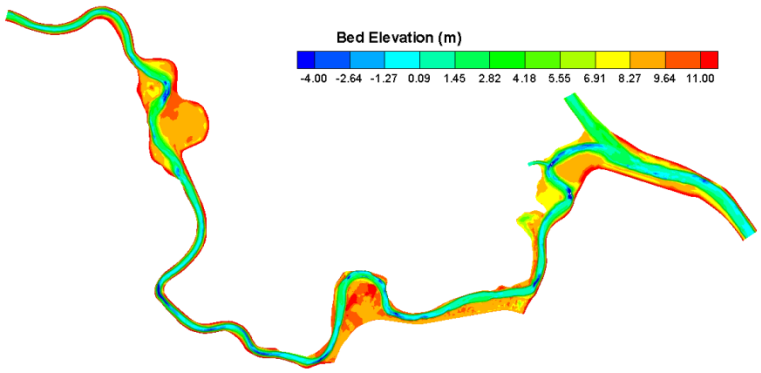

(b) Terrain represented by the mesh

Figure 22.—The model domain, the horizontal 2-D mesh and the 2015 terrain of the fine resolution model.

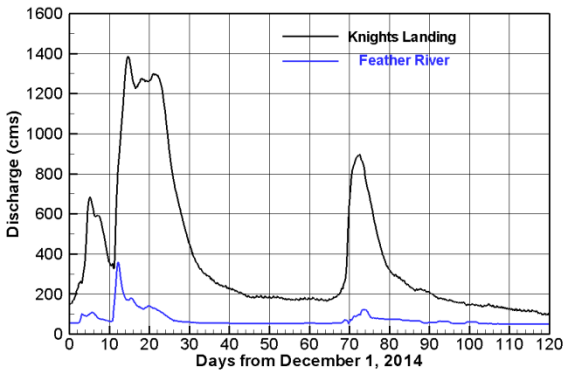

(a) Discharges

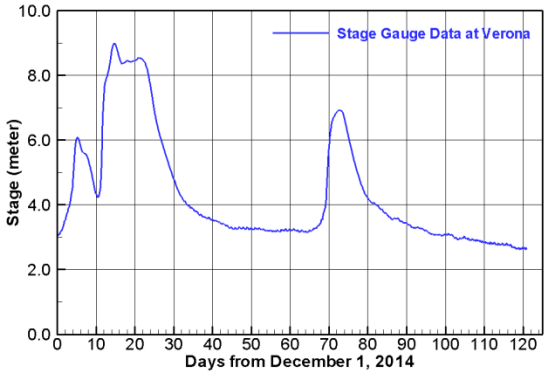

(b) Stage

Figure 23.—Boundary conditions for the fine resolution model.

2-D modeling is carried out first. The predicted discharge is compared with the gauge data at Verona station in Figure 24a while the predicted stage at Fremont Weir is in Figure 24b. Discharges are almost the same between the model and gauge data; and the agreement between the predicted and gauge stages is very good, particularly in at high flows. It is encouraging that the agreement is achieved without further model calibration of the Manning's coefficient. Next, the 2-D results are compared with ADCP data; results are presented when 3-D model results are discussed below. It will be shown that the 2-D model predicts the depth-averaged velocity very well.

ADCP data was collected by USGS on three dates within the model domain: January 26, February 11, and February 18, 2015. The discharges of these days at Verona station are marked in Figure 24a. The daily discharge at Verona is 232, 995, and 423 cms, respectively. ADCP survey was carried out at ten river transects along the Fremont Weir section of the river as shown in Figure 25. Two dates are selected for 3-D modeling: January 26 and February 11, 2015 so that both low and high flows are simulated and compared with the ADCP data.

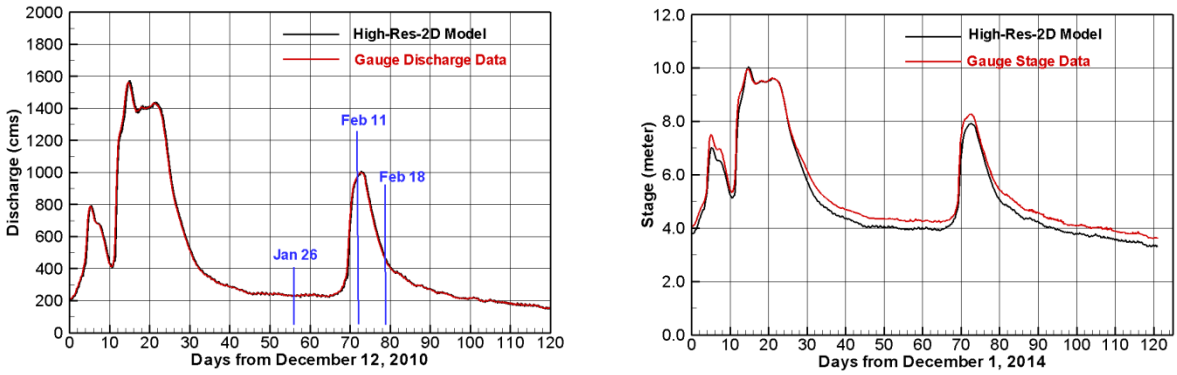

(a) Discharge at Verona

(b) Stage at Fremont Weir

Figure 24.—Comparison of predicted and recorded gauge data between December 1, 2014 and April 1, 2015.

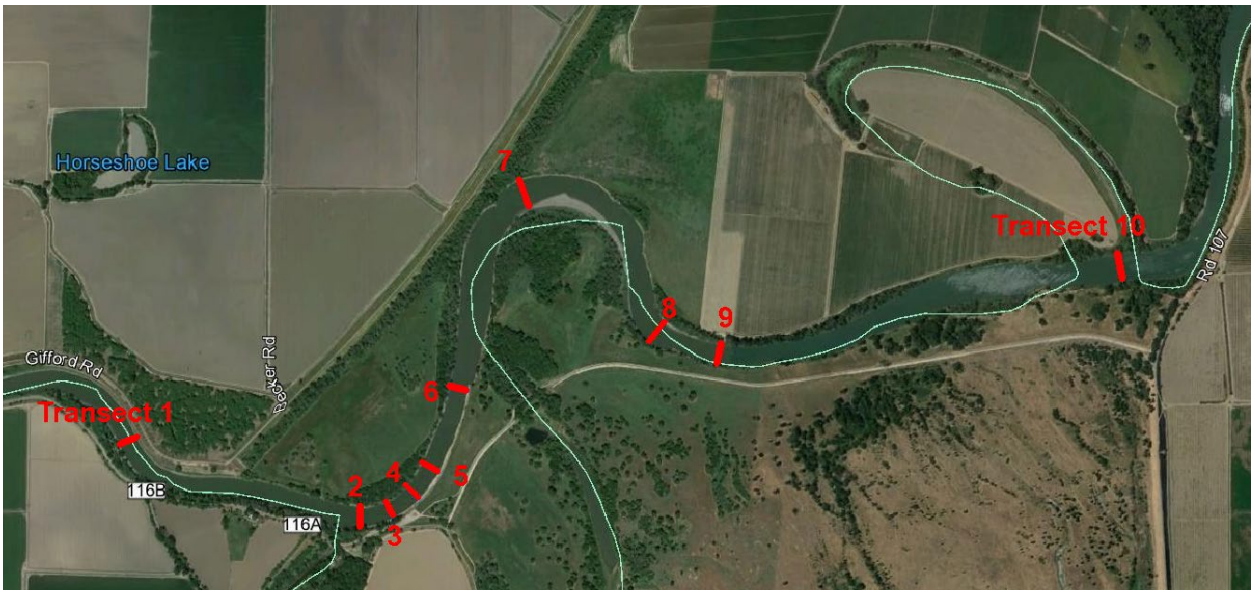

Figure 25.—Ten transects where the ADCP measurement was carried out.

The low discharge (232 cms) run corresponds to January 26, 2015. The 3-D and 2-D model results are compared with the ADCP data for the depth-averaged velocity in Figure 26. It is seen that 2-D and 3-D model results agree very well with the ADCP velocity data at most transects except for Transect 8. At Transect 8, the models predict that the maximum velocity remains near the left bank but the ADCP data shows that the maximum velocity has been shifted towards the right bank. The probable cause for the mismatch is the high uncertainty of the local river bathymetry used by the numerical models. This will be discussed later when the secondary flow patterns are compared.

It is also found that 3-D and 2-D model results are very similar in most locations, including the velocity distribution in the sharp bend. This is a confirmation that 2-D depth-averaged model is a reliable tool in predicting the depth-averaged velocity for natural channels with even sharp bends. If engineers are interested in the depth-averaged velocity only and if there are no major in-stream geometrical features that may cause significant local flow changes, 2-D model may be sufficient for flow prediction of a natural channel. A 3-D model is needed only when there are in-stream structures in the model domain or one is interested in the secondary flow patterns.

The high discharge (995 cms) run corresponds to February 11, 2015. The 3-D and 2-D model results are compared with the ADCP data for the depth-averaged velocity in Figure 27. The conclusions reached with the low discharge run are still valid with the high discharge case and so is not dependent on the flows. At the high flow, the agreement of the mode with ADCP data at transect 8 is much better than the low flow run. Improved modeling at Transect 8 reflects the fact that local river bathymetry mismatch usually has a lesser impact on velocity of a high flow than a low flow.

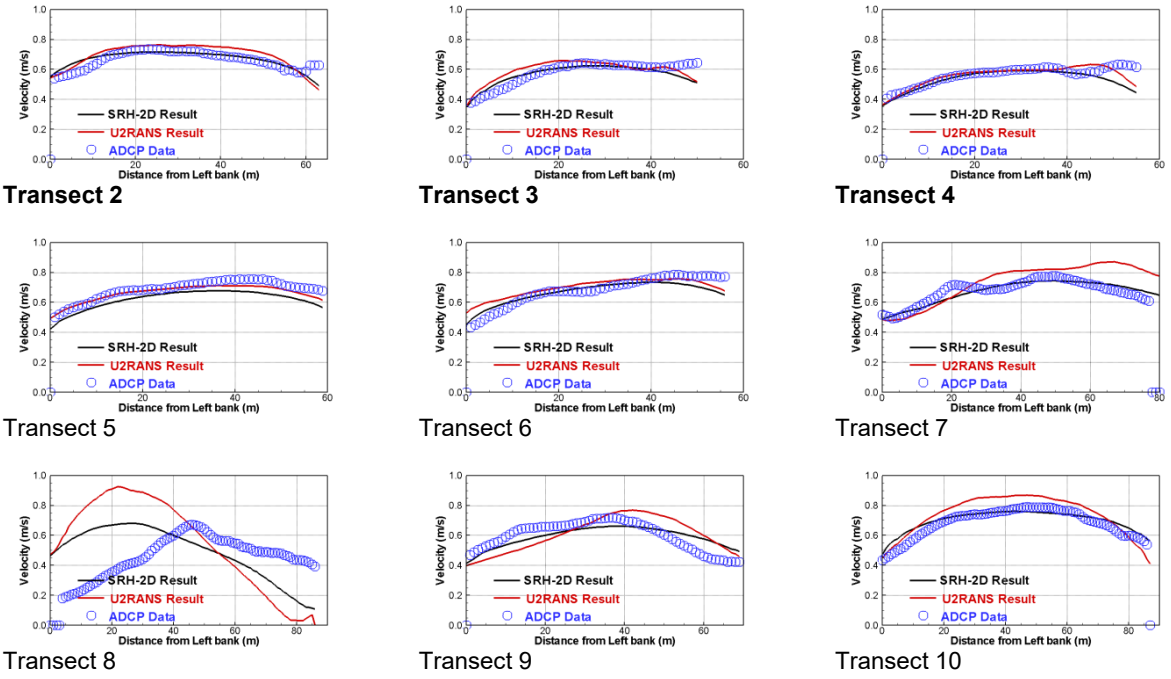

Figure 26.—Comparison of depth-averaged velocity at low flow.

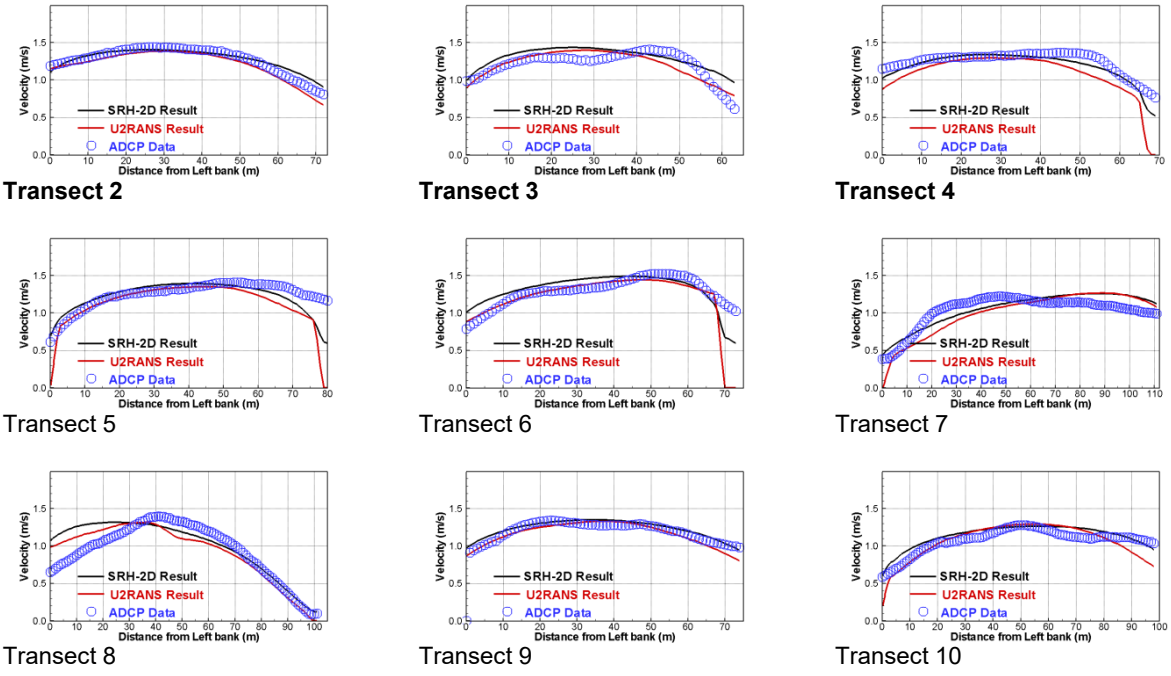

Figure 27.—Comparison of depth-averaged velocity at high flow.

A primary reason to use 3-D models is that complex flow patterns may be predicted due to in-stream structures or local bathymetric features. For example, secondary flow patterns may be

predicted in a curved section of a stream. In Figure 28 and Figure 29, the 3-D model predicted secondary flow patterns are compared with the ADCP data at selected transects for both the low and high discharge runs. In these figures, the total velocity magnitudes are also compared as color contours. In general, field measurements of secondary flows are different but the data possesses high uncertainty. Therefore, the comparison of the present 3-D model with the ADCP data can only be done qualitatively. Overall, the 3-D results agree with the ADCP data well in terms of the secondary flow patterns at most transects except for Transect 8. The mismatch in results at Transect 8 may be caused by the local river bathymetry. The cross-section bed elevation comparison shows that the river cross section used by the model is different from ADCP data. For example, the ADCP cross section has a deeper thalweg and a higher right bar than the numerical model. It was reported by the survey crew that flow in the Transect 8 area was very unsteady/dynamic and bed morphology was subject to significant change. This may explain why the bathymetry used by the model, surveyed at a different time, is different from the ADCP data bed profile and the mismatch of the model with the data.

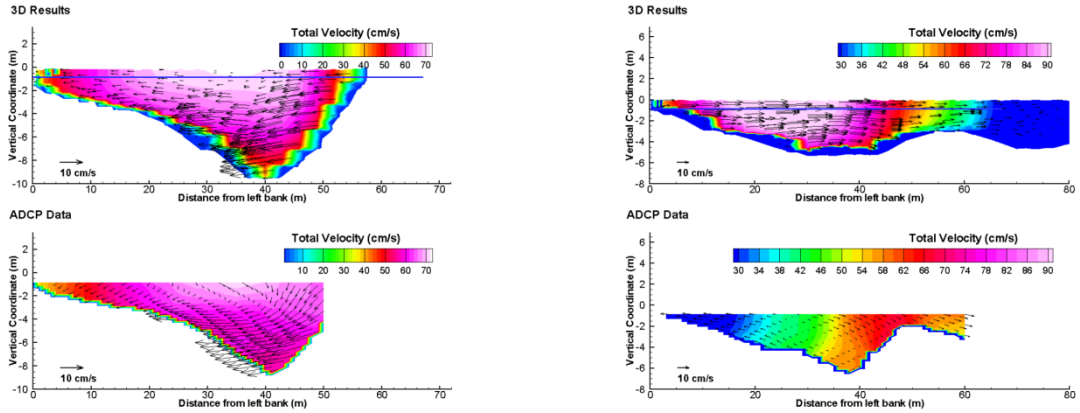

(a) Transect 3 (b) Transect 8

Figure 28.—Predicted (top) and ADCP measured (bottom) secondary flow patterns at selected transects for the low discharge run.

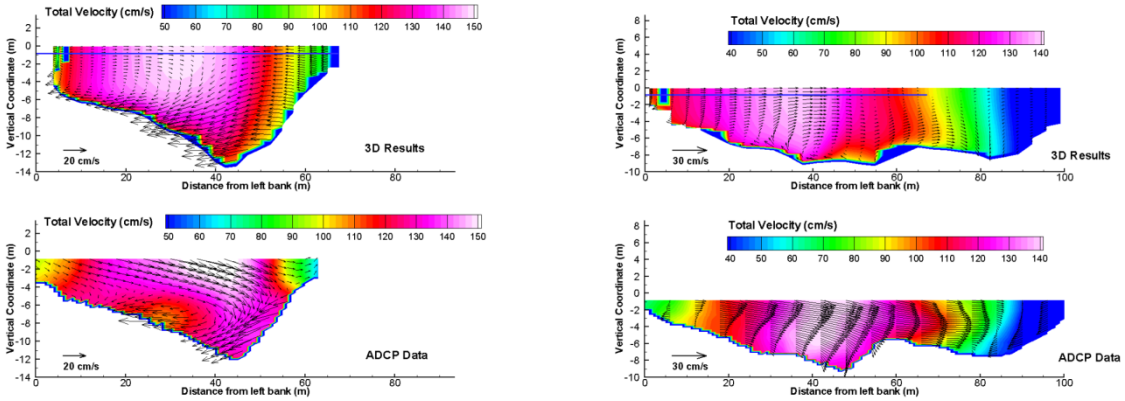

(c) Transect 3 (d) Transect 8

Figure 29.—Predicted (top) and ADCP measured (bottom) secondary flow patterns at selected transects for the high discharge run.

Concluding Remarks

Both 2-D and 3-D CFD simulations have been carried out along the Fremont Weir section of the Sacramento River. Results are also compared with the field data. The following conclusions may be obtained from this study:

- The SRH-2D low-resolution model agrees with the ADH model results very well. The two models used quite different numerical methods, discretization schemes, and physical process models, e.g., turbulence and energy loss equations. The close agreement between the two proves that both models have solved the same set of governing equations correctly.
- Large scale models such as the present 2-D low resolution model may have difficulty in taking all water inflows and outflows into account, particularly at high flows.
- A very coarse mesh may be used for 2-D modeling for natural streams. Such modeling is much quicker to perform, and overall flow patterns and velocity distribution can be predicted reasonably well. Very high-resolution mesh may not be needed in 2-D modeling.
- Both 2-D and 3-D models predict very well the depth-averaged velocity as measured by the ADCP. Similar results of 2-D and 3-D models for the depth-averaged velocity confirm that 2-D models are adequate in predicting depth-averaged velocities in natural rivers with even sharp bends.
- A main advantage of 3-D models is the ability to predict secondary flow patterns and large local velocity changes impacted by in-stream structures. A comparison of the 3-D predicted secondary flows with the ADCP data shows that the 3-D model can capture the secondary flow patterns observed at most transects of the ADCP data.

5.0 Fish Entrainment Modeling at Junctions

In this chapter, the juncture flow of Ramamurthy et al. (2007) is used to shed light on fish entrainment characteristics at typical diversion junctures; the track tools are based on the flow results in the previous chapter. The objective is to show that: (a) fish distribution across the cross-section upstream of the junction has a significant impact on the fish entrainment rate; (b) presence of a secondary flow upstream of the junction may redistribute fish before they enter the side channel and alter fish entrainment; and (c) local bathymetry features may be manipulated upstream of the diversion junction to increase or decrease fish entrainment.

An extensive number of studies have been reported to investigate the complex flow dynamics at a flow diversion junction as reviewed in chapter 3. A few studies have also been carried out to shed light on how the flow features at a junction may impact the sediment entrainment. However, few studies have been carried out investigating the relationship between flow features and fish entrainment at flow junctions. In the past, studies were primarily of the field measurement nature; measured data were primarily used to develop empirical relations to correlate the fish entrainment to flow variables such as the flow ratio (Perry et al. 2010; 2014; 2015; Cavallo et al. 2015; Romine et al. 2017). There is a lack of studies using numerical models, to my knowledge. An exception is the modeling study by Ramon et al. (2018) who dealt with numerical model applications at the Georgiana Slough junction of the Sacramento River. This study indeed touched on the issues of the impact of a nonuniform distribution of the passively driven particles on fish entrainment, along with the effect of the secondary flows in the bend. This study differs from the Ramon study in several aspects: (1) the 3-D flow model is based on a 3-D URANS solver without invoking the hydrostatic assumption, while the Ramon study adopted the 3-D model with the hydrostatic assumption; (2) the effect of non-uniform fish distribution upstream of the junction on the fish entrainment rate is investigated explicitly, including both the vertical and lateral fish distributions; and (3) the effect of secondary flows is studied explicitly.

Hance et al. (2020) recently proposed a conceptual model predicting fish entrainment using the concepts of streamline, entrainment zone and fish distribution. This study makes the same assumptions as Hance et al. (2020) except that the streakline and entrainment zone are predicted by a 3-D CFD model, not from the field-data based statistical models.

5.1. Entrainment at a Junction with a Straight Main Channel

Fish entrainment characteristics is first investigated at a 90-dgeree diversion junction along a straight main channel, using the Ramamurthy et al. (2007) case. The case is representative of most flow diversion junctions and flow results have been validated already in the previous chapter. Besides the baseline case with 83.8% diversion, two additional diversion rates are also simulated: 50% and 20%. The selected three rates are used to shed light on the impact of upstream fish distribution on the fish entrainment rate. All flow input conditions are kept the same except that the diversion rate through the side channel is varied.

The modelling study of the case aims to quantitatively demonstrate that the upstream fish distribution has a profound impact on the fish entrainment rate. Such impact has been studied in the past, but only in qualitatively. For example, Perry et al. (2014) discussed that both the flow entrainment rate and spatial distribution of fish approaching a river junction would influence the probability of fish entering a side channel. Based on the measured fish tracking data at the junction of Georgiana Slough and Sacramento River, Perry et al. (2014) showed that the probability of fish entrained into the Georgiana Slough branch from the Sacramento River was much higher for fish positioned on the entrainment side than on the opposite side. Their field results were reproduced in Figure 30 below. Higher flow increased the fish entrainment probability, consistent with the fact that fish would be more likely to move with the flow (i.e., act passively). The study of Perry et al. (2014) showed also that the discharge rate and cross-stream distribution of fish influenced also the performance of a non-physical fish barrier called a BioAcoustic Fish Fence (BAFF). They stated that "Ultimately, the location of fish approaching the BAFF proved to be the most important factor affecting migration routing." They concluded that "fish location in the cross-section was the most important determinant of an individual's probability of entrainment into Georgiana Slough."

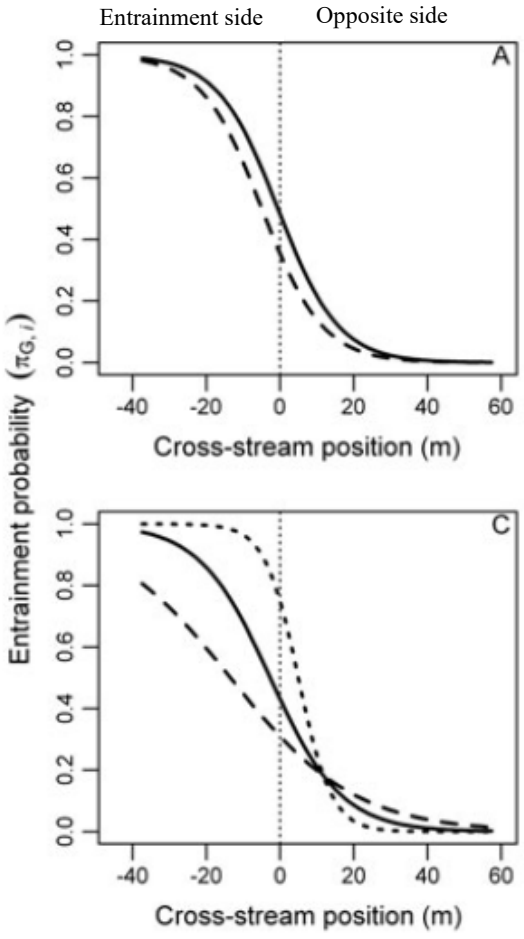

Figure 30.—Probability of entrainment into Georgiana Slough versus the lateral location (cross-stream position) of a fish based on the field data

of Perry et al. (2014). Top figure shows the effect of day (dashed line) and night (solid line); the bottom shows the differences at the 5th (dashed line), 50th (solid line) and 95th (dotted line) percentiles of discharge. Source of the figure: Perry et al. (2014).

To study the impact of non-uniform fish distribution, four upstream fish distributions are simulated using the Eulerian fish track model developed in this research. The four, named top, bottom, attraction side and rejection side, respectively, is graphically illustrated in Figure 31. Two runs explore the effect of vertical distribution upstream of the junction (surface-oriented versus deep water bottom-oriented), while the other two examine the effect of lateral distribution (left bank oriented versus right bank oriented). The rationale for the vertical and lateral fish distribution choices are discussed in Section 3.3. A total of twelve (12) Eulerian track model runs are carried out and tabulated in Table 1. Note that the same numerical model can be applied to any known or prescribed fish distribution if it is available.

For example, it could be a unimodal distribution where fish are concentrated in the center of the channel with less probability of being near either bank; or alternatively, a U-shaped distribution where fish are more likely to be at either banks than in the center.

(a) Top (red) or Bottom (blue) Distribution

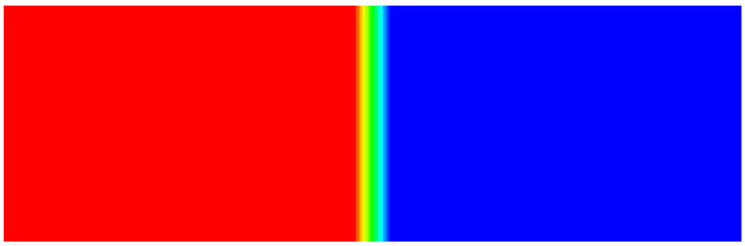

(b) Attraction (red) and Rejection (blue) Distribution

Figure 31.—Assumed fish distribution: top- or bottom-half and attraction-side or rejection-side distribution is simulated.

Table 1.—Model run labels and the corresponding diversion rate and fish distribution scheme

Scenario Label	% of Flow Diverted	Fish Distribution at Main Channel Inlet Upstream
84T	83.8	Top Half
84B	83.8	Bottom Half
84A	83.8	Attraction Side Half
84R	83.8	Rejection Side Half
50T	50	Top Half
50B	50	Bottom Half
50A	50	Attraction Side Half
50R	50	Rejection Side Half
20T	20	Top Half
20B	20	Bottom Half
20A	20	Attraction Side Half
20R	20	Rejection Side Half

Given an initial fish distribution at the upstream boundary (top, bottom, attraction or rejection) and a given flow diversion rate (83.8%, 50% or 20%), the fish distribution function (FDF) is transported by flowing water through an unsteady simulation using the Eulerian track model. Example FDF evolution results under the 50T and 50R runs (i.e., 50% diversion rate with top and rejection-side fish distribution runs) are shown in Figure 32 and Figure 33 at four times. For the top-half distribution, FDF remains on the top half of the main channel before the junction; and it is split into the side and the main channels once reaching the junction. Due to the complex secondary flows and recirculation flows at the junction, as discussed in Section 4.1, FDF is distributed over the entire depth after the junction. For the rejection-side distribution run, FDF mostly remains on the rejection side of the channel and majority of FDF is within the branching main channel. A small portion of FDF is entrained into the side channel, primarily through the near-bed flow as shown in Figure 34.

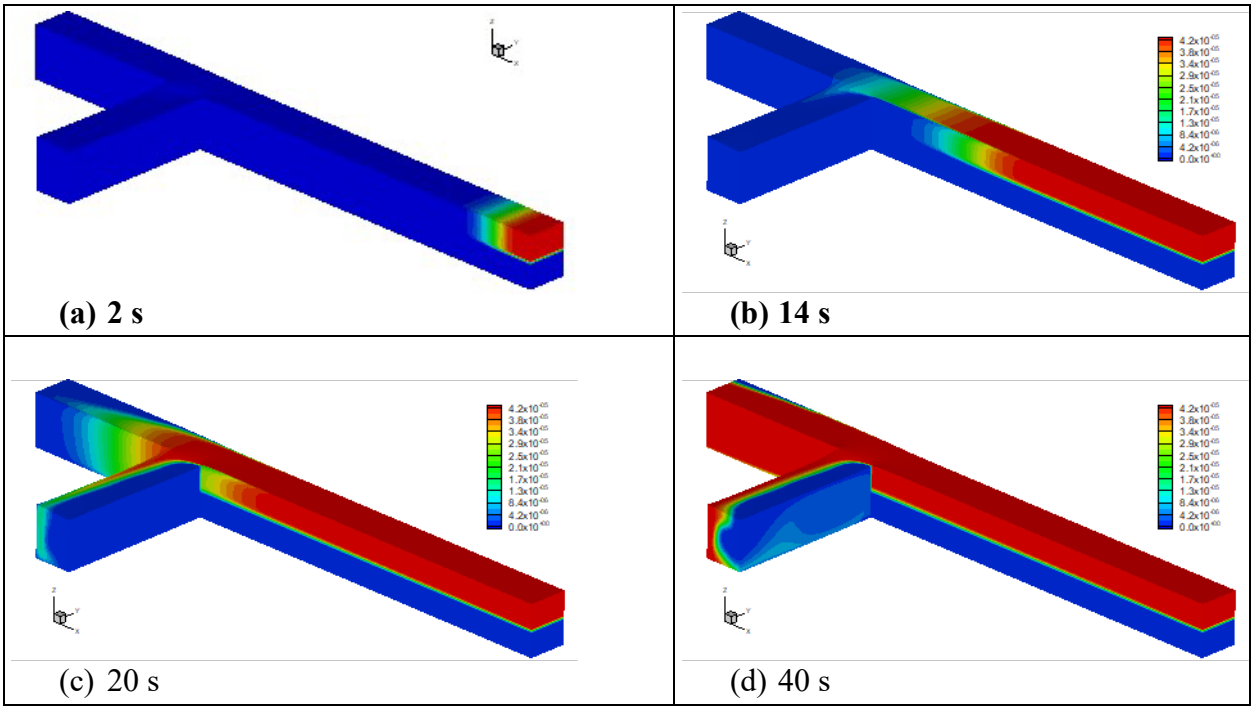

Figure 32.—Evolution in time of the fish distribution function (FDF) entering the main channel at inlet and diverting into the side channel for Run 50T (note: vertical direction is enlarged 4 times).

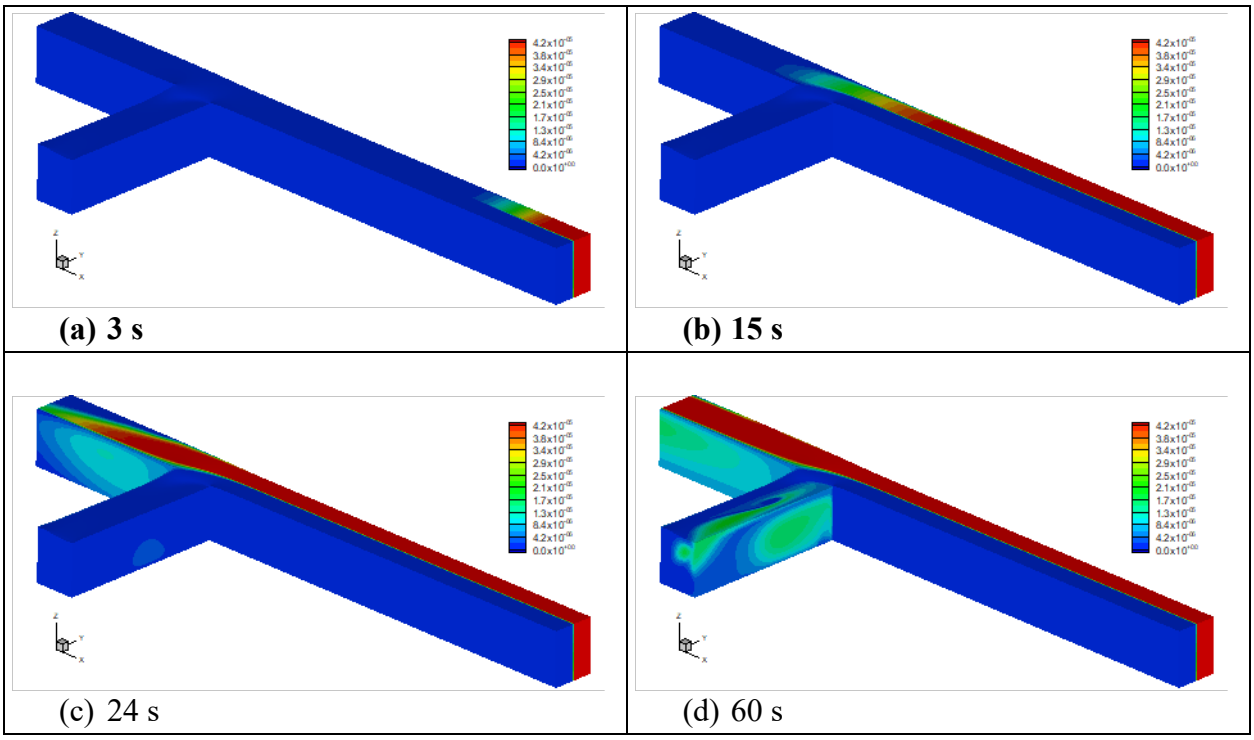

Figure 33.—Evolution in time of the fish distribution function (FDF) entering the main channel at inlet and diverting into the side channel for Run 50R (note: vertical direction is enlarged 4 times).

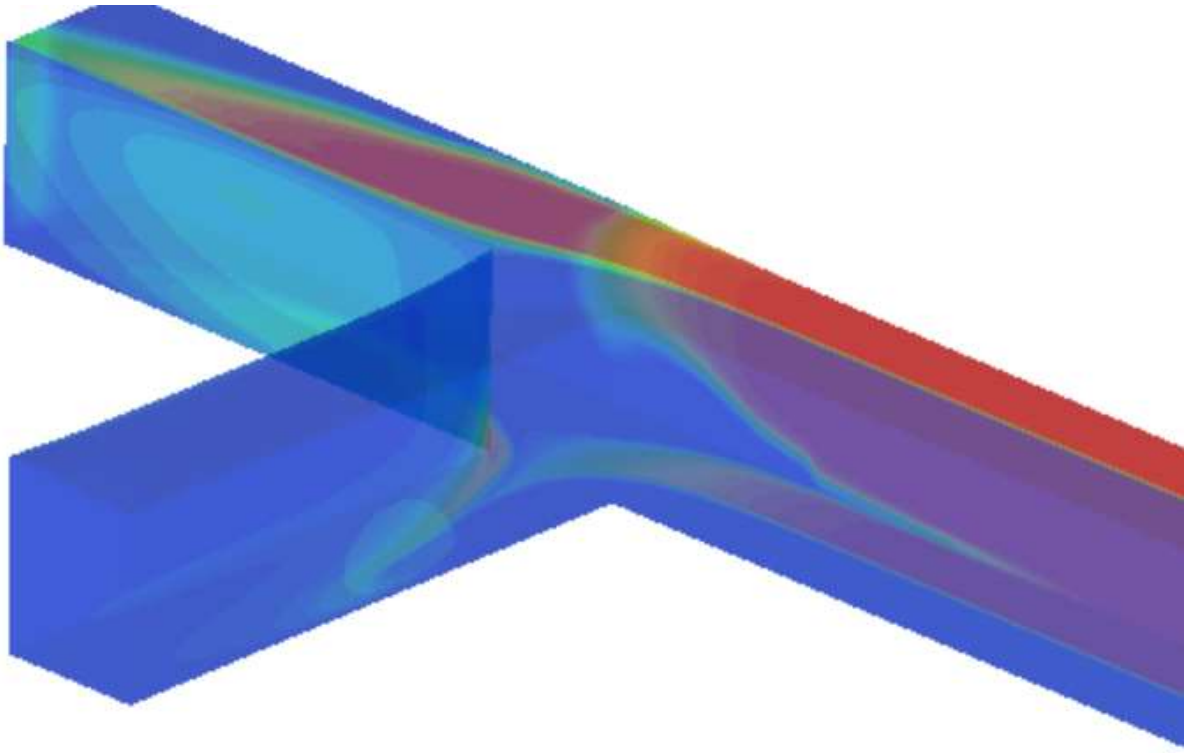

Figure 34.—Fish distribution function (FDF) contours at time 24 s for Run 50R (note: vertical direction is enlarged 4 times).

In this study, fish entrainment efficiency (ϵ) is defined at a flow junction in order to quantify the fish entrainment efficiency under different scenarios; it is expressed as:

$$\epsilon = PP/PW$$

where:

PP = Percentage of passive fish diverted into the side channel
PW = Percentage of water diverted into the side channel

The entrainment efficiency 1.0 means that the entrainment rate matches exactly the flow rate. This idealistic efficiency would be the case if fish is assumed passive and distributed uniformly at the cross section upstream of the junction. This has been numerically confirmed in the present study with the Eulerian track model: When the fish (FDF) is distributed uniformly at the inlet, unity efficiency is indeed obtained. The present study, however, shows that the efficiency other than unity would be obtained if fish distribution at the upstream cross section were non-uniform. A value above one indicates enhanced entrainment - a desirable feature for a junction designed for fish attraction – and a value below 1.0 is effectiveness for fish rejection.

The entrainment efficiency, computed at the exits of both the side and main channels, is plotted in Figure 35 for the four fish distributions at the 50% diversion rate. It is seen that fish entrainment is not unity if fish is distributed unevenly across the approach channel cross section. Entrainment is above unity if fish is bottom-oriented (deep water) or attraction-side oriented (on the side channel side). The results are not surprising as previous studies have shown that near-bed sediments moved predominantly into the side channel – termed Bulle Effect – as discussed in Section 2, and diverted water comprises primarily of those on the side channel side.

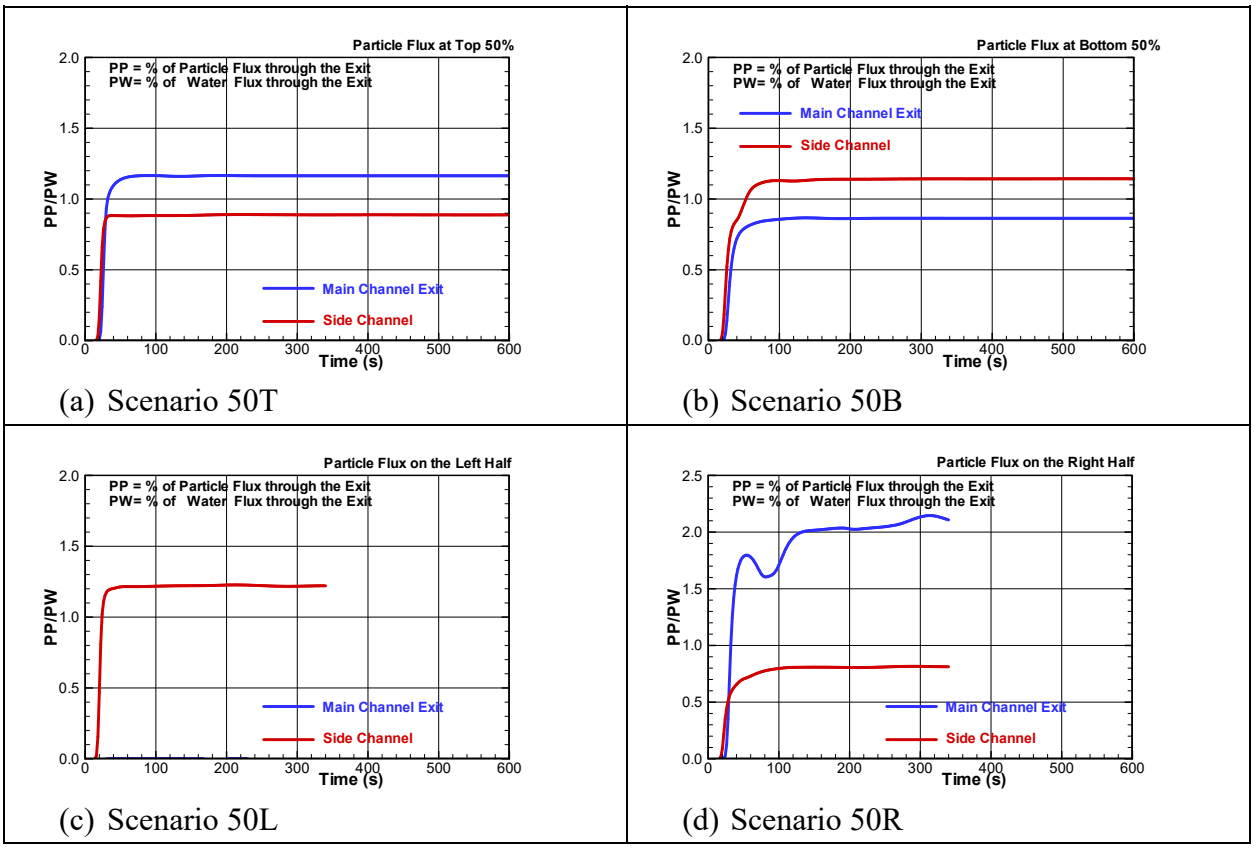

Figure 35.—Time history of fish entrainment efficiency through side and main channels for the case of 50% diversion rate. Red line is the side channel entrainment rate.

Finally, fish entrainment rate and efficiency through the side channel at the steady state condition (taken at time 600 s) are tabulated in table 2 for all 12 scenarios. The data are also plotted in Figure 36 and Figure 37. The results show that the bottom fish have a higher rate of entrainment into the side channel than the surface-oriented fish. At 20% diversion rate, e.g., the efficiency difference between the two is about 25%. The difference between surface-oriented and bottom-oriented fish entrainment rates, however, decreases with increasing diversion rate and approaches to zero at 100% diversion rate. The result is significant as most diversions in the field has less than 50% diversion rates, suggesting that fish entrainment rate may differ appreciably (up to 25%) between surface-oriented or bottom-oriented. Further, efficiency difference is even

efficiency difference is even more significant between the attraction-side or rejection-side fish distribution. It is found that almost all fish would enter the side channel if fish were distributed over the attraction side of the half channel (efficiency is almost 2.0). When fish is distributed on the rejection side half, fish diversion into the side channel is possible only at a high flow diversion rate (e.g., more than 30-40%).

As a comparison, in Figure 36, we add the linear regression line developed by Cavallo et al. (2015) who used fish telemetry data measured at seven flow junctions on the Sacramento River. Additionally, we plot also the fish tracking data obtained by Romine et al. (2017) at the Sutter and Steam Boat junctions of the Sacramento River. In the study of Cavallo et al. (2015), it was concluded that entrainment rate varied between 10% to 60% with the diversion ratio of 18% to 60%. Although the flow dynamics at the Georgiana Slough junction is quite different from the idealized junction simulated here (e.g., complex unsteady flow dynamics induced by tides), the measured fish entrainment curve falls within the region bounded by the top-half and rejection-half lines of the numerical model. The field entrainment results now may be explained based on the present study results. It was reported by Perry et al. (2014) that migrating juveniles at the Georgiana Slough section of the Sacramento River stayed mostly near top 4 meters of the water depth and fish distribution curve had its peak located on the rejection side at the Georgiana Slough junction. Both features would reduce the fish entrainment efficiency. At the Sutter junction, the entrainment rate was lower than the rejection-side curve of the numerical model once the flow rate is above 50%. We believe it was due to that entrainment beyond 50% was due to the reverse flow of the Sacramento River during flood period of the tidal influence. Lower fish entrainment rate at the Sutter than the Steam Boat may be explained by fish distribution approaching each junction: more fish is distributed on the rejection side of the Sacramento River before reaching the Sutter junction than the Steam Boat junction. The conjecture is yet to be confirmed in the field though.

Table 2.—Fish entrainment efficiency for the case of Ramamurthy et al. (2007)

Scenario Label	% of Fish Diverted (Eulerian)	Entrainment Efficiency (Eulerian)	% of Fish Diverted (Lagrangian)	Entrainment Efficiency (Lagrangian)
84T	79.4	0.947	74.4	0.888
84B	90.3	1.078	95.6	1.141
84L	100.0	1.200	100.0	1.2
84R	68.2	0.813	66.4	0.792
50T	44.4	0.888	43.2	0.864
50B	57.1	1.143	53.1	1.062
50L	91.0	1.820	92.5	1.850
50R	9.9	0.194	5.2	0.104
20T	17.9	0.897	16.03	0.802
20B	23.0	1.152	14.4	0.718
20L	40.0	2.0	30.8	1.54
20R	0.006	0.0	0.0	0.0

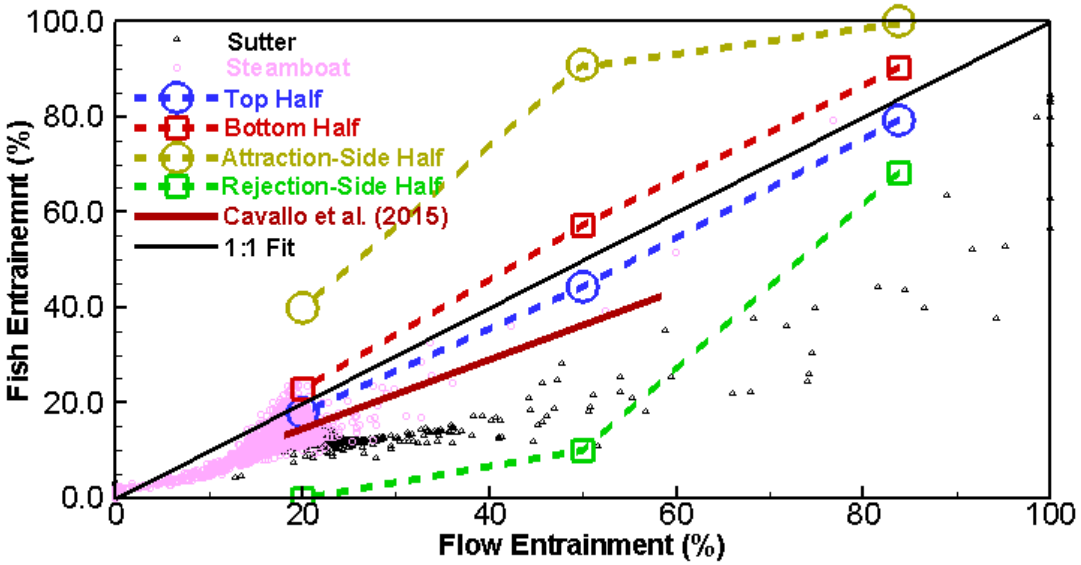

Figure 36.—Fish entrainment rate versus the flow diversion rate into the side channel with the 90-degree junction of Ramamurthy et al. (2007).

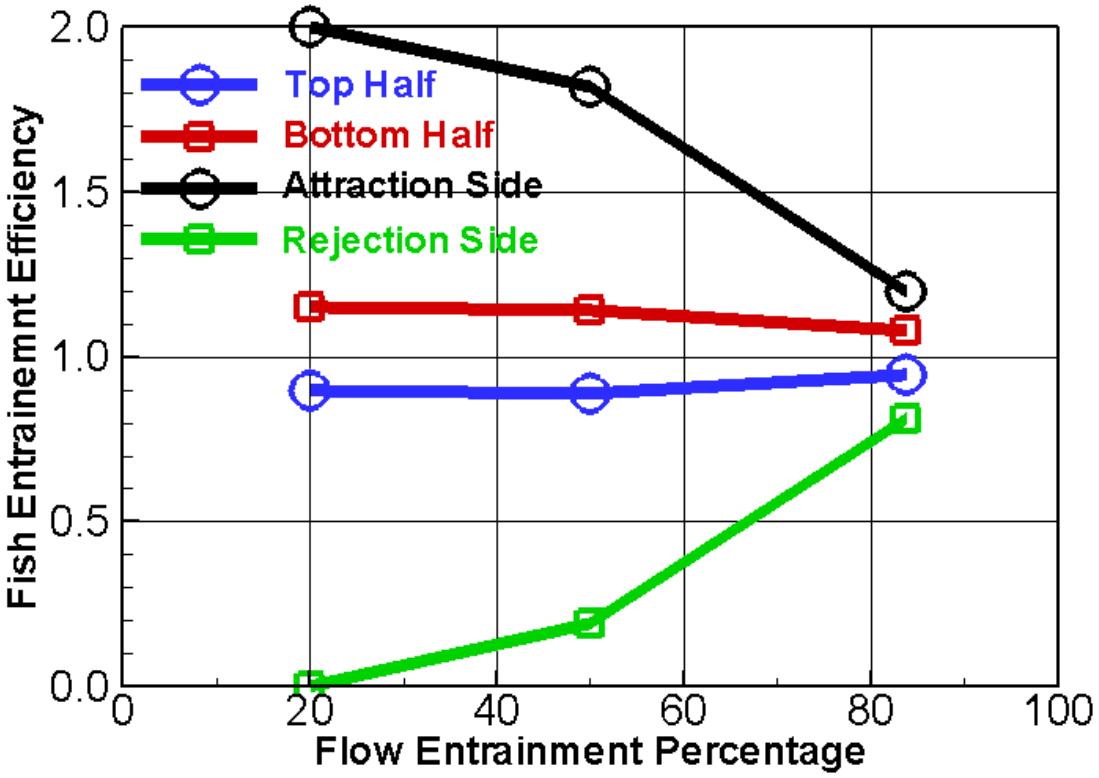

Figure 37.—Fish entrainment efficiency through side channel as a function of the percentage of diverted flow into the side channel with the 90-degree junction of Ramamurthy et al. (2007).

It is also noted that a similar entrainment plot was reported by Cavallo et al. (2015) based on the field data of the Sacramento River and it is reproduced in Figure 38, which may be used for further comparison with the present model results. Only the best-fit linear regression line is plotted in Figure 36 above. Following is noted with regard to the field results: (a) fish entrainment is higher at DCC and lower at GEO which may be explained by the possibility that fish was distributed more towards the outer bank at DCC than GEO due to the secondary flow created by the bend; (b) entrainment at GEO is mostly below the best-fit line while entrainment at the Head of the Old River is above (we know the fish distribution is on the rejection side at GEO; is it possible that fish is distributed towards the attraction side at the Old River?); (c) fish entrainment has a faster rate of increase with the flow entrainment rate once diversion is above 50%; the present numerical model results have a similar trend. Of course, this may also be attributed to the site difference.

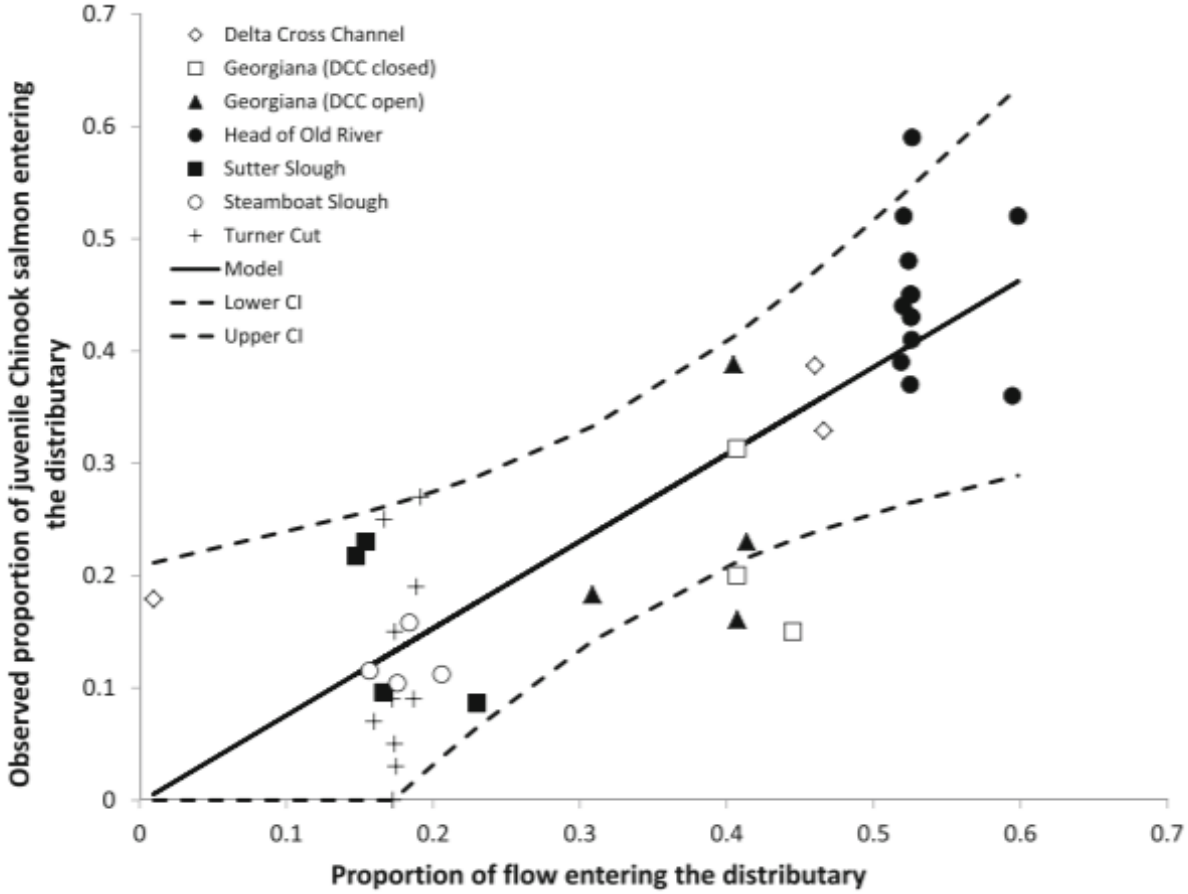

Figure 38.—Fish entrainment rate versus water entrainment rate relation based on the field fish tracking data at seven Delta junctions. The figure is from figure 4 of Cavello et al. (2015). Solid line is the best-fit linear line; the dashed lines are the 95% confidence interval. (This figure may be used as justification of my numerical study).

5.2. Results with the Lagrangian Track Model

The Lagrangian particle track model is also used to perform the same modeling of the case discussed above (Section 5.1). The results are reported for two purposes: (a) show that the Lagrangian track model developed in this research works well, despite challenges; and (b) the Lagrangian model results are in general agreement with the Eulerian track model. It is commented that the Lagrangian track model is much more challenging to develop due to the complexity of moving individual particles (fish) through a digital space. In this research, the Lagrangian track model is not explored further beyond the passive assumption, as the USACE's ELAM model may be applied for more general and comprehensive track simulations.

The same 12-case runs are carried out using the Lagrangian track model, and the predicted fish entrainment efficiency is tabulated in Table 2 above and plotted also in Figure 39. The Lagrangian model efficiency results are in overall agreement with the Eulerian model in Figure

37. Major differences between the two models are the predictions for the top half release of the 20% diversion case. The Lagrangian model predicted smaller percentage of fish into the side channel. It is primarily due to the different ways of computing the fish entrainment. The Lagrangian model counts only the particles that move out of the side channel exit boundary; this leads to a portion of the particles unaccounted, as these particles enter the side channel but do not exit the side channel due to the large flow recirculation near the side channel entrance.

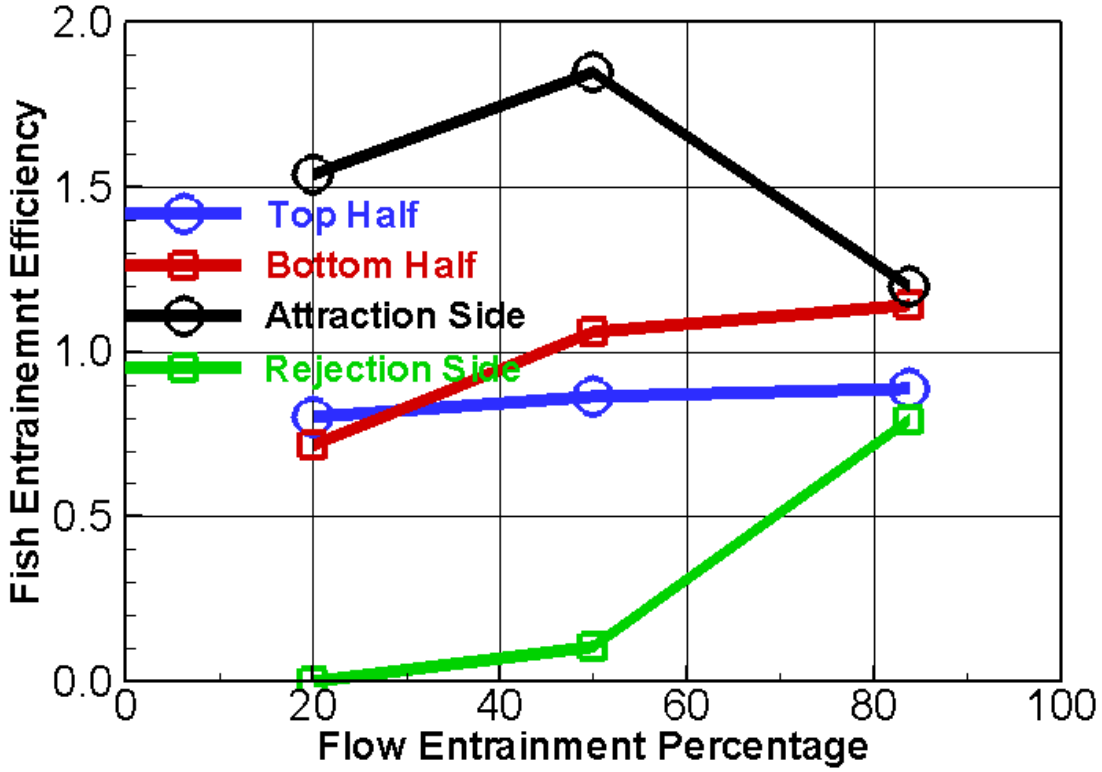

Figure 39.—Lagrangian track model result of fish entrainment efficiency through side channel as a function of the percentage of diverted flow into the side channel.

In summary, the above results demonstrate that the development of the Lagrangian model is a success. Since no new insights are produced by the Lagrangian model, it is not explored further in this study. The results also point to a potential strategy to attract or reject fish entrainment at flow junctions: local terrains or flows may be manipulated upstream of the junction to redistribute the fish upstream to alter the fish entrainment rate.

For example, with a 20% flow diversion at the 90-degree diversion channel of the Ramamurthy et al. (2007) case, more than 10% increase in fish diversion rate is possible with bottom-oriented

fish distribution alone in comparison with the uniformly distributed fish depth-wise. In the following more modeling studies are carried out to explore the impact of the secondary flows and local instream structures.

5.3. Secondary Flow Effect on Fish Entrainment

The above results show that fish distribution upstream of a junction is important in determining the fish entrainment efficiency. Under the existing conditions, field tracking of fish movement may be performed so that the non-uniform fish distribution upstream of junctions may be determined and used for a subsequent fish entrainment estimate (e.g., Hance et al. 2020). If such a distribution is available at a particular site, fish entrainment may be predicted using the model developed in this study. However, such studies are practical primarily for the existing-condition simulations. For future conditions, the fish distribution itself needs to be simulated; it can be done with more sophisticated fish tracking models such as USACE's ELAM model.

In this sub-section, the Eulerian fish tracking model is used further to show that secondary flows upstream of a junction are important in determining the entrainment rate, in addition to the approaching fish distribution. It is motivated by the results in the sub-section above: a strategy to attract or reject fish entrainment may be adopted by finding ways to redistribute fish towards desirable areas upstream of a junction. Since our knowledge of fish vertical distribution is limited, the lateral fish distribution may be manipulated to attract or reject fish. For example, a potential way to make fish distribute towards the attraction side is to create a secondary flow upstream of the junction so that top portion of the water is flowing towards the side channel side. This is in accordance with the findings by Blake and Horn (2004) and Blake et al. (2012) that strong secondary circulation developed at a river bend could influence the salmon lateral distribution.

Telemetry fish tracking data conducted by Steele et al (2017) on the Fremont Weir section of the Sacramento River showed that fish tend to be distributed along the outer bank within a bend. It was believed to be the result of the secondary circulation within the bend. Their data showed that there was a moderate shift in the spatial distribution to the outside bend of approximately 5 to 8 m away from the channel center. The channel width was approximately 70 m with the centerline being 35 m away from either bank.

The existence of a secondary flow upstream of the junction may have an additional impact on entrainment. A counter-rotating upstream secondary flow can weaken and even overwhelm the helical circulation created by the diversion flow into the side channel. Therefore, it is conjectured that the so-called Bulle Effect can be reduced, or the trend be reversed. This conjecture is supported by the study of Ramon et al. (2018) who showed large effects of upstream secondary flows on flow and fish entrainment into side channels.

Simulation of Secondary Flow Effect on Fish Entrainment

The Eulerian fish tracking model is used to study the effect of secondary flow on fish entrainment rate. The secondary flow is created by attaching a 180-deg bend to the main channel upstream, as shown in Figure 40a. All boundary conditions are the same as the straight channel case of Ramamurthy et al. (2007) simulated above. The only difference is that the flow undergoes a 180-deg bend upstream of the junction. The total number of horizontal mesh cells is 18,760 and the 3-D mesh has 30 cells in the vertical direction resulting in a total of 562,800 3-D mesh cells.

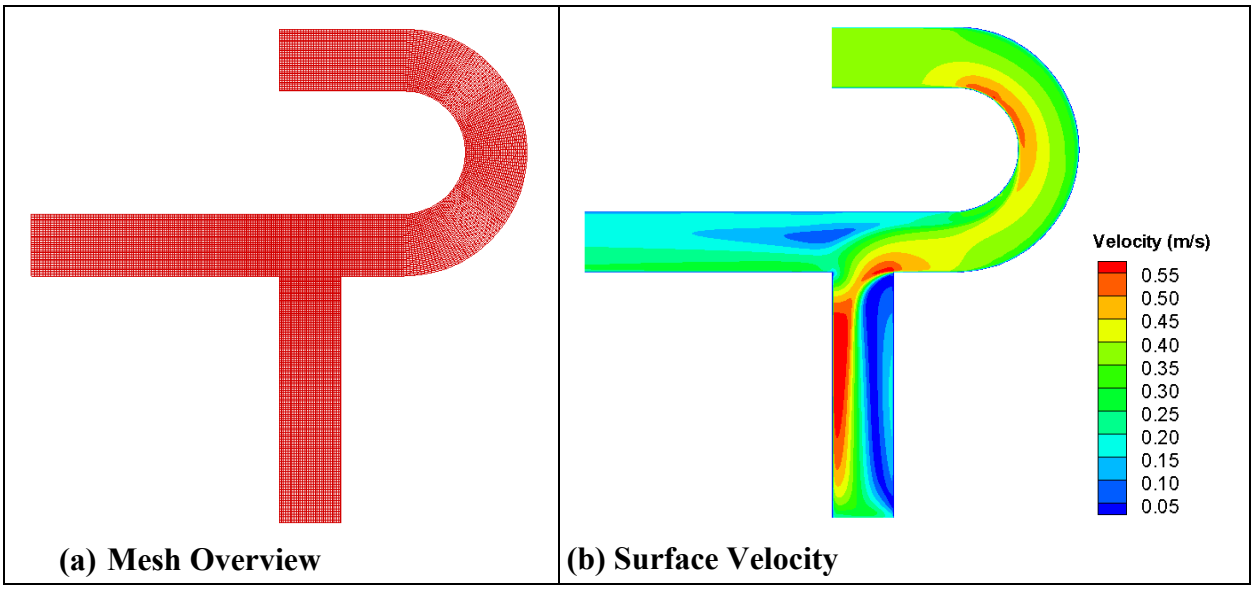

Figure 40.—Plan view of the model domain, mesh and computed flow velocity at the water surface with the 50% diversion rate case.

Three model runs are carried out to examine the effect of secondary flows on fish entrainment with fish distribution function (FDF) only in the top-half of the inlet: 20%, 50% and 83.8% of diversion rates. To gain an understanding of the flow field of the combination of bend and junction flows, the simulated surface flow velocity is plotted in Figure 40b with the 50% diversion rate case. It is seen that floe entrainment pattern has been altered due to the upstream bend flows. Further, the model predicted FDF contours at the steady state condition is plotted in Figure 41, while the secondary flow created by the bend and the FDF distribution are displayed in Figure 42 at the cross section 0.5 channel width (0.305 m) upstream of the junction.

The following observations may be made with regard to the predicted results:

- A secondary flow is developed after the waters enter the channel and move through the 180-deg bend. At the exit of the bend, about half-channel-width upstream of the junction, the secondary flow velocity on average is about 12% of the streamwise velocity component. The secondary flow moves the upper 82% of the waters towards the outer bend, which would redistribute the fish distribution based on the field observation.
- If fish respond passively, the FDF computed represents the fish distribution and it is displayed in Figure 42b. It is seen that fish distribution is switched from top-half regime at the entry to mostly outer-bend regime (or the attraction side). This transition by the secondary flow can have an important impact on the fish entrainment rate, based on the study results in the previous sub-section.

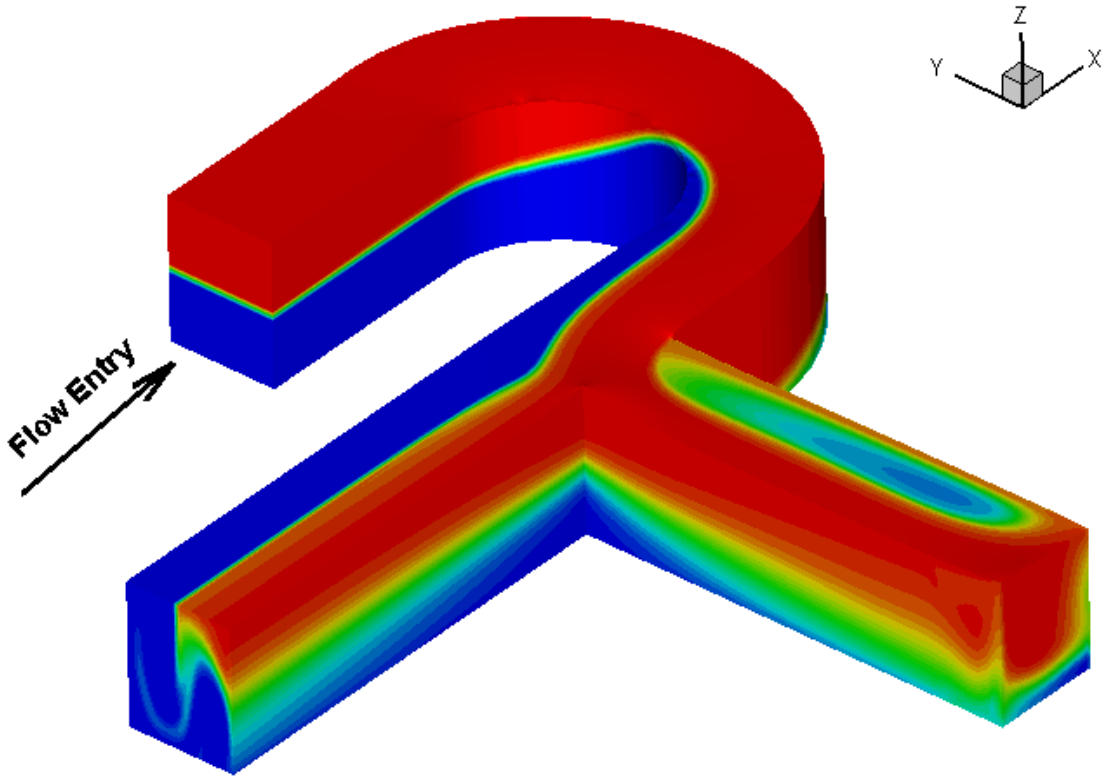

Figure 41.—Fish distribution function (FDF) contours at steady state (time 24 s) for the run of 40% flow rate and top-half distribution at the inlet (note: vertical direction is enlarged 4 times).

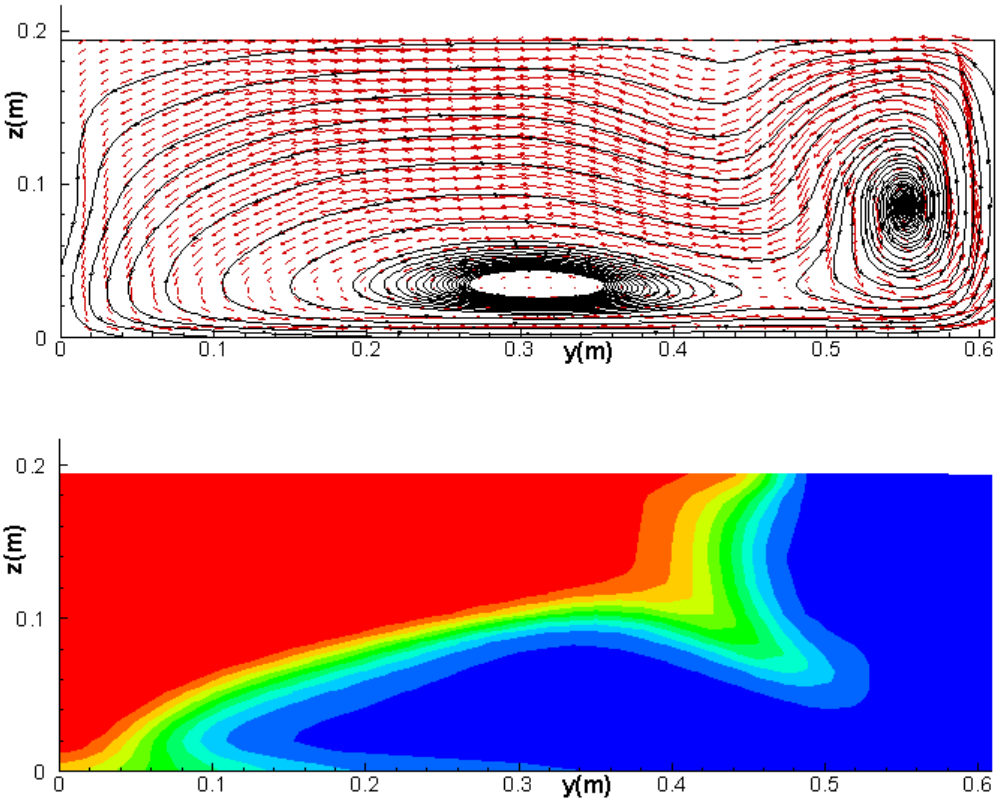

Figure 42.—Secondary flow and FDF distribution on the cross section 0.5 channel width upstream of the junction.

Fish entrainment through the side channel is quantitatively computed and results are shown in Figure 43. As expected, the fish entrainment rate of the bend case is like the attraction-side curve of the straight channel. This is due to the impact of the bend flow (i.e., secondary flow) which caused the top-surface fish redistributed towards the attraction-side of the channel before the junction. Fish efficiency is similarly moving towards the attraction-side curve of the straight channel, as shown in Figure 43.

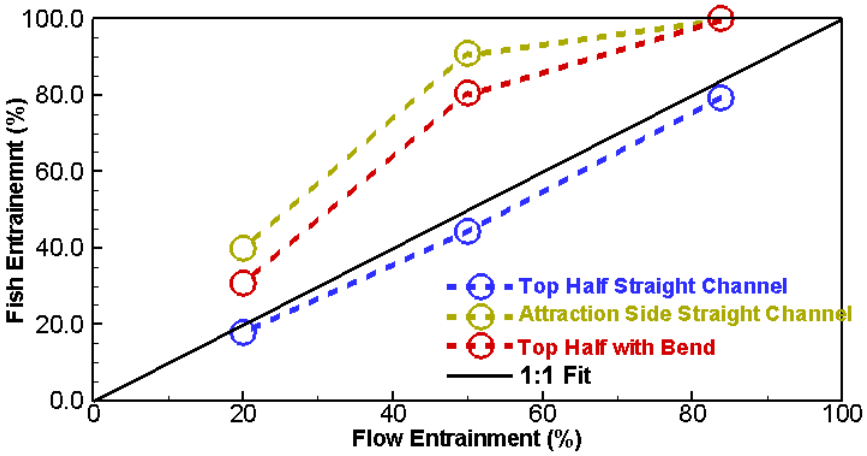

(a) Fish entrainment rate

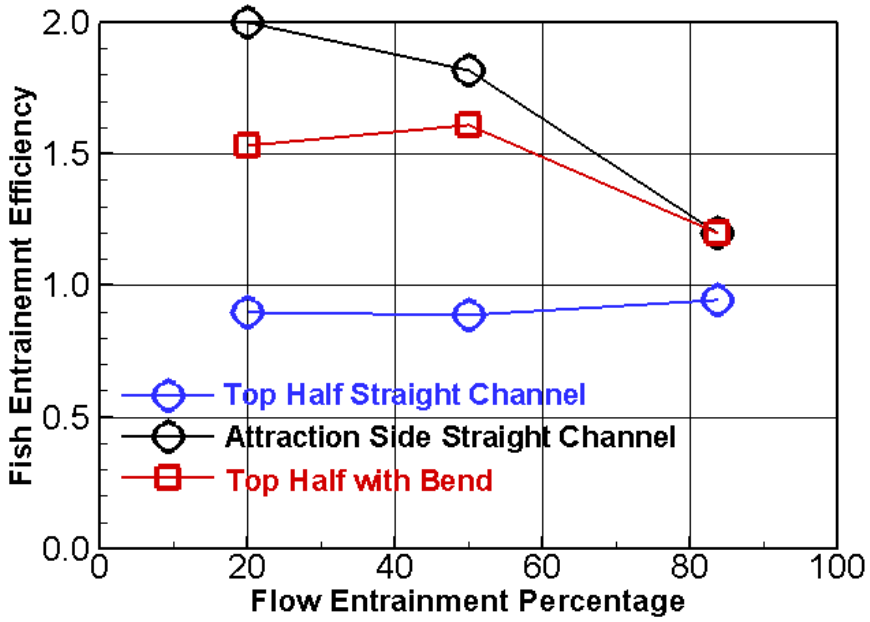

(b) Entrainment Efficiency

Figure 43.—Computed fish entrainment rate and efficiency with varying flow rate with the top-half fish distribution through a 180 deg bend before the junction, along with results from the straight channel.

5.4. Impact of Local Instream Structures on Fish Entrainment

The above results show that one way to attract or reject fish entrainment at a junction is to locally generate or disrupt a secondary circulation upstream of the junction. Such management options may be achieved by, for instance, using submerged vanes such as the Iowa vane, bendway weir, floating curtain, or large woody structures.

Submerged vanes are frequently used for applications such as bank erosion protection (Odgaard and Wang 1991a; b), sediment exclusion from water intake (Barkdoll 1997), and channel deepening for navigation (Wang 1991). For the interest of present study, these structures may be placed on stream beds upstream of a junction to create or reduce secondary current (Marelius and Sinha 1998). In the study of Daniels and Rhoads (2003), for example, the effect of submerged obstructions on secondary circulation in curved streams was demonstrated with the large woody structures. Both the location of the maximum velocity and strength of the secondary flow were altered. Perry et al. (2014) suggested that simple guiding structures, such as a floating boom, could be effective to shift the cross-stream fish distribution. For example, a floating log boom was successful at guiding migrating juvenile salmon toward a surface passage structure at the Lower Granite Dam on Snake River (Cash et al., 2002).

In this study, a simple straight plate vane is placed in the straight main channel upstream of the side channel; it is to demonstrate that a secondary flow may be generated by such a submerged vane. It is further shown, using the fish track model, that it may alter the entrainment rate through the side channel. The setup of the case is shown in Figure 44. The plate has a length of 0.5B, thickness of 0.01B, and 50% submerged. The center of the plate is about 1.612B upstream of the side channel and the plate has a 40^o angle from the flow direction. The study of Marelius and Sinha (1998) concluded that a 40^o angle is an optimum for such a purpose.

Simulation cases are selected corresponding to 20T, 50T and 84T of the no-vane cases in Section 5.1. That is, the flow entrainment is 20%, 50% and 83.8%, respectively, and the fish is distributed on the top half of the channel inlet. Simulated flow and FDF results with the 50% entrainment run are displayed in Figure 45 through Figure 47.

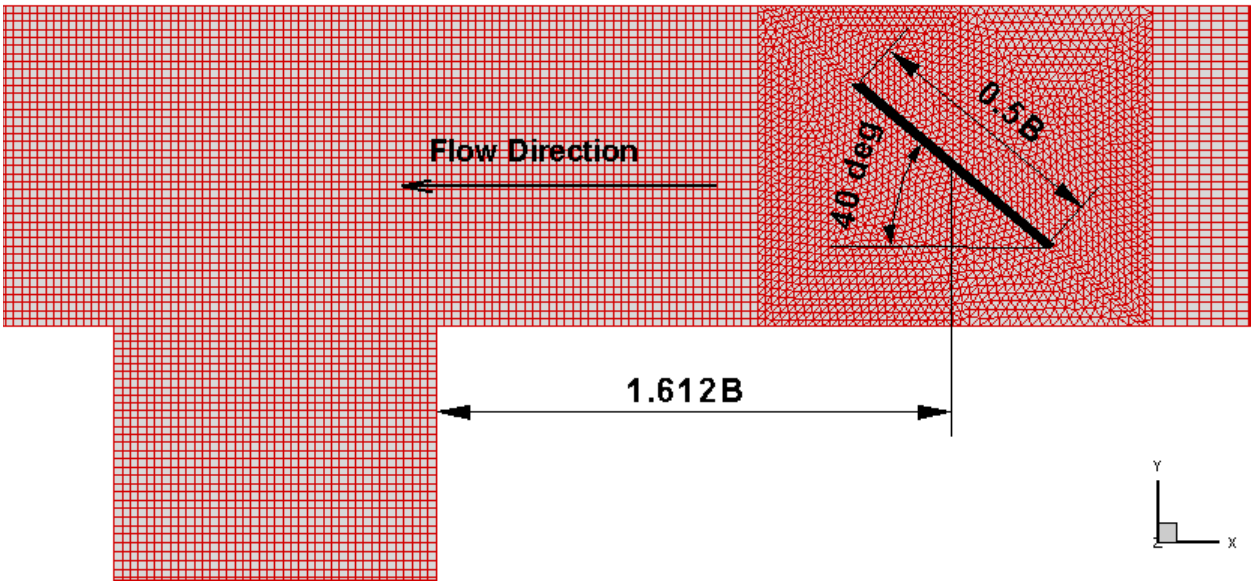

Figure 44.—Schematic of a straight vane placed in the middle of a main channel upstream of the side channel with 40-deg angle from the flow. B is the channel width

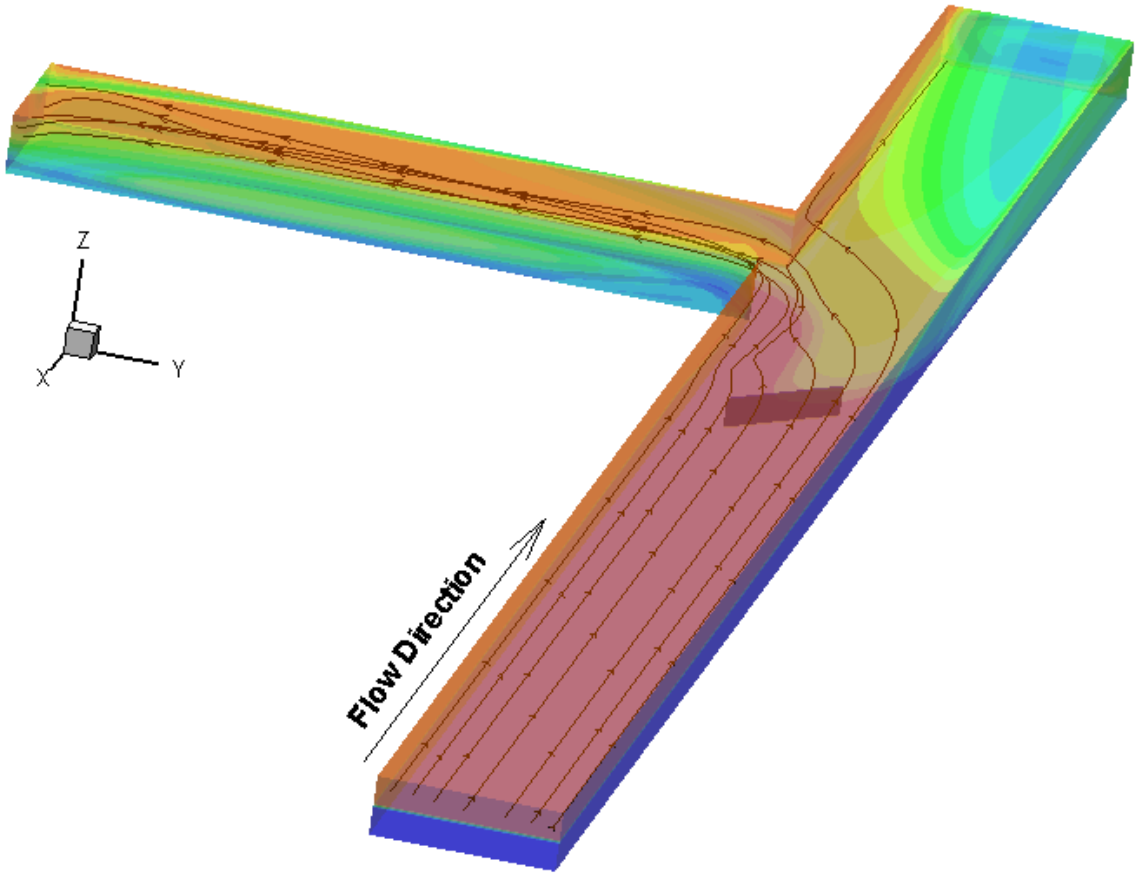

Figure 45.—3-D perspective view of FDF field and flow streamlines for the case of vane in the middle of the main channel.

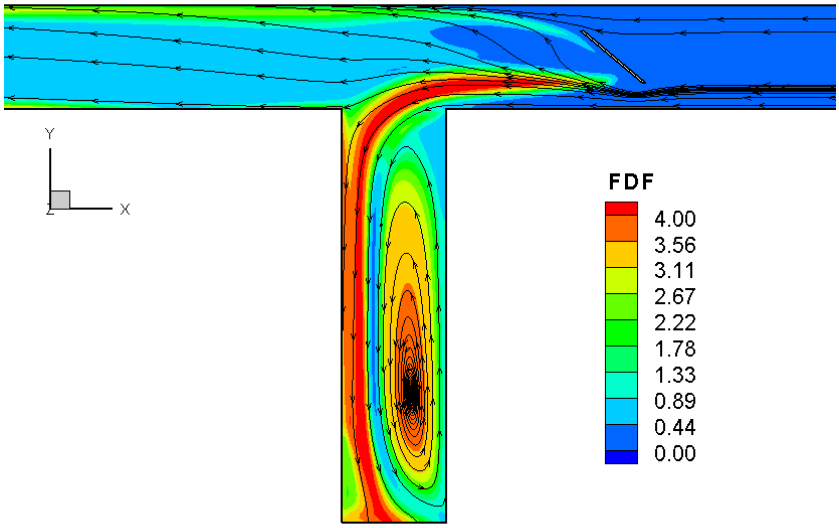

(a) Z = 0.05 m

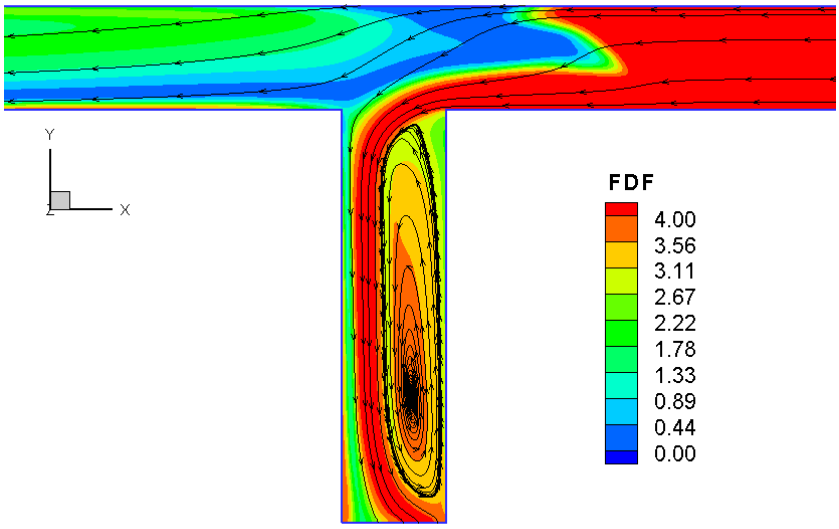

(b) Z = 0.15 m

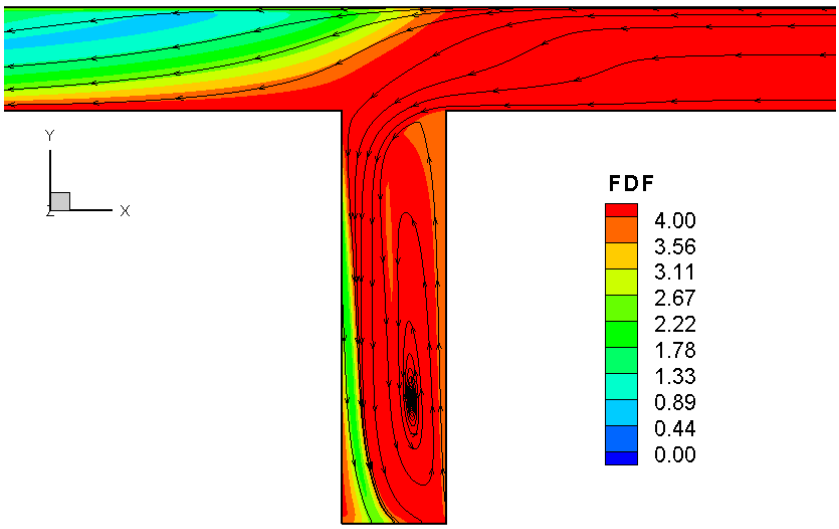

(c) At free surface (Z=0.19764 m)

Figure 46.—FDF distribution and flow streamlines at three horizontal planes for the case of vane in the middle of the main channel.

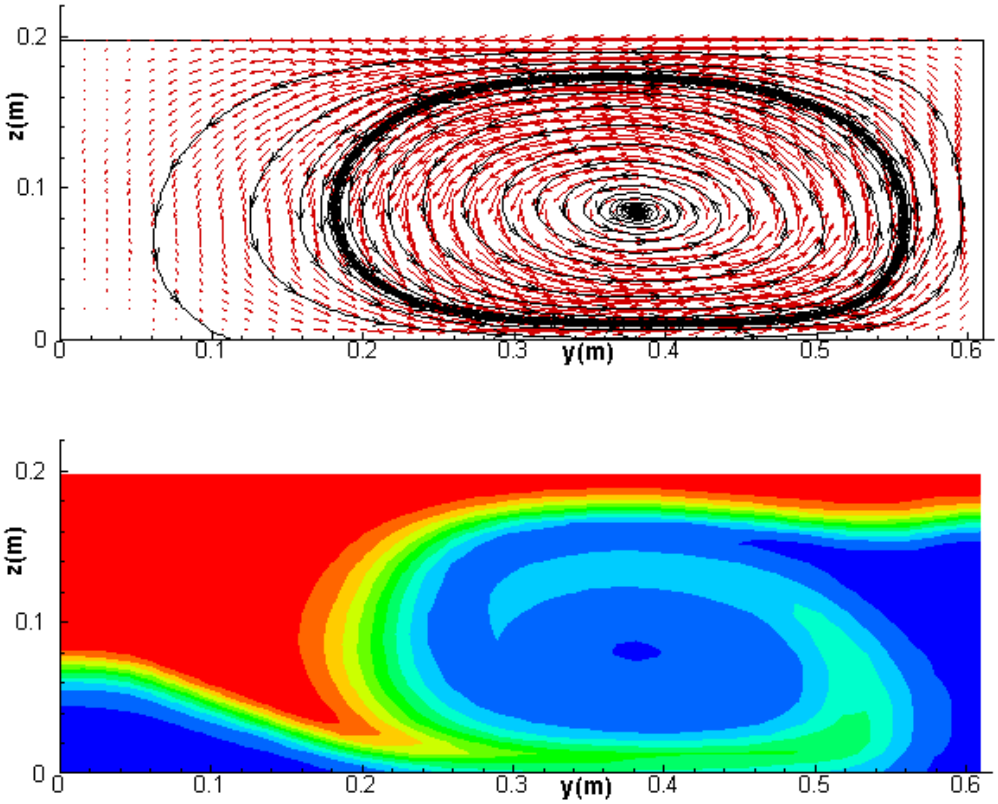

Figure 47.—Secondary flow (top) and FPF distribution (bottom) at the cross-section x=0.305m within the main channel (0.5B upstream of the side channel) for the case of vane in the middle of the main channel.

Fish entrainment through the side channel is also quantitatively computed and results are shown in Figure 48. As expected, the fish entrainment rate of the vane case is between the without-vane straight channel case and the without-vane entrainment-side fish distribution case. It is the consequence of top-surface fish redistributed towards the attraction side of the channel before the junction. Fish efficiency is similarly moving towards the attraction-side curve of the straight channel.

Other side channel entrance geometric features may be explored. For example, the entrance width may be studied. According to John et al. (2009), “in order to encourage schooling behavior, which has been associated with more direct passage habits, a route should be wide enough to accommodate the entire school of fish if fish passage is to be encouraged. Alternatively, a potential passage route may be designed to be narrower if the structure is to discourage fish passage.”

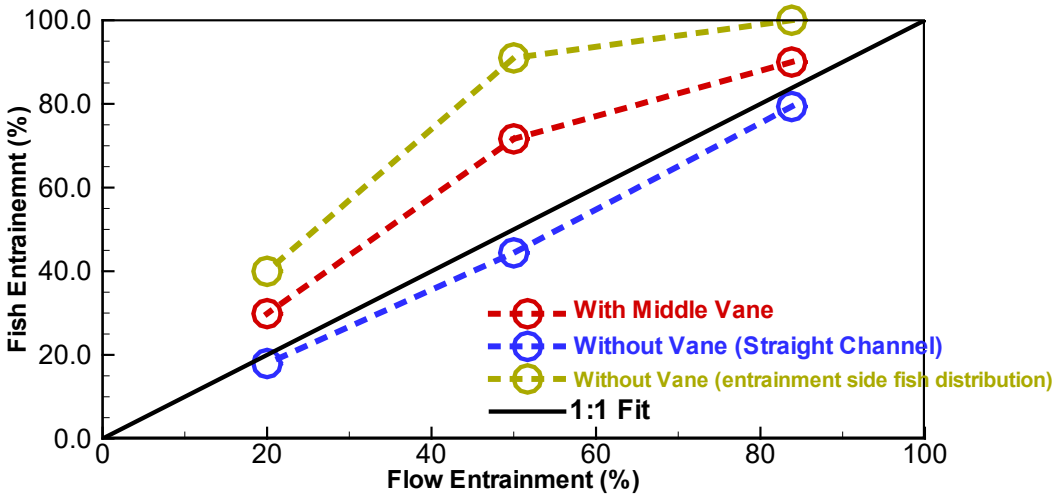

(a) Fish entrainment rate

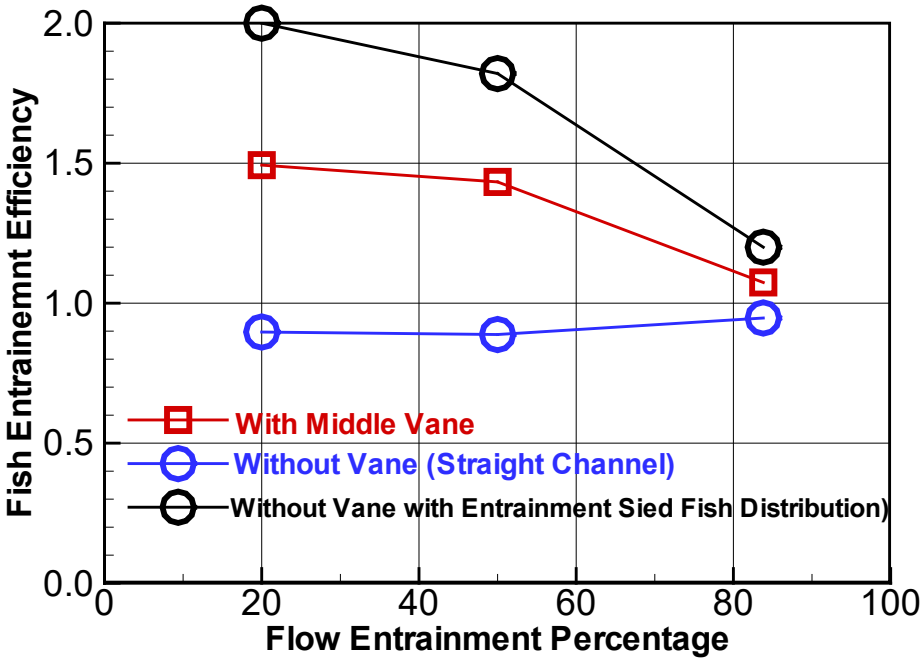

(b) Entrainment Efficiency

Figure 48.—Computed fish entrainment rate and efficiency with the top-half fish distribution through the straight main channel with a middle vane before the junction (results from the no-vane runs are also shown).

6.0 Fish Track Studies in the Field

In this chapter, field applications of the model tools are documented.

6.1. Study at Georgiana-Slough of the Sacramento River, CA

Background

Juvenile salmonids encounter multiple routes to the Pacific Ocean as they out-migrate downstream through California's San Joaquin and Sacramento rivers. Juvenile salmon that are routed through the interior delta may exhibit reduced survival from a number of stressors including: predation, water quality, water temperatures, and pumping facilities. Both physical barriers (PB) and non-physical barriers (NPB) for fish have been engineered to deter fish from sub-optimal routes (Bowen and Bark 2010; Zielinski et al. 2014). There are number of factors that have been identified to influence barrier effectiveness. The relative importance of many of these factors may vary spatially, temporally, and by the species of concern or the stage of life-cycle of the species. Estimates of the extent to which barrier effectiveness varies as a function of these factors is still an emerging science. Results from previous barrier studies at Georgiana Slough and elsewhere indicate that the barrier effectiveness is dependent on fine scale and bulk flow hydrodynamics. Therefore, good flow model results, coupled with fish track models, may be used to further the analysis of NPB and PB effectiveness to help develop reliable design criteria.

The junction of the Sacramento River and the Georgiana Slough, near Walnut Grove, California is selected as a case study. The flows at the junction are oscillatory and complex due to tidal influence, so the modeling is challenging. In this study, 3-D CFD modeling is carried out, and the flow results are then used as inputs to ELAM to systematically analyze how measured fish movement, using acoustic-tag telemetry, may be linked to the water flow patterns. Note that this study was a collaborative effort among multiple agencies. The study results have been documented by Goodwin et al. (2023) in which Dr. Lai was the second author. The paper, however, focused primarily on ELAM fish results. Therefore, the primary focus below is to document the flow results and ELAM results are only briefly summarized. Refer to Goodwin et al. (2023) for details of the ELAM results.

Study Site and ADCP Data

The study site is the junction of the Georgiana Slough and the Sacramento River, near Walnut Grove, California (Figure 49). In the figure, WGA, WGB, GEO and DCC are the river flow monitoring stations, corresponding to the U.S. Geologic Survey Station numbers 1447890, 11447905, 11447903, and 11336600, respectively. The Sacramento River flows southeast and turns west through a bend. Flow diversion to Georgiana Slough is on the south side of the bend. Flow at this area displays complex eddy patterns due to flow reversal from the Sacramento River branch caused by tides. Perry et al. (2014) stated that "Tidal forcing causes the Sacramento River

to reverse direction twice daily at river flows less than about 20,000 CFS (as measured at Freeport, U.S. Geological Survey station number 11447950). This tidal forcing can cause the relative distribution of flows among the three channels to vary over hourly time scales (note that during the time period this analysis was conducted the DCC gate was closed preventing flow from the Sacramento River). For example, nearly all of the river's flow is diverted into Georgiana Slough during reverse-flow flood tides." While these complex tidal flow patterns are occurring, the bulk flow in the Georgiana Slough branch is always unidirectional.

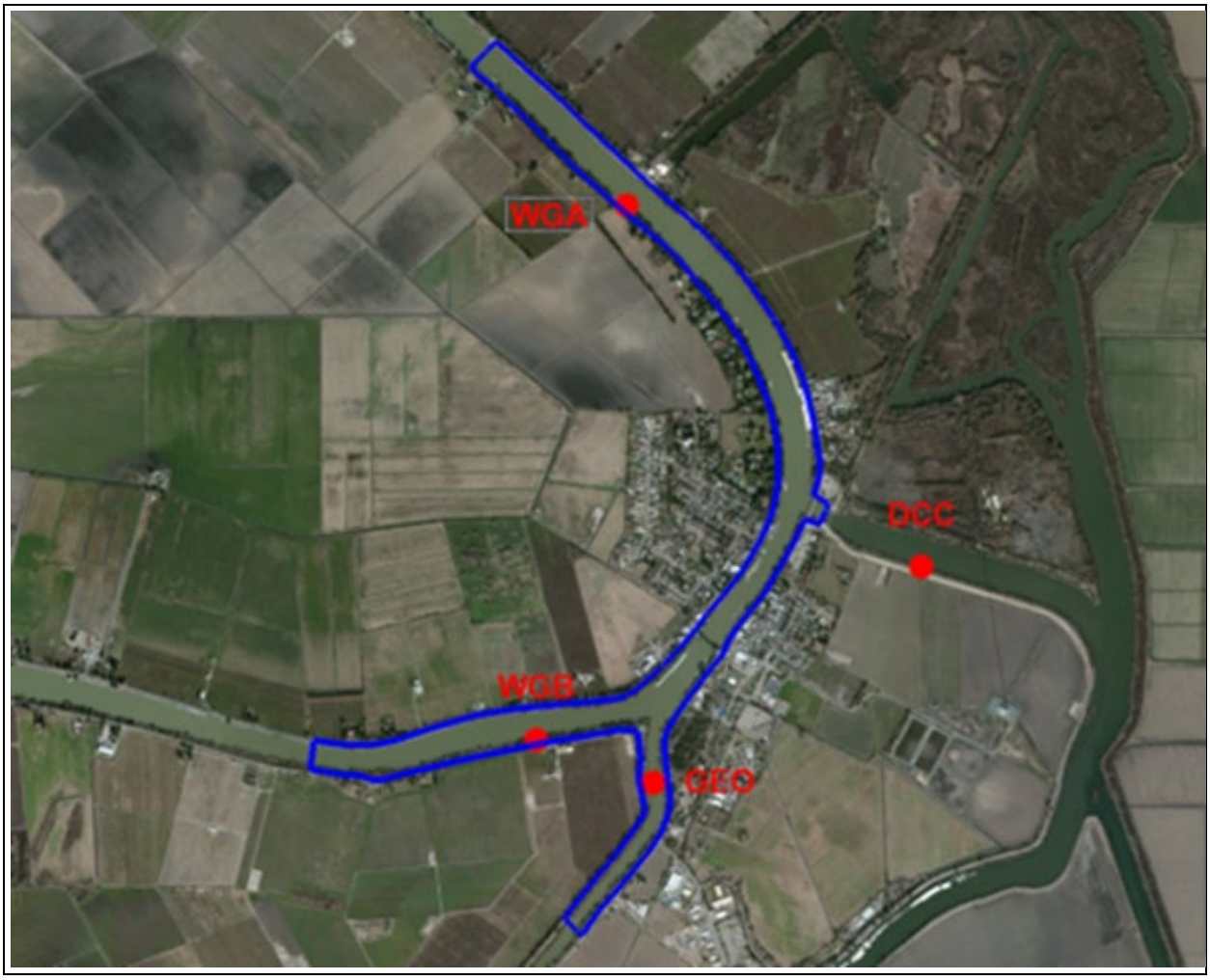

Figure 49.—Junction of Sacramento River and Georgiana Slough.

The bathymetric data of the study site was collected by CDWR's North Central Region Office (NCRO) on three separate trips in 2013 and 2014. The data set is used by the flow model to represent the river bathymetry. The river bathymetry is relatively stable.

Separate acoustic Doppler current profiler (ADCP) measurements were carried out by USGS engineers over number of years. A set of ADCP data measured on January 16, 2009 was available and is used for model validation. The ADCP data provides 3-D velocity at two transects (Figure 50) and at various times of the day.

The raw ADCP velocity must be properly processed to obtain the secondary flow patterns. The USGS team used VMT software available from the following website: http://hydroacoustics.usgs.gov/movingboat/VMT/VMT.shtml. The approach was described by Parsons et al. (2013). Different data processing approaches have led to different secondary flow patterns so the measured secondary flows can only be regarded as qualitative based on our discussion with the data collection engineers.

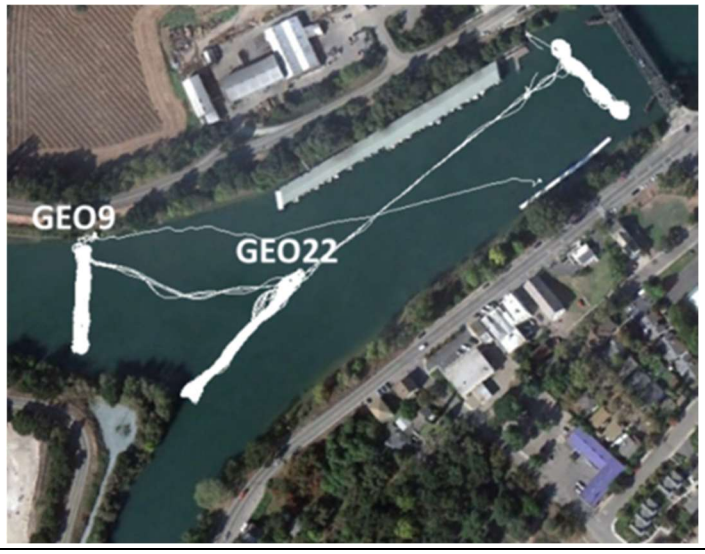

Figure 50.—Repeated ADCP measurement transects.

3-D Mesh Generation

3-D CFD modeling is carried out for the flow processes at the study site; the results are used as inputs to ELAM to understand fish movement behaviors. The model domain covers a 4.6 km (2.9 mile) reach of the Sacramento River (figure 49). A 2-D mesh, consisting of 36,362 cells, is generated first. The mesh size is about 3 meters by 3 meters at the junction area. 3-D mesh is then developed using the sigma-mesh approach. This means the horizontal mesh does not change but vertical coordinate changes with the free surface. The 3-D mesh at time zero is displayed in Figure 51 and it has about 1.3 million mesh cells.

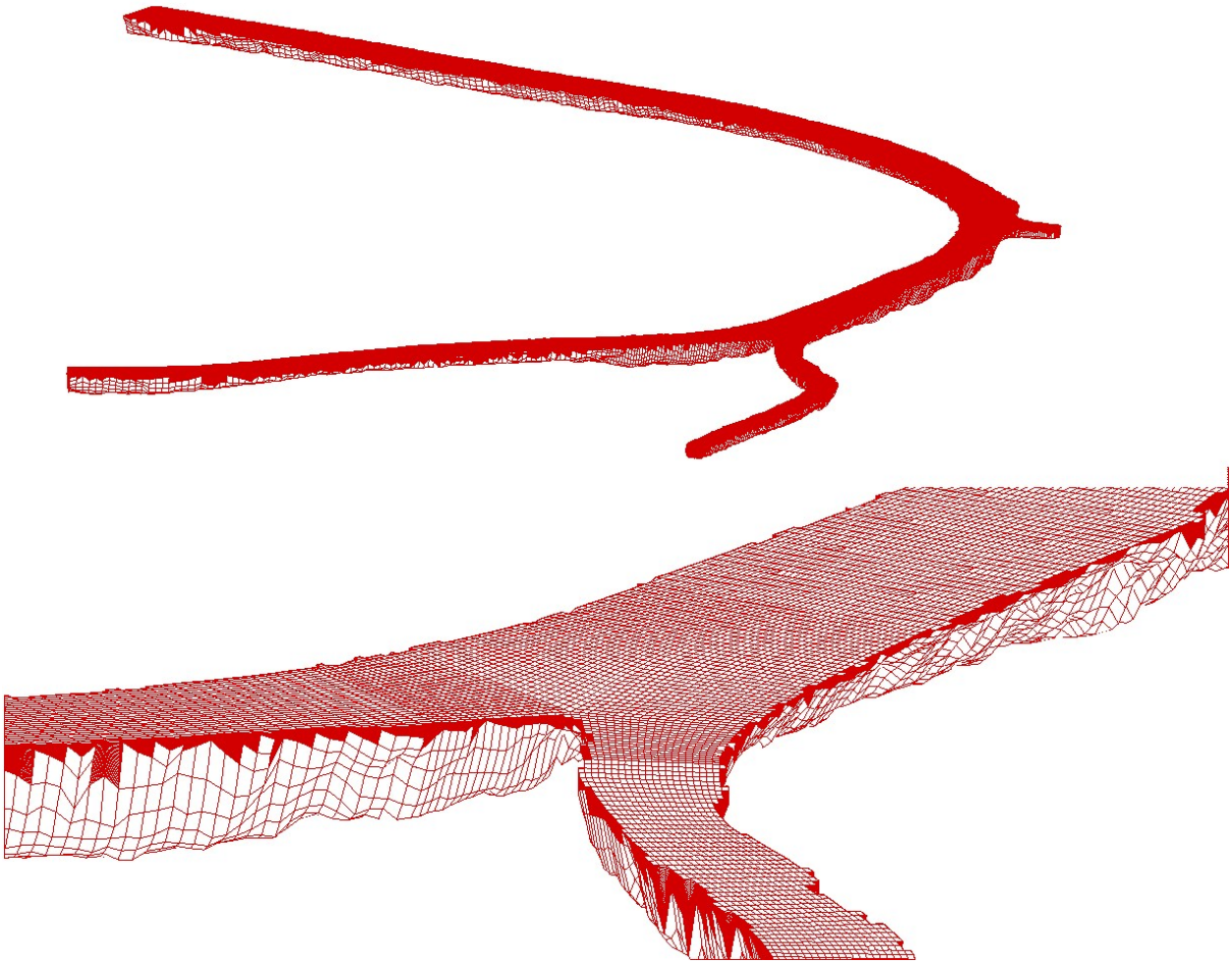

Figure 51.—3-D mesh at time zero (top is an overview and bottom is the zoom-in view).

Boundary Conditions

Flow discharge and water surface elevation are available at four nearby gauge stations (WGA, WGB, GEO and DCC in (figure 49); they provide the needed boundary conditions at the four open boundaries. The discharges on January 16, 2009 at the four boundaries are shown in Figure 52. Note that the flow reverses direction twice during the day.

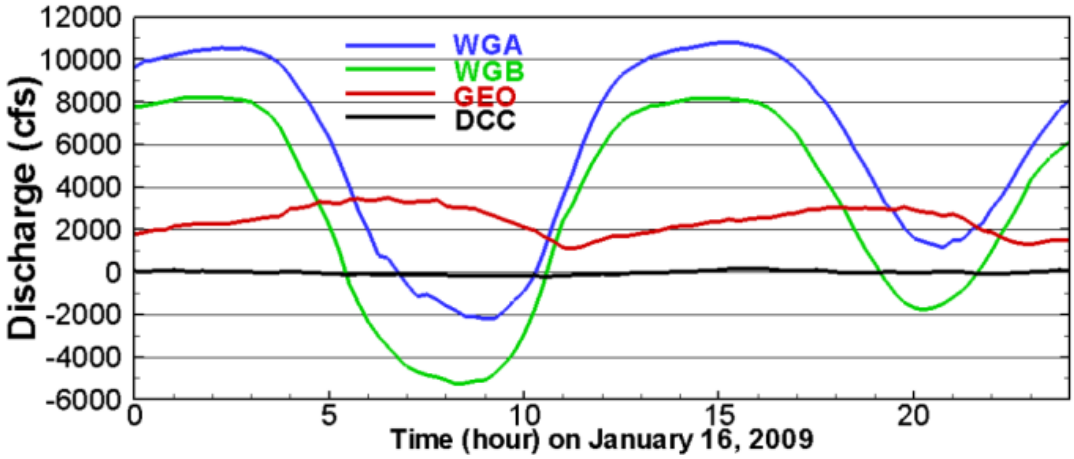

Figure 52.—Discharges at the four gages on January 16, 2009.

Results and Comparison

Unsteady 3-D flow modeling of the site is performed for the 24-hour period of January 16, 2009. The predicted velocity and flows patterns are shown in Figure 53 at two different times. At hour 3.5, the flow moves downstream along the Sacramento River; the flow, however, reverses its direction at hour 8.15.

According to the model, macroscale vortices and eddies are generated at the junction and change rapidly in time. The results have been animated to show the flow patterns and their changes. Snapshots of the animation at three different times of the day are shown in Figure 54, Figure 55, and Figure 56. The results demonstrate that complex multiple vortices are generated at the junction when flow reverses.

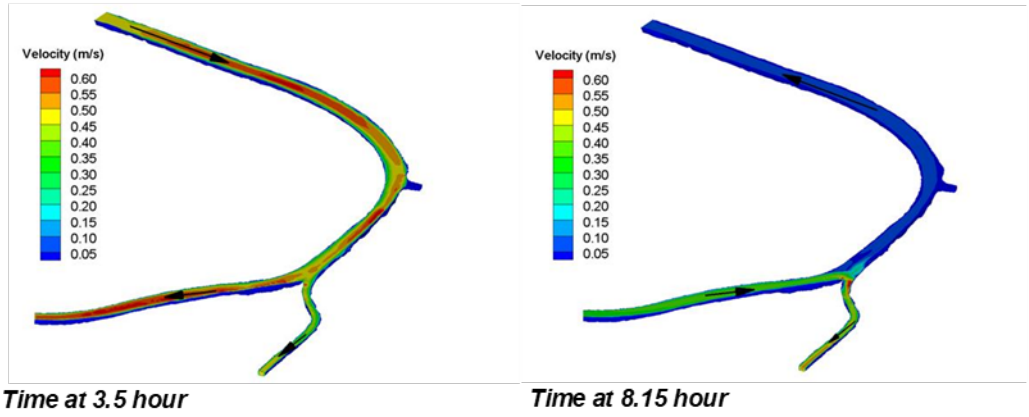

Figure 53.—3-D model predicted surface velocity.

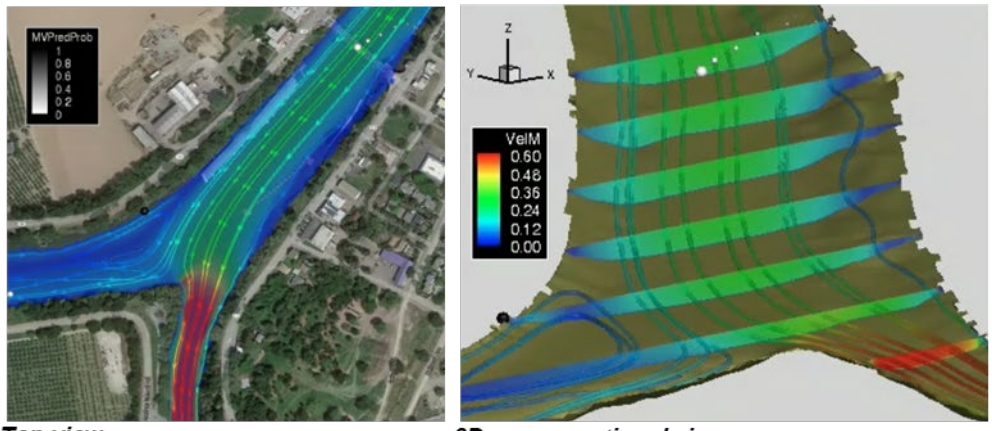

Top view *3D cross-sectional view*

Figure 54.—Flow patterns at time 5:20 am.

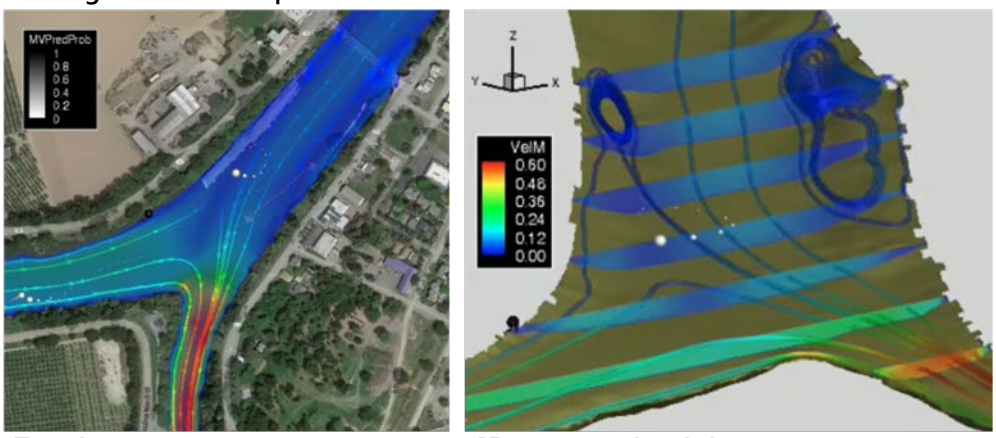

Top view *3D cross-sectional view*

Figure 55.—Flow patterns at time 6:17 am.

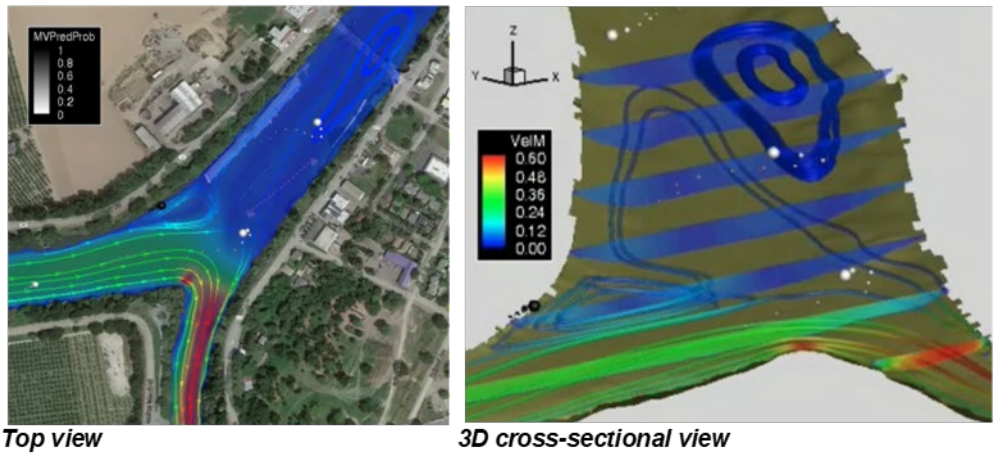

Top view *3D cross-sectional view*

Figure 56.—Flow patterns at time 6:53 am.

The CFD model results are next compared with the ADCP velocity data at two transects (GEO9 and GEO22 in Figure 57). Plan-view velocity is compared for GEO9 at hour 3.5 and for GEO22 at hour 8.15. The numerical model results are in satisfactory agreement with the ADCP data, with the major discrepancy at the tip of GEO22 which was caused by high uncertainty of bathymetry used in the area, along with the potential vegetation impacts on local flows.

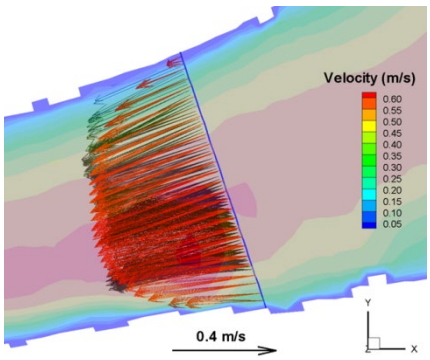

(a) Transect GEO9 at 3.5 hour

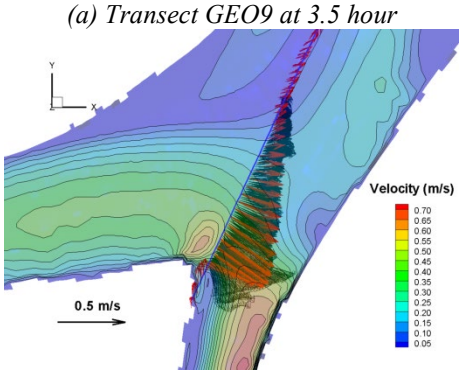

(b)Transect GEO22 at 8.15 hour

Figure 57.—Comparison of predicted and measured velocity (red: 3-D model results; black: ADCP).

Secondary flows are difficult to measure in the field. Much research and effort have been conducted on how to process the raw ADCP data so that reasonable secondary flow patterns may be extracted (Dinehart and Burau 2005a, b). Several methods were investigated and discussed by Parsons et al. (2013). Secondary flow pattern is compared at transect GEO9 at time 3.5 hour in Figure 58. In the plot, three different ADCP data processing methods are shown: “No Rotation” means the data are obtained as field measured and no velocity vector rotation is applied; “ZNSFDM” means that secondary flow is obtained by applying an extra constraint so that the net secondary discharge is zero; and “Rozovskii” means that the method of Rozovskii was applied in obtaining the secondary flow. The comparison shows that the 3-D model prediction is in qualitative agreement with the measured secondary flow data. However, secondary flows based on the ADCP data may have high variability as evidenced by the different results produced with different processing methods with the same ADCP data set.

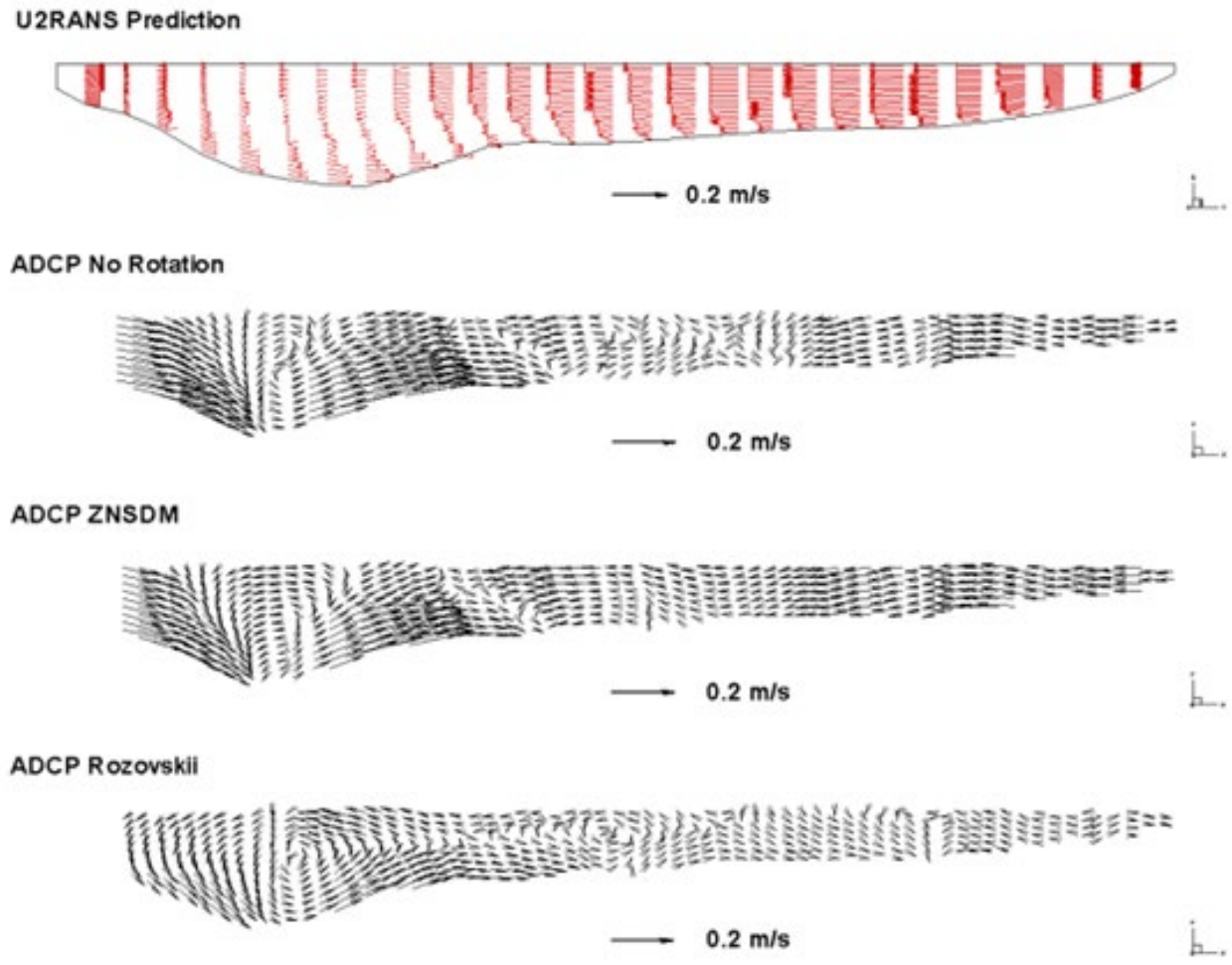

Figure 58.—Comparison of predicted (top) and measured secondary flow pattern at GEO9 at time 3.5 hour.

Fish Movement Behaviors

CFD flow results may be used to interpret fish movement behaviors that underly the route selection; that is, why some fish move downstream through the junction area along a path that leads to the Sacramento River while others move downstream through Georgiana Slough.

In the first step, ELAM is used in the passive-particle mode using the CFD flow output. By comparing the characteristics of measured fish trajectories against the simulated passive particles, an insight is gained into the decision-making of individual fish movement. The passive fish results suggest that numerical particles, released at the same times and positions that real fish are first observed (example Figure 59), enter Georgiana Slough in greater numbers than remain in the Sacramento River. The two time periods we evaluated are: 1-7 January 2009 (53.6%

Georgiana versus 46.4% Sacramento) and 16-22 January 2009 (55.8% Georgiana versus 43.5% Sacramento; 0.7% exit upstream).

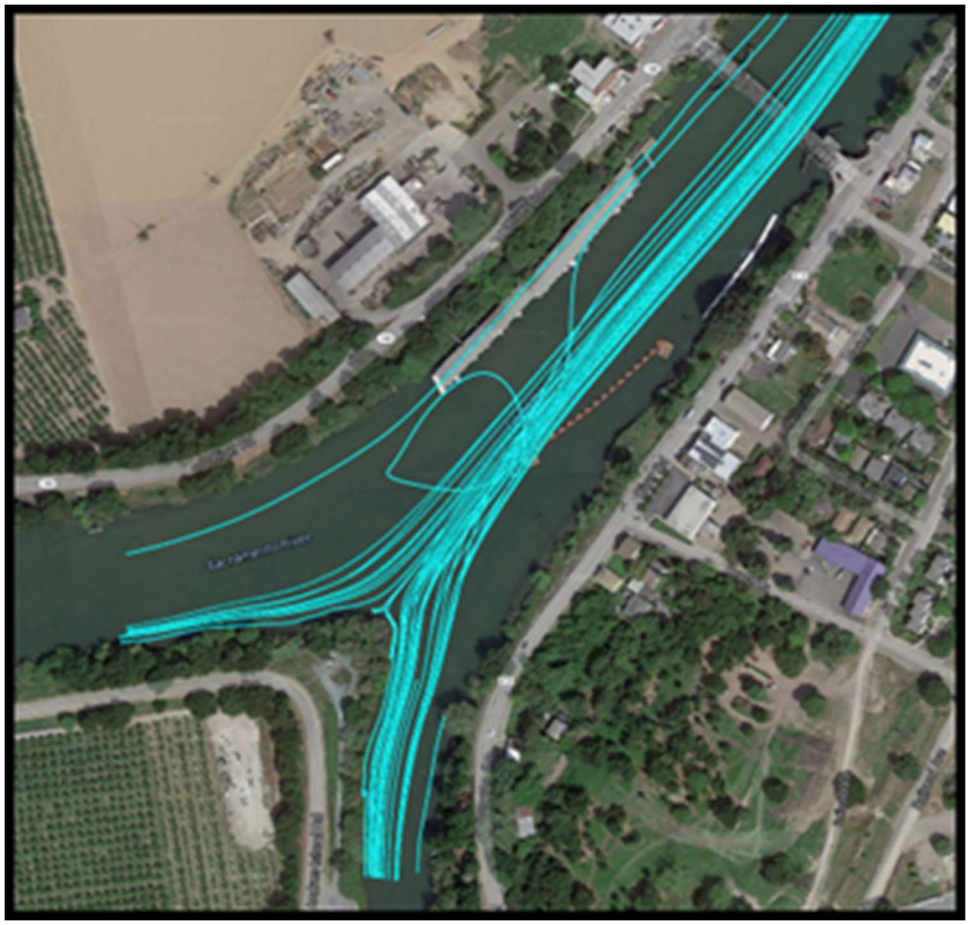

Figure 59.—Passive particles released on 16 January 2009 at the same times and positions that real fish are first observed. Here, particles are removed once they sufficiently pass into either channel.

A preliminary ELAM modeling, however, showed that addition of subtle fish behaviors can have a large effect on an individual's trajectory and ultimate fate within the river. Example fish movement results are shown in figure 60, by adding simple fish behavior rules in ELAM. This shows that there is a need to adopt the full ELAM capability, exploring fish behaviors.

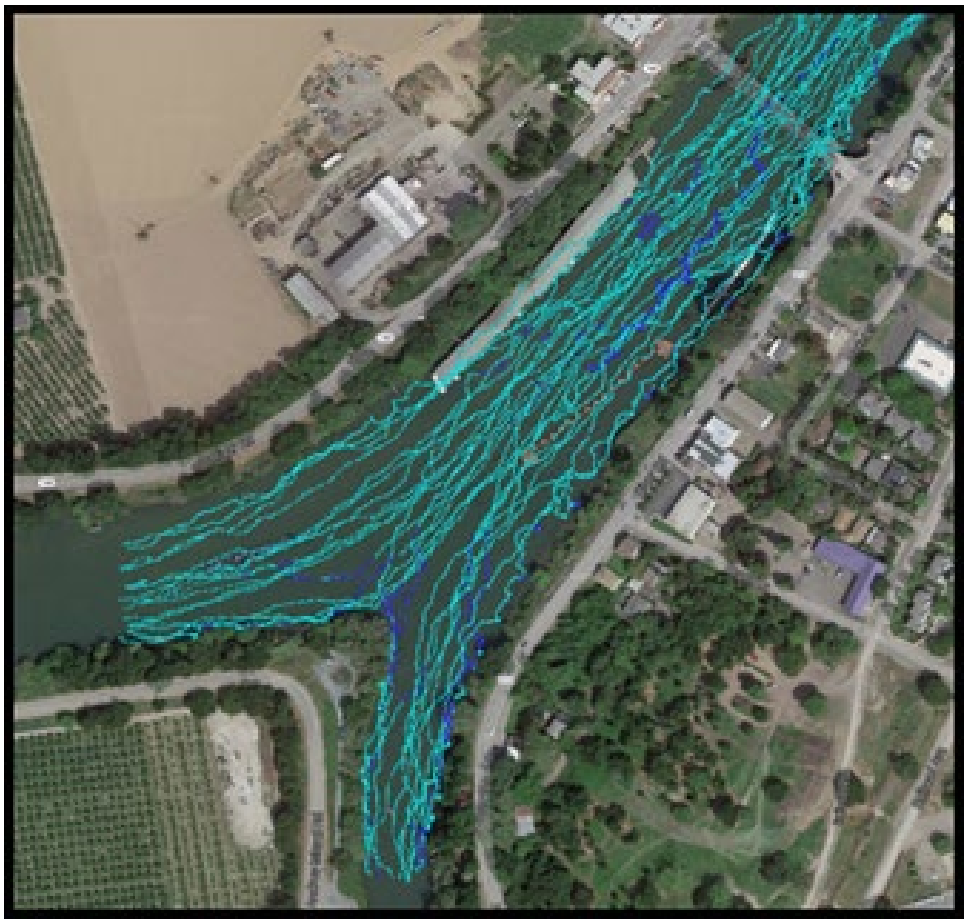

Figure 60.—Example of the same particles in Figure 59, but with a small amount of behaviors (B{1}: cyan; B{2}: blue from Goodwin et al. (2014) and movement stochasticity added to their trajectories.

In a second step, behavior rules are used to track the fish movement. The ELAM modeling process us as follows. ELAM dynamically extracts from the CFD results the hydraulic information for a given time period. Hydraulic data of the time period is then loaded into a behavior decision algorithm that computes a volitional orientation and speed for each fish. This volitional information is added to the passive movement for a given particle to compute the overall simulated 'fish' movement during the time period. For this study, ELAM uses a 2-second time step to compute fish movement behavior. The hydraulic information from the CFD model is at 3-min time intervals and interpolated in time and space to the fish and then interpreted by ELAM in the context of recent past hydraulic information and the recent experiences of the individual. Recent past information and experience contribute to the selection of one behavior among the alternative behaviors possible. The alternative behaviors that are explored in the study include four behaviors, $B\{1\text{-}4\}$, first proposed by Goodwin et al. (2014). Using $B\{1\text{-}4\}$ as the initial set of behaviors, the simplest suite of one or more behaviors are sought that can reproduce observed fish movement patterns. If no combination of $B\{1\text{-}4\}$ prove sufficient, other behaviors can be revised to replace $B\{1,2,3,4\}$.

The final ELAM results performed in the present Step 2 study have been documented in a journal paper in Goodwin et al. (2023). Only the Abstract of the journal paper is reproduced below; readers are referred to the paper itself for details.

Abstract of Goodwin et al. (2023):

"Predicting the behavior of individuals acting under their own motivation is a challenge shared across multiple scientific fields, from economic to ecological systems. In rivers, fish frequently change their orientation even when stimuli are unchanged, which makes understanding and predicting their movement in time-varying environments near built infrastructure particularly challenging. Cognition is central to fish movement, and our lack of understanding is costly in terms of time and resources needed to design and manage water operations infrastructure that is able to meet the multiple needs of human society while preserving valuable living resources. An open question is how best to cognitively account for the multi-modal, -attribute, -alternative, and context-dependent decision-making of fish near infrastructure. Here, we leverage agent- and individual-based modeling techniques to encode a cognitive approach to mechanistic fish movement behavior that operates at the scale in which water operations river infrastructure is engineered and managed. Our cognitive approach to mechanistic behavior modeling uses a Eulerian-Lagrangian-agent method (ELAM) to interpret and quantitatively predict fish movement and passage/entrainment near infrastructure across different and time-varying river conditions.

A goal of our methodology is to leverage theory and equations that can provide an interpretable version of animal movement behavior in complex environments that requires a minimal number of parameters in order to facilitate the application to new data in real-world engineering and management design projects. We first describe concepts, theory, and mathematics applicable to animals across aquatic, terrestrial, avian, and subterranean domains. Then, we detail our application to juvenile Pacific salmonids in the Bay-Delta of California. We reproduce observations of salmon movement and passage/entrainment with one field season of measurements, year 2009, using five simulated behavior responses to 3-D hydrodynamics. Then, using the ELAM model calibrated from year 2009 data, we predict the movement and passage/entrainment of salmon for a later field season, year 2014, which included a novel engineered fish guidance boom not present in 2009.

Central to the fish behavior model's performance is the notion that individuals are attuned to more than one hydrodynamic signal and more than one timescale. We find that multi-timescale perception can disentangle multiplex hydrodynamic signals and inform the context-based behavioral choice of a fish. Simulated fish make movement decisions within a rapidly changing environment without global information, knowledge of which direction is downriver/upriver, or path integration. The key hydrodynamic stimuli are water speed, the spatial gradient in water speed, water acceleration, and fish swim bladder pressure. We find that selective tidal stream transport in the Bay-Delta is a superset of the fish-hydrodynamic behavior repertoire that reproduces salmon movement and passage in dam reservoir environments.

From a cognitive movement ecology perspective, we describe how a behavior can emerge from a repertoire of multiple fish-hydrodynamic responses that are each tailored to suit the animal's recent past experience (localized environmental context).

From a movement behavior perspective, we describe how different fish swim paths can emerge from the same local hydrodynamic stimuli. Our findings demonstrate that a cognitive approach to mechanistic fish movement behavior modeling does not always require the maximum possible spatiotemporal resolution for representing the river environmental stimuli although there are concomitant tradeoffs in resolving features at different scales. From a water operations perspective, we show that a decision-support tool can successfully operate outside the calibration conditions, which is a necessary attribute for tools informing future engineering design and management actions in a world that will invariably look different than the past."

6.2. Study at the Fremont Weir of the Sacramento River, CA

The flow results produced by Dr. Lai have also been used for ELAM fish track modeling at the Fremont Weir section of the Sacramento River, California – the objective is to perform a fish entrainment study for the evaluation of the best notch design along the Fremont Weir.

Flow modeling was performed by Dr. Lai and the key results are discussed in chapter 4 already. ELAM modeling was performed by David Smith at USACE, through a collaborative agreement; the results were documented separately in Smith et al. (2017). Readers are referred to the USACE report for details as it is not repeated here.

For reference purpose, the abstract of the USACE report is reproduced below (Smith et al. 2017):

"The United States Bureau of Reclamation and the California Department of Water Resources are planning a notch in the Fremont Weir on the Sacramento River. The notch is intended to provide access to the Yolo Bypass floodplain for juvenile salmon across a range of flows and to provide passage for adult anadromous fishes, and to increase floodplain inundation. This study estimated the entrainment rate of 12 separate notch scenarios. Entrainment estimates vary from approximately 1 to 25%. Across all scenarios larger notch flows entrain greater fish numbers, although not proportionally to the volume through the notch. West located notches entrain more fish than central and east and intakes perform better than shelfs. However, intakes and shelfs both performed poorly, regardless of notch flows, when intake channels were angled from the mainstem. Entrainment estimates are comparable to measured entrainment rates elsewhere in the Sacramento River suggesting that the modeled estimates are reasonable. The results further suggest that the approach used is valuable for incorporating structural modifications and evaluating expected outcomes." .

7.0 References

Acierto, K.A., J. Israel, J. Ferreira, and J. Roberts. 2014. Estimating juvenile winter-run and spring-run Chinook Salmon entrainment onto the Yolo Bypass over a notched Fremont Weir. *California Fish and Game* 100 (4): 630–639.

Acosta, M., M. Anguita, F.J. Rueda, and F. Fernández-Valdomero. 2010. Parallel implementation of a semi-implicit 3-D lake hydrodynamic model. In Proc., Int. Conf. on Computational and Mathematical Methods in Science and Engineering, 1026–1037. Madrid, Spain: Addlink/COMSOL.

Arenasa, A., Politano, M., Weber, L., and Timko, M. 2015. Analysis of movements and behavior of smolts swimming in hydropower reservoirs. Ecological Modelling, 312:292-307.

Babagoli Sefidkoohia, R., Shahidib, A., Ramezani, Y., Kahed, M. 2017. Simulation of flow pattern in intake by using a numerical model. Water Harvesting Research, 2(1): 24-36. DOI: 10.22077/jwhr.2017.593

Barkdoll, B.D., Hagen, B.L. and Odgaard, A.J. 1998. Experimental comparison of dividing open-channel with duct flow in T-Junction. *Journal of Hydraulic Engineering, ASCE* 124: 92–95.

Bellmore J.R., Baxter C.V., Martens K., Connolly P.J.2013. The floodplain food web mosaic: a study of its importance to salmon and steelhead with implications for their recovery. Ecological Application 23:189–207

Bever, A.J., and MacWilliams, M.L.2015. Factors Influencing the Calculation of Periodic Secondary Circulation in a Tidal River: Numerical Modelling of the Lower Sacramento River, USA. Hydrological Processes.

Blake, A., and M.J. Horn. 2004. Acoustic tracking of juvenile Chinook salmon movement in the vicinity of the delta cross channel, Sacramento river, California—2001 study results. USGS Open-File Rep. USGS. Washington, DC:

Blake, A., J.R. Burau, and N.S. Adams. 2012. “Outmigration behavior of juvenile Chinook salmon in a river bend in the Sacramento river at Clarksburg, California.” In Proc., Fisheries Networks: Building Ecological, Social, and Professional Relationships. 142nd Annual Meeting of the American Fisheries Society, Minneapolis, MN.

Blake, A., P. Stumpner and J. Burau. 2017. A Simulation Method for Combining Hydrodynamic Data and Acoustic Tag Tracks to Predict the Entrainment of Juvenile Salmonids onto the Yolo Bypass Under Future Engineering Scenarios. USGS. West Sacramento, California: 105.

Bowen, M.D. & Bark, R. 2010. 2010 Effectiveness of a Non-Physical Fish Barrier at the Divergence of the Old and San Joaquin Rivers (California). Technical Memorandum 86-68290-10-07, Bureau of Reclamation.

Brandes P.L., McLain J.S. 2001. Juvenile Chinook salmon abundance, distribution, and survival in the Sacramento-San Joaquin Estuary. In: Brown, R.L ed. Contributions to the Biology of Central Valley Salmonids. Fish Bulletin 179, pp 39-99

Buchanan R.A., Skalski J.R., Brandes P.L., Fuller A. 2013 Route use and survival of juvenile Chinook salmon through the San Joaquin River Delta. N Am J Fish Manag 33: 216–229

Buckley, J., & Kynard, B. 1985. Vertical distribution of juvenile American Shad and Blueback Herring during the seaward migration in the Connecticut River. Massachusetts Cooperative Fishery Research Unit, Department of Forestry and Wildlife Management, Amherst, Maryland.

Bulle, H. 1926. Untersuchungen uber die Geschiebeableitung bei der Spaltung von Wasserlaufen. VDI Verlag, Berlin (in German).

Carlson A.J., Rahel F.J. 2007. A basin wide perspective on entrainment of fish in irrigation canals. T Am Fish Soc 136:1335–1343

Cash, K.M., Adams, N.S., Hatton, T.W., Jones, E.C., Rondorf, D.W. 2002. Three dimensional fish tracking to evaluate the operation of the Lower Granite surface bypass collector and behavioral guidance structure during 2000. US Geological Survey Report to U.S. Army Corps of Engineers: Walla Walla, Washington; 73.

Cavallo, B., P. Gaskill, J. Melgo, and S.C. Zeug. (2015). Predicting juvenile Chinook salmon routing in riverine and tidal channels of a freshwater estuary. Environ. Biol. Fishes 98 (6): 1571–1582. https://doi.org/10.1007/s10641-015-0383-7.

Coutant C.C. 2001a. Behavioral technologies for fish guidance. American Fisheries Society, Symposium 26: Bethesda, Maryland.

Coutant C.C. 2001b. Integrated, multi-sensory, behavioral guidance systems for fish diversions. In Behavioral technologies for fish guidance, Coutant CC (ed.). American Fisheries Society, Symposium 26: Bethesda, Maryland; 105–114.

Crowder, D.W., and P. Diplas. 2000. Evaluating spatially explicit metrics of stream energy gradients using hydrodynamic model simulations. Can. J. Fish. Aquat. Sci. 57 (7): 1497–1507. https://doi.org/10.1139/f00-074.

Crowder, D.W., and P. Diplas. 2002. "Vorticity and circulation: Spatial metrics for evaluating flow complexity in stream habitats." Can. J. Fish. Aquat. Sci. 59 (4): 633–645. https://doi.org/10.1139/f02-037.

Dabiri, J.O. 2017. Biomechanics: How fish feel the flow. Nature 547:406-407.

Daniels, M.D., and Rhoads, B.L. 2003. Influence of a large woody debris obstruction on three-dimensional flow structure in a meander bend. Geomorphology 51 (1): 159–173. https://doi.org/10.1016/S0169-555X(02)00334-3.

Dinehart, R.L. & Burau, J.R. 2005b. Averaged indi-cators of secondary flow in repeated acoustic Doppler current profiler crossings of bends. Water Resource Research, 41(9), pp.1-18.

Dutta, S. 2017. Bulle-Effect and Its Implications for Morphodynamics of River Diversions.

DWR (California Department of Water Resources). 2017. Evaluating juvenile Chinook Salmon entrainment potential for multiple modified Fremont Weir configurations: Application of Estimating juvenile winter-run and spring-run Chinook Salmon entrainment onto the Yolo Bypass over a notched Fremont Weir, Acierto et al. (2014). Technical memorandum for the Yolo Bypass Salmonid Habitat Restoration and Fish Passage Project. Sacramento, California.

Dynamic Solutions LLC. 2011. Hydrodynamic Model of the Sacramento River from Freeport to Wilkins Slough using AdH and Delta EFDC-ELAM Model Linkage. Project Report, Knoxville, Tennessee.

Faber, D., Weiland, M., Moursund, R., and Carlson, T. 2001. Evaluation of the Fish Passage Effectiveness of the Bonneville I Prototype Surface Collector using Three-Dimensional Ultrasonic Fish Tracking. US Army Corps of Engineers, Pacific Northwest Laboratory.

Faber, D.M., Ploskey, G.R., Weiland, M.A., Deng, D., Hughes, J.S., Kim, J., Skalski, J.R. 2011. Evaluation of behavioral guidance structure on juvenile salmonid passage and survival at Bonneville Dam in 2009. Richland, WA: Pacific Northwest National Laboratory.

Friesen, T., Vile, J., & Pribyl, A. 2007. Outmigration of juvenile Chinook salmon in the lower Willamette River, Oregon. Northwest Scientist 81:173-190.

Gohari, S. (2012). Laboratory investigation of separation line at the intake sand its relation to sediment control. 9th Int. Congress on Civil Engineering, Isfahan University of Technology, Isfahan, Iran.

Goodwin, R. A. 2004. Hydrodynamics and juvenile salmon movement behavior at Lower Granite Dam: decoding the relationship using 3-D space-time (CEL Agent IBM) simulation. Ph.D. Dissertation. Cornell University, Ithaca, New York.

Goodwin, R.A., J.M. Nestler, J.J. Anderson, L.J. Weber, and D.P. Loucks. 2006. Forecasting 3-D fish movement behavior using a Eulerian-Lagrangian-agent method (ELAM). Ecological Modelling. Ecol. Modell. 192 (1–2):197–223. https://doi.org/10.1016/j.ecolmodel.2005.08.004.

Goodwin, R.A., M. Politano, J.W. Garvin, J.M. Nestler, D. Hay, J.J. Anderson, L.J. Weber, E. Dimperio, D.L. Smith, and M.A. Timko. 2014. Fish navigation of large dams emerges from their modulation of flow field experience. Proceedings of the National Academy of Sciences of the United States of America 111:5277-5282.

Goodwin, R.A., Lai, Y., Smith, D.L., Reeves, R., and McQuirk, J. 2018. Juvenile salmon movement/passage through the tidal free-flowing Georgiana Slough and Sacramento River junction emerge from swim orientation based on their recent past experience in water speed, the velocity gradient, water acceleration, and pressure. Final Report.

Goodwin, R.A., Lai, Y., Taflin, D.E., Smith, D.L., McQuirk, J., Trang, R., and Reeves, R. 2023. Predicting near-term, out-of-sample fish passage, guidance, and movement across diverse river environments by cognitively relating momentary behavioral decisions to multiscale memories of past hydrodynamic experiences. Front. Ecol. Evol. 11:703946. doi: 10.3389/fevo.2023.703946

Grace, J.L., and Priest, M.S. 1958. Division of flow in open channel junctions. Bulletin No. 31, Engineering Experimental Station, Alabama, Polytechnic Institute, Auburn, Ala.

Gualtieri, C., M. Ianniruberto, N. Filizola, R. Santos, and T. Endreny. 2017. Hydraulic complexity at a large river confluence in the Amazon basin. Ecohydrology 10 (7): e1863. https://doi.org/10.1002/eco.1863.

Hager, W.H. 1984. An approximate treatment of flow in branches and bends. Proc., Instn. Mech, Engrs., 198C(4), 63–69.

Hammack, E.A., Threadgill, T.L., Smith, D.L., & Sanborn, S. 2013a. Calibration of a Two-Dimensional Hydraulic Model of the Sacramento River Using a Coarse , Large Domain Mesh – Data Report. Vicksburg, MS.

Hammack, E.A., Threadgill, T. L., Smith, D. L., & Sanborn, S. 2013b. Calibration of a Two-Dimensional Hydraulic Model of the Sacramento River Using a Refined , Small Domain Mesh – Data Report. Vicksburg, MS.

Hance, D.J., Perry, R.W., Burau, J.R., Blake, A., Stumpner, P., Wang, X., Pope, A. 2020. Combining Models of the Critical Streakline and the Cross-Sectional Distribution of Juvenile Salmon to Predict Fish Routing at River Junctions. San Franc Estuary Watershed Sci.18(1):3. https://doi.org/10.15447/sfews.2020v18iss1art3

Heer, A. de, Mosselman, E. 2004. Flow structure and bedload distribution at alluvial diversions. River Flow 2004, Second International Conference on Fluvial Hydraulics, Napoli, Italy, 1:801-806.

Huusko, R. 2018. *Downstream Migration of Salmon Smolts in Regulated Rivers: Factors Affecting Survival and Behaviour.* University of Oulu, Thesis for PhD A-709.

Issa, R.I., and Oliveira, P.J. 1994. Numerical Prediction of Phase Separation in Two-Phase Flow Through T-Junction. Computers Fluids Vol. 23, No. 2, pp. 347-372.

Jeffres CA, Opperman JJ,Moyle P.B. 2008. Ephemeral floodplain habitats provide best growth conditions for juvenile Chinook salmon in a California river. Environ Biol Fish 83:449–458

Kemp, P.S., Gessel, M.H., and Williams, J. G. 2005. Fine-scale behavior responses of pacific salmonid smolts as they encounter divergence and acceleration of flow. Transactions of the American Fisheries Society, 134(2), 390-398.

Lai, Y.G. 2000. Unstructured Grid Arbitrarily Shaped Element Method for Fluid Flow Simulation. AIAA Journal, 38 (12): 2246-2252.

Lai, Y.G., Weber, L.J., Patel, V.C. 2003a. Non-Hydrostatic Three-Dimensional Method for Hydraulic Flow Simulation - Part I: Formulation and Verification. J. Hydraulic Engineering, 129(3): 196-205.

Lai, Y.G., Weber, L.J., Patel, V.C. 2003b. Non-Hydrostatic Three-Dimensional Method for Hydraulic Flow Simulation - Part II: Application. J. Hydraulic Engineering, 129(3): 206-211.

Lai, Y.G. 2008. SRH-2D version 2: Theory and User's Manual, Sedimentation and River Hydraulics Group, Technical Service Center, Bureau of Reclamation, Denver, CO 80225. website: www.usbr.gov/pmts/sediment/

Lai, Y.G. 2010. "Two-Dimensional Depth-Averaged Flow Modeling with an Unstructured Hybrid Mesh." J. Hydraulic Engineering, ASCE, 136(1), 12-23.

Lai, Y.G., and Bandrowski, D.J. 2014. Large Wood Flow Hydraulics: a 3-D Modelling Approach. Proc. 7th International Congress on Environmental Modelling and Software, International Environmental Modelling and Software Society, San Diego, California, D.P. Ames, N. Quinn (Eds.).

Lai, Y.G., Smith, D.L., Bandrowski, D.J., Liu, X., Wu, K. 2017a. Three Dimensional Computational Modeling of Flows through an Engineered Log Jam. ASCE World Environmental and Water Resources Congress, Sacramento, California, May 21-25, 2017.

Lai, Y.G., Goodwin, R.A., Smith, D.L., Reeves, R.L. 2017b. Complex Unsteady Flow Patterns at a River Junction and Their Relation with Fish Movement Behavior." ASCE World Environmental and Water Resources Congress, Sacramento, California, May 21–25, 2017.

Larinier, M., & Travade, F. 2002. Downstream Migration: Problems and Facilities. Bulletin Francias de la Penche et de la Pisciculture 364 Suppl:181-207 Ch.13.

Launder, B.E., and Spalding, D.B. 1974. The numerical computation of turbulent flows. Comput. Methods Appl. Mech. Eng., 3, 269–289.

Law, S.W., and Reynolds, A.J. 1966. Dividing flow in an open channel. J. Hydr. Div., 92(2), 4730–4736.

Liepsch, D., Moravec, S., Rastogi, A.K., and Vlachos, N.S. 1982. Measurement and Calculations of Laminar Flow in a Ninety Degree Bifurcation, Journal of Biomechanics, Vol. 15, pp. 473-485.

Marelius, F. and Sinha, S.K. 1998. Experimental Investigation of Flow Past Submerged Vanes. J. Hydraul. Eng. 124(5): 542-545.

McNamara, J.M., T.W. Fawcett, and A.I. Houston. 2013. An adaptive response to uncertainty generates positive and negative contrast effects. Science 340:1084-1086.

Miller, J.A., A. Gray, and J. Merz. 2010. Quantifying the contribution of juvenile migratory phenotypes in a population of Chinook Salmon Oncorhynchus tshawytscha. Marine Ecology Progress Series 408: 227–240.

Mulligan, K. 2014. An Analysis of Partial-Depth, Floating, Impermeable Guidance Structures for Downstream Fish Passage at Hydroelectric Facilities. Final Report, Hydro Research Foundation, Environmental and Water Resources Engineering, Department of Civil and Environmental Engineering, University of Massachusetts Amherst.

Murota, A. 1958. On the flow characteristics of a channel with a distributory. Technology Reports of the Osaka University, 6(198).

Neary, V.S., and Odgaard, A.J. 1993. Three-dimensional flow structure at open channel diversions. J. Hydraul. Eng., 119(11), 1223–1230.

Neary V., Sotiropoulos F. 1996. Numerical investigation of laminar flows through 90-degree diversion of rectangular cross-section, Computer and Fluids 25, 95-118.

Neary, V.S., Sotiropoulos, F., and Odgaard, A.J. 1999. Three dimensional numerical model of lateral-intake inflows. J. Hydraul. Eng., 125(2), 126–140.

Nelson, W.R., L.K. Freidenburg, and D.W. Rondorf. 1994. "Swimming performance of subyearling Chinook salmon." In Identification of the spawning, rearing, and migratory requirements of fall Chinook salmon in the Columbia river basin, edited by D. W. Rondorf and V. H. Miller, 39–62. Portland, OR: Bonneville Power Administration.

Nestler, J.M., R.A. Goodwin, D.L. Smith, J.J. Anderson, and S. Li. 2008. Optimum fish passage and guidance designs are based in the hydrogeomorphology of natural rivers. River Res. Appl. 24 (2): 148–168. https://doi.org/10.1002/rra.1056.

Newman KB, Brandes P.L. 2010. Hierarchical modeling of juvenile Chinook salmon survival as a function of Sacramento–San Joaquin Delta water exports. N Am J Fish Manag 30: 157–169

Nichols F.H., Cloern J.E., Luoma S.N., Peterson D.H. 1986. The modification of an estuary. Science 231:567–573

NMFS (National Marine Fisheries Service). 2011. Anadromous Salmonid Passage Facility Design. NMFS, Northwest Region, Portland, Oregon.

NPCC (Northwest Power and Conservation Council). 2000. Return to the river. Portland, OR: Northwest Power and Conservation Council.

Noatch M.R., Suski C.D. 2012. Non-physical barriers to deter fish movements. Environmental Reviews 20: 1–12. DOI: 10.1139/A2012-001.

Odeh M. 1999. Innovations in fish passage technology. American Fisheries Society: Bethesda, Maryland.

Odeh M. 2000. Advances in fish passage technology: Engineering design and biological evaluation. American Fisheries Society: Bethesda, Maryland.

Oteiza, P., I. Odstrcil, G.V. Lauder, R. Portugues, and F. Engert. 2017. A novel mechanism for mechanosensory-based rheotaxis in larval zebrafish. Nature 547:445-448.

Parsons, D.R., P.R. Jackson, J.A. Czuba, F.L. Engel, B.L. Rhoads, K.A. Oberg, J.L. Best, D.S. Mueller, K.K. Johnson & J.D. Riley. 2013. Ve-locity Mapping Toolbox (VMT): a processing and visualization suite for moving-vessel ADCP measurements. Earth Surf. Process. Landforms 38, 1244-1260.

Patankar, S.V. 1980. Numerical heat transfer and fluid flow, McGraw-Hill, New York.

Perry, R.W., J.R. Skalski, P.L. Brandes, P.T. Sandstrom, A.P. Klimley, A. Ammann, and B. MacFarlane. 2010. Estimating survival and migration route probabilities of juvenile Chinook salmon in the Sacramento–San Joaquin river delta. North Am. J. Fish. Manage. 30 (1): 142–156. https://doi.org/10.1577/M08-200.1.

Perry R.W., Brandes P.L., Burau J.R., Klimley A.P., MacFarlane B, Michel C, Skalski J.R. 2013. Sensitivity of survival to migration routes used by juvenile Chinook salmon to negotiate the Sacramento–San Joaquin River Delta. Env Biol Fish 96:381–392. doi: http://dx.doi.org/10.1007/s10641-012-9984-6

Perry, R.W., Romine, J.G., Adams, N.S., Blake, A.R., Burau, J.R., Johnston, S.V., Liedtke, T.L. 2014. Using a non-physical behavioural barrier to alter migration routing of juvenile Chinook Salmon in the Sacramento−San Joaquin River Delta. River Res Appl. 30(2):192–203. Available from: https://doi.org/10.1002/rra.2628

Perry, R.W., Brandes, P.L., Burau, J.R., Sandstrom, P.T., and Skalski, J.R. 2015. Effect of Tides, River Flow, and Gate Operations on Entrainment of Juvenile Salmon into the Interior Sacramento–San Joaquin River Delta, Transactions of the American Fisheries Society, 144:3, 445-455, DOI: 10.1080/00028487.2014.1001038.

Perry, R.W., Buchanan, R.A., Brandes, P.L., Burau, J.R., Israel, J.A. 2016. Anadromous salmonids in the Delta: new science 2006−2016. San Franc Estuary Watershed Sci.14(2):7. *https://doi.org/10.15447/sfews.2016v14iss2art7*

Pope, S.B. 2000. Turbulent flows, Cambridge University Press, Cambridge.

Popper, A. and Carlson, T. 1998. Application of sound and other stimuli to control fish behavior. Transactions of the American Fisheries Society 127:673-707.

Post J.R., van Poorten B.T., Rhodes T, Askey P, Paul A 2006. Fish entrainment into irrigation canals: an analytical approach and application to the Bow River, Alberta, Canada. N Am J Fish Manag 26:875–887

Qu, J. 2005. Three-dimensional turbulence modeling for free surface flows, Ph.D. thesis, Concordia Univ., Montreal, Canada.

Ramamurthy, A.S., Qu, J., and Vo, D. 2007. Numerical and Experimental Study of Dividing Open-Channel Flows. J. Hydraul. Eng., 133(10): 1135-1144.

Ramon, C.L., Acosta, M., and Rueda, F.J. 2018. Hydrodynamic Drivers of Juvenile-Salmon Out-Migration in the Sacramento River: Secondary Circulation. J. Hydraul. Eng., 144(8): 04018042J.

Reebs, S.G. 2002. Plasticity of diel and circadian activity rhythms in fishes. Reviews in Fish Biology and Fisheries 12:349–371.

Rhie, C.M., and Chow, W.L. 1983. Numerical study of the turbulent flow past an airfoil with trailing edge separation. AIAA J., 21(11),1526–1532.

Roberts J.J., Rahel F.J. 2008. Irrigation canals as sink habitat for trout and other fishes in a Wyoming drainage. TAmFish Soc 137:951–961

Romine, J.G., Perry, R.W., Stumpner, P.R., Blake, A.R., and Burau, J.R. 2017. Effects of tidally varying river flow on entrainment of juvenile salmon into Sutter and Steamboat Sloughs. San Francisco Estuary and Watershed Science.

Rueda, F.J., and G.S. Schladow. 2003. Dynamics of large polymictic lake. II: Numerical simulations. J. Hydraulic Eng. 129 (2): 92–101. https://doi.org/10.1061/(ASCE)0733-9429(2003)129:2(92).

Rueda, F.J., S.G. Schladow, and J.F. Clark. 2008. Mechanisms of contaminant transport in a multi-basin lake. Ecol. Appl. 18 (sp8):A72–A87. https://doi.org/10.1890/06-1617.1.

Schroeder, R.K., B. Cannon, L.D. Whitman, and P. Olmsted. 2013. Willamette spring Chinook-life history and habitat connections. Poster. Oregon Dept. Fish and Wildlife, Corvallis.

Schroeder, R.K., L.D. Whitman, B. Cannon, and P. Olmsted. 2016. Juvenile life-history diversity and population stability of spring Chinook salmon in the Willamette River basin, Oregon. Can. J. Fish. Aquat. Sci. 73: 921–934.

Shettar A., and Murthy K. 1996. A numerical study of division of flow in open channels, Journal of Hydraulic Research 34, 651-675.

Smith, D. L., J. M. Nestler, G. E. Johnson, and R. A. Goodwin. 2010. Species-specific spatial and temporal distribution patterns of emigrating juvenile salmonids in the Pacific Northwest. Reviews in Fisheries Science 18:40-64.

Smith, D.L., Threadgill, T., Lai, Y., Woodley, C., Goodwin, R.A., and Israel, J. 2017. Scenario Analysis of Fremont Weir Notch – Integration of Engineering Design, Telemetry, and Flow Fields. Final Report ERDC TR/EL-17-Draft, The US Army Engineer Research and Development Center (ERDC).

Smith, P., J. Donovan, and H. Wong. 2005. Applications of 3-D hydrodynamic and particle tracking models in the San Francisco bay-delta estuary." In 2005 World Water and Environmental Resources Congress. Reston, VA: ASCE.

Smith, P. 2006. A semi-implicit, three-dimensional model of estuarine circulation. Open File Rep. 2006-1004. Sacramento, CA: USGS.

Sommer T., Nobriga M.L., Harrell W.C., Batham W., Kimmerer W.J. 2001. Floodplain rearing of juvenile Chinook salmon: evidence of enhanced growth and survival. Can J Fish Aquat Sci 58:325–333

Steel, A., P. Sandstrom, P. Brandes, and A.P. Klimley. 2013. Migration route selection of juvenile Chinook salmon at the delta cross channel, and the role of water velocity and individual movement patterns. Environ. Biol. Fishes 96 (2–3): 215–224. https://doi.org/10.1007/s10641-012-9992-6.

Steel, A., Lemasson, B., Smith, D., Israel, J. 2017. Two-Dimensional Movement Patterns of Juvenile Winter-Run and Late-Fall-Run Chinook Salmon at the Fremont Weir, Sacramento River, CA. Draft report. ERDC/EL TR-17-10.

Stumpner, P., A. Blake, and J. Burau. 2017. Hydrology and Hydrodynamics on the Sacramento River near the Fremont Weir: Implications for Juvenile Salmon Entrainment Estimates.in U. S. G. Survey, editor. West Sacramento, California.

Tanaka, K. 1957. The improvement of the inlet of the Power Canal. Transactions of the Seventh General Meeting of I.A.H.R., 1, 17.

Taylor, E.H. 1944. Flow characteristics at rectangular open-channel junctions. Transactions, ASCE, 107: 893-912.

Tompkins, M., Anderson, J., Goodwin, P., Ruggerone, G., Speir, C., and Viers, J. 2017. Yolo Bypass Salmon Habitat Restoration and Fish Passage Analytical Tool Review. Delta Science Program.

Van Remoortere, P.H. 2014. A place to grow: prioritizing and designing habitat for juvenile Chinook salmon within the floodplain of the Willamette River. Master Thesis. University of Oregon.

Vasquez, J.A. 2005. Two-Dimensional Numerical Simulation of Flow Diversions. 17th Canadian Hydrotechnical Conference, Edmonton, Alberta, August 17–19, 2005.

Whitney, R., Calvin, L., Erho, M., & Coutant, C. 1997. Downstream passage for salmon at hydroelectric projects in the Columbia River basin: development, installation, and evaluation. Portland, OR: Northwest Power Planning Council.

Wilder, R. M., and J. F. Ingram. 2006. Temporal patterns in catch rates of juvenile Chinook Salmon and trawl net efficiencies in the lower Sacramento River. IEP (Interagency Ecological Program) Newsletter 19(1):18–28.

Zielinski, D.P., Voller, V.R., Svendsen J.C., Hon-dzo, M. Mensinger, A.F. & Sorensen P. 2014. Laboratory experiments demonstrate that bubble curtains can effectively inhibit movement of common carp. Ecological Engineering 67: 95-103

Appendix A

A Literature Review on the Downstream Juvenile Salmon Passage

Steve Hollenback, Physical Scientist
Sedimentation and River Hydraulics Group
Technical Service Center
Bureau of Reclamation, Denver, CO

Executive Summary

The cues that trigger juvenile salmon downstream migration vary by species, river reach, time of year, hydrological flows, and other environmental factors. Further, the swimming habits of juvenile salmon are variable, primarily by species, and size. The timing of migration and the understanding of when it typically occurs is important for any structure designed to assist with downstream migration, as the hydraulic conditions created by a structure may have significant differences with changes in flows at different times of year, also the longer a salmon waits before migrating the larger they will become which substantially modifies swimming abilities and habits.

However, juvenile salmon do exhibit a certain degree of consistency of migration habits within a population, especially if one focuses on the same species within the same river reach from one year to the next. The similarity of migration habits from one year to the next within a given river reach for a specific species often includes the timing of migration, the patterns of vertical migration, typical habitat selection, and preferred migration patterns through water control structures. These similarities of migration habits have effectively helped to design and build successful downstream fish passage facilities. However, as downstream juvenile salmon migration is a complex process which has not been examined as in-depth as other fish processes, such as upstream migration habits, the current depth and breadth of studies available does not effectively define the migration habits and variability of most species within the majority of reaches. As such, the best practice towards confidently developing a fish passage or fish exclusion structure should be based on multi-year monitoring of how a given fish species population reacts to changes in hydrological conditions within a given reach.
While monitoring downstream migration habits of juvenile salmon greatly assists in developing the best practical structure to properly guide migrating fish in the appropriate direction through defining specific characteristics, some basic guidance has been developed to help guide the planning, monitoring, and design processes which can be applied to the majority of downstream migrating salmonids. This guidance includes fundamental design criteria for structures to attract or exclude juvenile salmonids to/from an area such as basic behaviors of juvenile salmon to flow, depth, temperature, and other generalized changes in hydrological and hydraulic conditions. However, it should be noted that the majority of the guidance which was discovered in this literature review focuses on large scale dams as opposed to smaller scale water diversion structures.

Typically, if the migration habits of a species of juvenile salmon within a reach are reasonably understood, and the hydrology of a waterway is known within a reasonable level of confidence, this data may be developed into a model with a reasonable level of confidence in the output. Models which have been previously employed to predict the response of juvenile salmon in response to changing hydraulic conditions may be simple, or complex, and each carries distinct benefits and limitations.

In general, modeling juvenile fish behavior has resulted in limited success, but as the science develops modeling predictions have become more precise, accurate, and complex which is trending towards the ability of developing highly managed waterways which can safely guide

migrating salmonids to sea.
One crucial key of developing better structures to properly guide fish downstream has been the continual advancement and refinement of models to better predict how a structure will impact fish movements in a waterway.

A1. Introduction

Increasing juvenile salmon survival during their downstream migration in regulated rivers is an important issue as survival of juvenile salmon in regulated rivers is often many-fold lower than a corresponding section of free-flowing river (Huusko, 2018). In future initiatives to rebuild salmon stocks, safeguarding downstream migration should be considered equally as important as upstream migration of spawning salmon.

However, downstream fish passage technologies are much less advanced than upstream fish passage. Largely, this is because the focus of efforts to re-establish free movement of migrating fish has traditionally been on upstream passage facilities, and because facilities which assist in downstream migration are often much more difficult to design and develop (Larinier & Travade, 2002).

One prime challenge in enhancing the success of downstream juvenile salmonid migration is fish entrainment. Fish entrainment occurs whenever water is diverted through a structure, such as a diversion canal, and fish are diverted with the water. In order to reduce undesirable fish entrainment both attraction and repulsion of juvenile salmon must be understood to effectively develop a migration pathway.

Here, we describe the current state of the science in downstream juvenile salmonid migration with a focus on entrainment. Give an overview of salmon development, describe basic habits of downstream migrating fish, discuss basic fish guidance design and monitoring, then consider some of the more successful models which have been employed to understand and predict the movements and choices of juvenile salmon as they migrate to sea.

A2. Salmon Development

In the months following salmon egg fertilization, a salmon embryo develops from a unicellular fertilized egg into an alevin hatchling with limited mobility, lack of pigment, and an attached yolk sack. Salmon egg fertilization may happen throughout the year. However, as warmer waters generally lead to faster development, most adult salmon tend to spawn in warmer months, giving emerging fry the greatest chance of survival. (Quinn, The Behavior and Ecology of Pacific Salmon and Trout, 2018).

Alevin movement in natural streambeds is not well studied, but in general they first move deeper in gravel after hatching. Then, after their yolk is mostly absorbed, they move upward to emerge from the gravel bed. Following streambed emergence, the juvenile salmon (fry) of some species such as chum, or pink salmon typically migrate directly downstream and usually at night.

However, many salmon species mill about for an indeterminate amount of time before migrating downstream.

After salmon develop into fry they continue to mature into parr as they switch their food source from plankton to invertebrates, a salmon may remain a parr for years, or for just a few months. Just before salmon transition from freshwater to saltwater they further develop into a smolt, in which they undergo a color transition and other physiological changes which allow them to survive the shift from freshwater to salt water. After the post-smolt salmon enters the ocean it will spend the first year in schools with other post-smolt salmon as its swimming and reproductive abilities develop into the adult stage. As an adult they may spend three of four more years at sea before returning to freshwater to spawn. However, in some salmon species all or some of the migrating populations do not migrate to sea at all. (Quinn, The Behavior and Ecology of Pacific Salmon and Trout, 2018)

A3. Swimming Habits

The swimming habits of juvenile salmon exhibit a wide range of variability. However, some patterns in migration tendencies do exist which may be employed to help understand and model the swimming patterns of a juvenile population during downstream migration. Here we describe the trends in migration timing, vertical migration habits, typical habitat selection during migration, migration choices through a water control structure, and generally discuss the impacts of turbulence on small fish.

A3.1. Migration Timing Window

Historically, because of the expense associated with monitoring fish migrations, monitoring seasons have been shorter than ideal, as such the appreciation of how variable salmon migration timing can be has previously been limited. However, with more advanced monitoring techniques such as acoustic doppler, it is becoming clearer that salmon migrate downstream at many times of year (Quinn, The Behavior and Ecology of Pacific Salmon and Trout, 2018). The variability of migration timing, duration, and scope, in each species, each waterway, and each year has been found to be influenced by a complex of environmental factors such as temperature, turbidity, daylight, etc., as well as various biotic and hydrologic factors (Pavlov, Kirillova, & Kirillov, 2008).

The environmental cues that stimulate salmon and trout do not only vary between years, and reaches, but also among species in curious ways. This variation may be used to help distinguish sub-yearling migrating juveniles from parr older than a year. In species which tend to migrate almost immediately after emerging from gravel, such as Chum and Pink Salmon, the timing of migration is primarily determined by the timing of when their parents spawned and the temperature (linked with rate of growth) the embryo was exposed to during development. Other species may spend a year, or more, in fresh water, and undergo significant changes in physiology during this time as they develop from fry to parr. Among pacific salmon who tend to spend a year or more in freshwater, Coho are the best studied, but Sockeye and Chinook tend to follow similar migration patterns. In these species the timing of migration appears to be primarily

controlled by photoperiod, and secondarily by water temperature experienced in the late spring, just prior to seaward migration. (Quinn, The Behavior and Ecology of Pacific Salmon and Trout, 2018).

Between these two migration types, immediate or delayed, the predictability of the migration timing is markedly different. In consideration of species which tend towards immediate migration, such as Chum, the timing can vary greatly from year to year, and closely tracks with the accumulated temperature units the embryo is exposed to. However, in species which tend towards delayed migration, such as Coho, migration timing occurs at about the same time each year, with only slightly earlier migration when the spring is warmer. This difference in temperature response is demonstrated in one study in which stream temperatures increased after experimental logging removed much of the streams shade. In this study the Coho migration only shifted an average of six days, but the Chum migration timing shifted nineteen days (Holtby, 1988). Additionally, a study of Pink Salmon helps to further demonstrate the link between incubation temperature and migration time of immediate migrating salmon. Over the duration of record of 34 years at Auke Creek in Alaska water temperatures during incubation only increased about 1°C, but during this time juvenile salmon migrations date shifted seventeen days. (Quinn, The Behavior and Ecology of Pacific Salmon and Trout, 2018).

While some species such as Chum and Coho Salmon are almost exclusively anadromous (migrate to the sea), some species occur in anadromous and nonanadromous forms. Chinook Salmon may produce a small number of nonanadromous males, but all females go to the sea. Kokanee Salmon (nonanadromous sockeye) populations are found in many lake systems in the pacific northwest and may produce some anadromous offspring. Masu Salmon, some trout, and all the char species commonly occur as both anadromous and nonanadromous within the same river (Quinn, The Behavior and Ecology of Pacific Salmon and Trout, 2018).

In general, the timing and age of salmon when they choose to migrate to the sea is variable. Because of these differences, the size and habits of downstream migrating salmon can be highly variable, as are the hydrologic conditions present during migration. These factors all must be at least generally understood in a given river reach before a successful structure to assist with downstream migration can be developed.

A3.2. Vertical Migration as a Response to Diel Cycles

Often, juvenile salmon migrating downstream exhibit diel vertical migration. The tendency is often for salmon to be more surface oriented at dusk, may be deeper at night during the summer, and are often deeper during the day (Faber, Weiland, Moursund, & Carlson, 2001). This characteristic has been hypothesized to be in reaction to predation, food sources, and temperature. It is likely in response to the availability of plankton, and lowered light conditions, when it is too dark for predators to forage successfully, that juvenile salmon are often found at the surface at dusk. Vertical migration at night often occurs after feeding in the summer when the surface waters are often too warm for optimal digestion efficiency, and as such- juvenile salmon move below the thermocline where they can digest the food more readily (Brett, 1971). This theory has been based on observations in natural settings as well as in simulations. Laboratory

feeding research has showed that at rations similar to what might be anticipated in a lake, Sockeye grew faster under a temperature regime simulating diel vertical migration patterns as opposed to constant temperature regimes (Biette & Green, 1980). Additionally, modeling based on observed patterns of temperature and zooplankton in a North Carolina reservoir also predicted a notable increase in growth for Kokanee which vertically migrated when optimal temperatures were below the depth where prey were concentrated (Bevelhimer & Adams, 1993). However, while vertical migrations are energetically sensible, nighttime vertical migrations have been observed when the water column is not stratified, indicating that this behavior is not fully understood (Steinhart & Wurtsbaugh, 1999).

While energetic efficiency of diving deeper in the water column may explain why juvenile salmon leave the surface at night, the reason for diving deeper during the day is likely a result of a different stimuli. Daytime vertical migration is likely due to them trying to avoid predation from birds and larger fish which feed by sight. As such, this migration is likely an attempt to strike a balance between the safest place in a lake, at the bottom, and the best location to feed, at the surface (Clark & Levy, 1988). Each population of salmon exhibit slightly different characteristics in striking this balance, but each tends to follow this same routine (figure A1). The daytime depth seems to be regulated not by water temperature, as in the night, but by water clarity. In general, each population seems to respond to water clarity, predation pressure, food availability, and water temperature among different waterways and seasons uniquely in regard to their variation in vertical migration habits (Quinn, The Behavior and Ecology of Pacific Salmon and Trout, 2018). As such, the pattern of vertical migration and its influences are not currently understood well enough to be able to model population dynamics accurately without observations of a population directly.

Vertical migration patterns of salmon may be important in understanding downstream migrations past water control structures as the vertical distribution of a population has a higher correlation to where they will attempt to pass the structure than the horizontal distribution does. Observations have explained that juvenile salmonid will often not take their first option in a horizontal direction for fish passage but will largely remain in the same area of the vertical water column during passage (Faber, Weiland, Moursund, & Carlson, 2001).

Fish species		Afternoon	Dusk	Night
Sockeye salmon	Shallow	0.1	4.3	16.3
	Intermediate	0.5	7.4	6.3
	Deep	2.8	3.4	2.3
Longfin smelt	Shallow	1.1	21.3	24.5
	Intermediate	1.9	20.5	33.9
	Deep	15.6	9.9	24.9
Threespine stickleback	Shallow	16.3	24.5	22.8
	Intermediate	6.3	33.9	15.4
	Deep	2.3	24.9	3.6

Figure A1.—Depth distribution of juvenile sockeye salmon and select other fish at different times of day in April, data averaged from 1997 to 2013. Depths are approximately defined as shallow: 12 meters, intermediate: 25 meters, and deep: 50-55 meters below water surface. Note, as this study took place in April waters were not warm enough to induce nighttime vertical migration (Quinn, Sergeant, Beaudreau, & Beauchamp, 2012).

A.3.3. Habitat Selection

Habitat selection of juvenile salmon is another important consideration when attempting to understand the downstream migration patterns of a population. While different species may exhibit differences in habitat selection, it is assumed that the majority of migrating juvenile salmon populations do tend to be drawn to similar habitats.

When not actively migrating downstream, young juvenile Chinook in rivers and streams are often associated with shallow, low velocity water near the inside of river bends rather than near the thalwag or outside bends where velocity is greater (Tompkins, et al., 2017). Additionally, young juvenile Coho tend to prefer habitats with slower and deeper water often found in pools and tend to spend less time in the faster moving waters found in riffles (Healy & Lonzarich, 2000) (figure A2). In many salmon species it is well documented that there are shifts in habitat preference as the fish become larger (>100 mm) towards spending more time in faster currents, this is likely related to increasing foraging opportunities while decreasing predation (Quinn, The Behavior and Ecology of Pacific Salmon and Trout, 2018). Regardless of size Coho, Steelhead, and Cutthroat have all been documented as selectively occupying deep pools with structure over shallower pools with structure and tend to avoid pools without cover or structure (Lonzarich & Quinn, 1995).

As Fry develop into parr they tend to exhibit more smolt like behavior in habitat selection as they tend towards higher velocities and are more likely to be associated with migrating towards the thalwag of a river or distributed across the mid-channel. While smaller fry (~30-70 mm) typically occupy more near shore areas of rivers and streams while migrating downstream (Friesen, Vile, & Pribyl, 2007).

Parr and smolt tend to exhibit similar habitat selection to lager fry in that they trend towards being near higher velocity currents and towards mid-channel preferences. But differ in that parr and smolt density tends to not be significantly influenced by bank cover, canopy cover, and mean or maximum depth but is increased by in-channel woody debris. One study reported a strong correlation between Parr and smolt distribution and woody debris, with the majority being observed within 1 meter of debris, and almost all observed within 2 meters of debris (figure A3). This may be because it creates slow currents near higher velocity waters and low light intensity, but it is not well documented what processes produce this attraction behavior (McMahon, 2011). Further, it has been documented that over the course of a smolt run migrating towards the sea, fish group size and density tend to increase (McMahon, 2011).

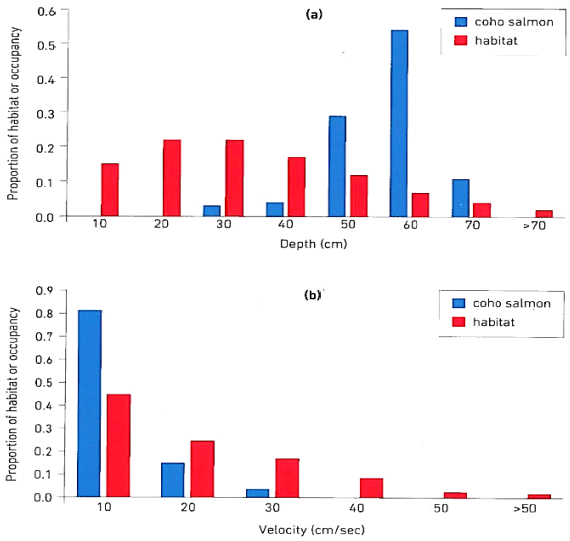

Figure A2.—Habitat occupancy selection tendencies of coho salmon compared to the habitat available in (a) water depth, and (b) water velocity (Healy & Lonzarich, 2000)

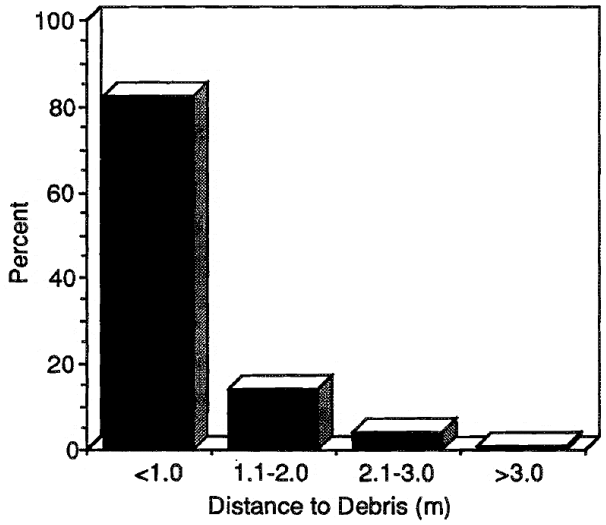

Figure A3.—Proximity of coho salmon smolts to large woody debris (McMahon, 2011).

A3.4. Migration choices through a water control structure

Similar to habitat selection and vertical migration response to diel cycles by juvenile salmonid, the migration habits through control structures vary significantly between fish populations, river reaches, species, and seasons. However, some general guiding principles can assist in developing basic predictions of downstream migrating juvenile salmonid response to water control structures. Nonetheless, it should be understood that in order to be able to accurately predict the typical response of a distinct salmonid population to a water control structure at a particular location the best method is to begin with collecting multiple years of data observing the specific river reach and species in question.

Analogous to vertical migration correlation to diel cycles, there is evidence that downstream migration may be linked with diel cycles during moderate flow conditions. It has been found that while many juvenile salmon actively migrate downstream at night, during the day they tend to hold in areas of cover near the shore or migrate upstream (Godin, 1982). This correlation between downstream migration and daylight tends to be higher in spatially constricted rivers with low turbidity which exhibit higher predation pressure during the day (Furey, 2016).
As a method to better discuss the response habits of a population of downstream migrating juvenile salmonids it can be helpful to break a population into three distinct groups: direct passage, searching, and milling. Direct passage fish being fish that pass through a water control structure within one hour. Searching fish are fish that actively searched for an exit and pass through a water control structure within one to four hours. Finally, milling fish are defined here as fish that move around a passage rout for more than four hours before passing through a water control structure.

The potential for different migration habits between different species is described well in a study at Bonneville Power Plant I (Faber, Weiland, Moursund, & Carlson, 2001) which found that Steelhead were observed to be twice as likely to mill during the day as during the night, while Chinook were equally likely to mill at day or night. Additionally, Steelhead were 10 times more

likely to direct pass at night than at daytime, and Chinook were twice as likely to direct pass at night as during daytime. Further, response of fish classified as “direct passage” appear to follow the main flow field during approach and passage, while “milling” fish showed a variety of response to the flow field (Faber, Weiland, Moursund, & Carlson, 2001).

At the Dalles Dam it was reported that schools tend to exhibit characteristics associated with “direct pass” or “searching” fish more so than individual fish which were more prone to be classified as “milling”. Additionally, it is reported that schools of fish were more prone to swim against the current for a period of time, than individual fish were. As a result, the majority of fish (60 to 90%) would swim against the current for a period of time before passing through the water control structure, and the time a school of salmon spent milling seemed to decrease with increased passage width (Johnson, et al., 2009).

Further studies have resolved general flow field effects on juvenile salmon swimming habits. In steady flow juvenile salmonids tend to drift downstream, and when encountering moderate flow acceleration, they swim across the streamlines into the higher velocity areas. Additionally, it was determined that in general, when they encounter strong flow acceleration they swim upstream against flow, and they tend to swim against changes in vertical velocity in order to maintain depth. (Tompkins, et al., 2017).

As a whole, larger juvenile salmon populations were observed to follow flow along the thalwag of the water control structure where water velocity magnitudes are greater than 3 cfs by the time they had reached within 200 feet of the water control structure (figure A4) (Faber, Weiland, Moursund, & Carlson, 2001). This general habit was observed to be less true during the day (figure A5) as compared to nighttime (figure A6). Vertical distribution patterns were also apparent in the juvenile fish populations passing at the Bonneville Dam in which Yearling Chinook and Juvenile Steelhead were observed to pass the dam more preferentially towards the surface at night (figure A7) as compared to during the day (figure A8) (Faber, Weiland, Moursund, & Carlson, 2001). Additionally, juvenile fish showed greater probability of movement against or orthogonal to the current when water velocity was lower than 3 cfs (Faber, Weiland, Moursund, & Carlson, 2001). As a note, the recommended maximum velocity for an upstream fish passage designed for juvenile salmonids of 80 to 100 mm is 3 to 4.5 cfs (NMFS, 2011).

Figure A4.—Horizontal Approach and Passage Distribution of Juvenile Steelhead and Yearling Chinook at Bonneville Dam Powerhouse I at all times. Line represents 50% fish passage entry route. (Faber, Weiland, Moursund, & Carlson, 2001).

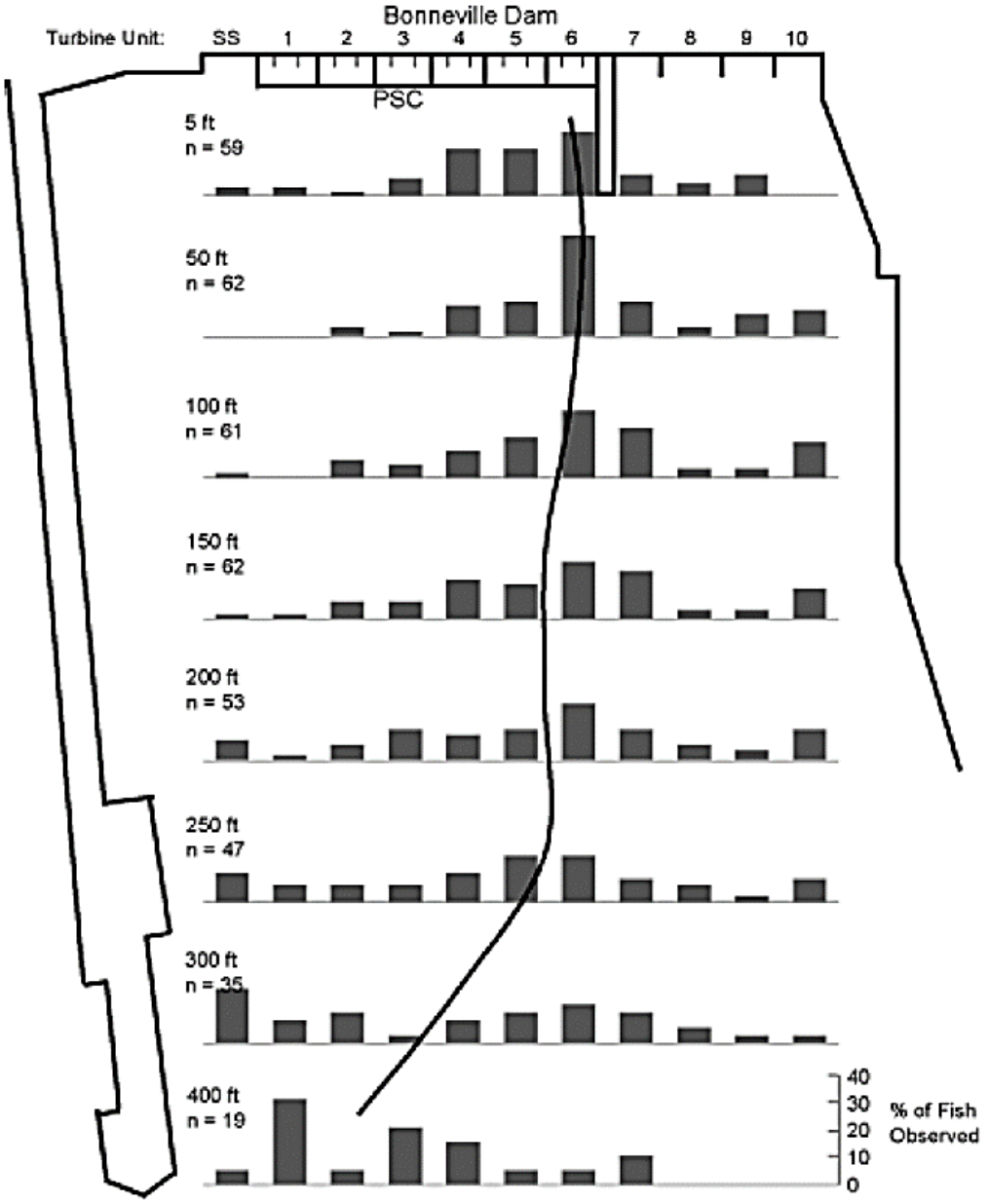

Figure A5.—Horizontal Approach and Passage Distribution of Juvenile Steelhead and Yearling Chinook at Bonneville Dam Powerhouse I during daylight hours. Line represents 50% fish passage entry route. (Faber, Weiland, Moursund, & Carlson, 2001).

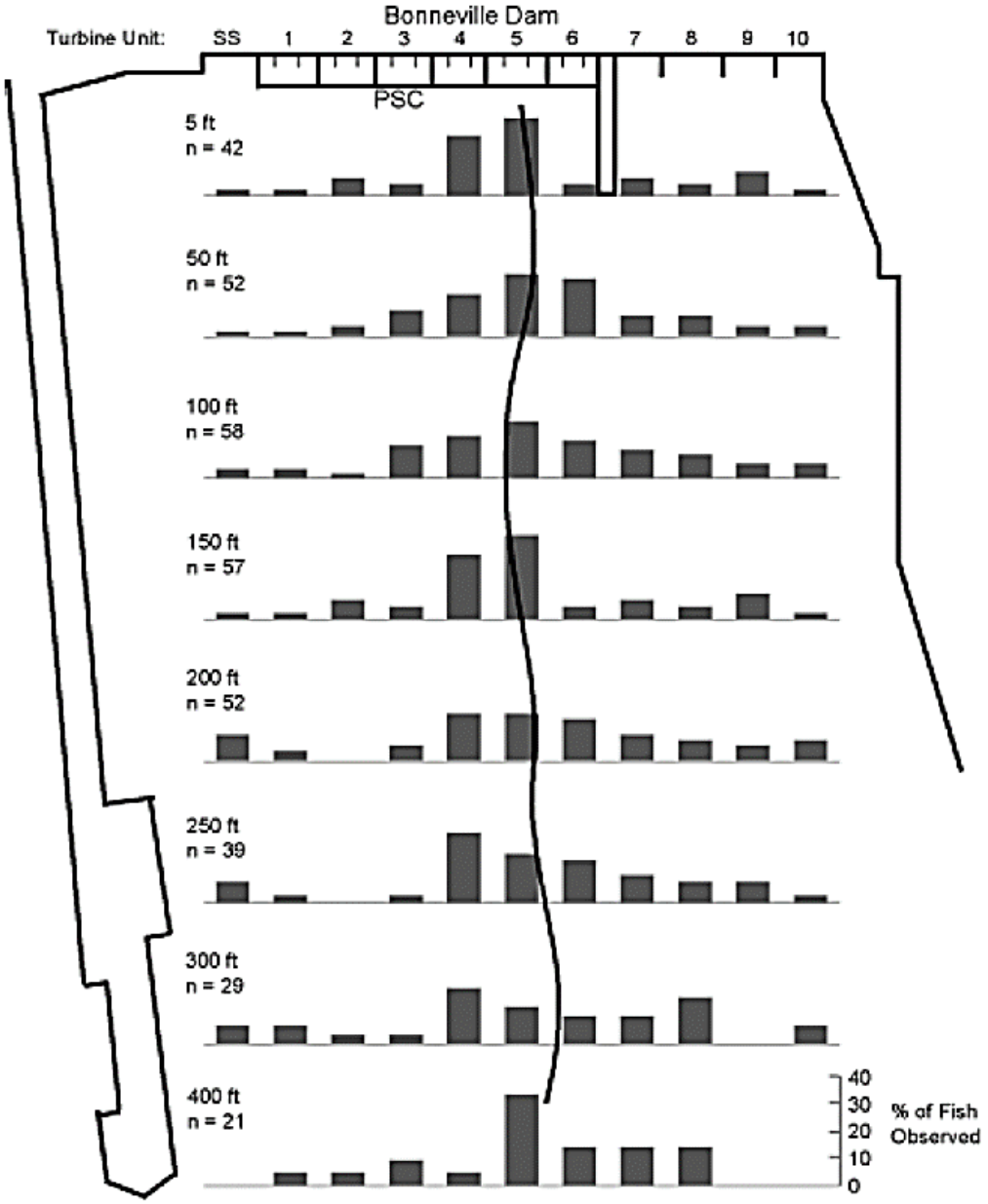

Figure A6.—Horizontal Approach and Passage Distribution of Juvenile Steelhead and Yearling Chinook at Bonneville Dam Powerhouse I during night hours. Line represents 50% fish passage entry route. (Faber, Weiland, Moursund, & Carlson, 2001).

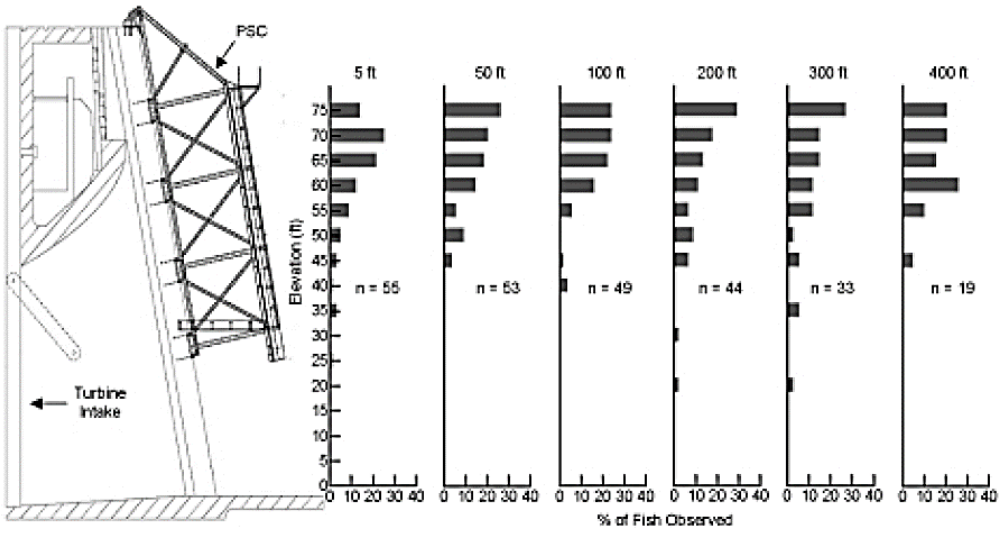

Figure A7.—Vertical Distribution of Yearling Chinook and Juvenile Steelhead at Bonneville Dam Powerhouse I during night hours. (Faber, Weiland, Moursund, & Carlson, 2001).

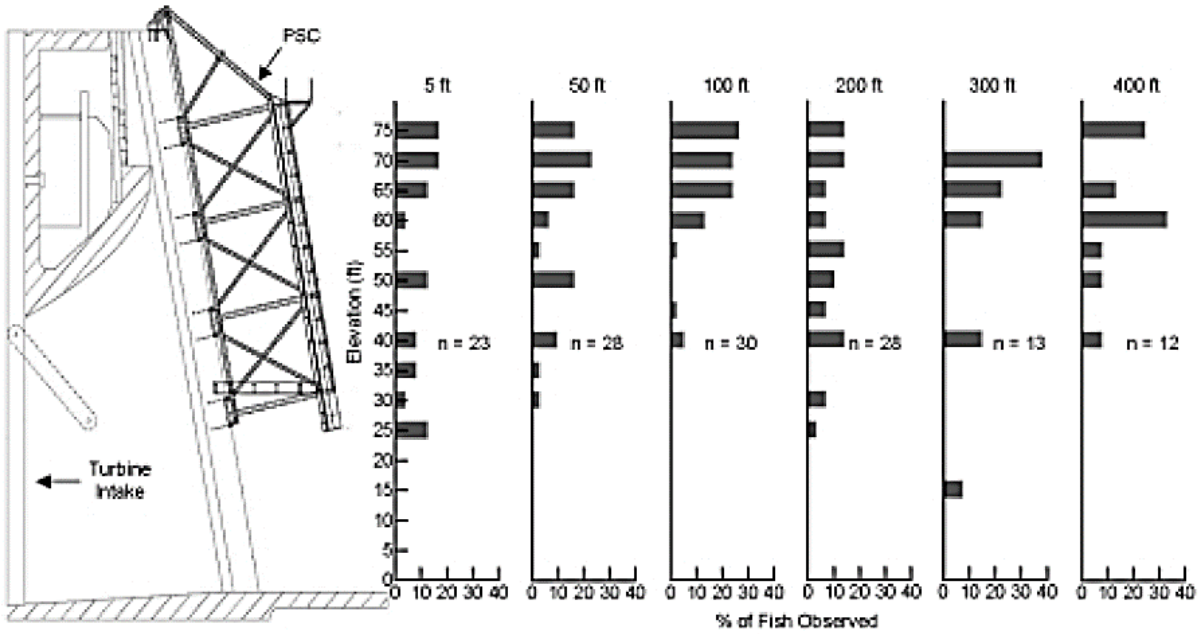

Figure A8.—Vertical Distribution of Yearling Chinook and Juvenile Steelhead at Bonneville Dam Powerhouse I during daylight hours. (Faber, Weiland, Moursund, & Carlson, 2001).

A3.5. Impacts of Turbulence on migrating fish

Analysis of turbulence on Cyprinids (to include minnows and carps) for the purpose of upstream fish passage can help to develop an understanding of how turbulence would be anticipated to impact small juvenile salmon while attempting downstream passage at a water control structure. In general, Reynolds shear stress and eddy size are the most important turbulence descriptions

when attempting to predict travel time, and assumed related effort, through a fish passage. With lower Reynolds number transit time increases, and when eddies are larger than a fish's body size a fish is much more likely to become disoriented. Further, small fish are found to prefer areas of low turbulence, especially when near an area of high turbulence with large eddies, as evident from the percent of time spent in a flow region (Silva, Katopodis, Santos, Ferreira, & Pinheiro, 2012).

A4. Monitoring

Monitoring of juvenile salmon has been subject to a number of different techniques in order to attempt to understand their behavior response. Some of these include direct capture, video, radio telemetry, and sonic telemetry. Because the majority of wild salmon stocks are listed under the Endangered Species Act techniques involving direct capture are limited in applicability. Video monitoring has limited success because it is best applied in close proximity to a structure, and as such, yields little information on approach behavior. Radio telemetry does not provide the information necessary for understanding fine-scale behaviors. As an alternative, in recent years, the emergence of sonic tag tracking systems, has gained favor with researchers. Unfortunately, current sonic tag technology requires use of a relatively large tag which may affect fish behavior, particularly for 0-age salmonid smolts (Johnson & Moutsund, 2000). However, developments in large-scale acoustic doppler monitoring has demonstrated that this technology is able to largely overcome many of the above disadvantages with other technologies.

Applying large-scale acoustic doppler velocimeter monitoring allows for the simultaneous monitoring of fish approach, passage, and water velocity with enough resolution to track individual fish. Deployment of this type of monitoring technology over multiple years allows the relationship between juvenile salmon response to various hydrodynamic conditions at a site to be better understood (Johnson, et al., 2009). As development of this technology continues, future sonar systems will likely be fully integrated systems with built-in real-time tracking capability. These systems may be used to track targets relative to physical guidance structures or other behavior-modifying stimuli such as light, turbulent flow, electrical/magnetic fields, or low-frequency sound and vibration. The combination of fine-scale fish behavior data and environmental parameters will likely yield better design criteria for structures to either enhance or reduce fish passage as desired (Johnson & Moutsund, 2000). Examples of methods for deploying acoustic monitoring systems and conducting analysis is presented in multiple documents to include (Adams & Evans, 2011), (Johnson, et al., 2009), and (Johnson, et al., 2006).

A5. Basic Fish Guidance Design

Prior to developing a design for a given structure to assist in or reduce fish passage, a study should be conducted of migration habits of the population within the reach where the structure will be placed. Migration habits may be different even within the same fish populations, which have been observed to behave differently in different river reaches (Furey, 2016). As such, having a thorough understanding of how water control structure operations and environmental conditions affect passage, survival, and migration choices on a population level is crucial.

Understanding how survival or passage varies in response to flow conditions requires data for a wide range of conditions. Studies conducted in a single year only consider a narrow range of environmental conditions, due to natural year-to-year variation in the environment. Furthermore, multiyear analyses benefit from the large sample sizes over multiple years, which can reduce statistical uncertainty and help to identify relations that might otherwise be statistically undetectable. (Adams & Hatton, 2012).

Movement of fish is influenced by environmental factors such as temperature, TDG, turbidity, and sunlight, through physical factors such as water speed, channel geometry, woody debris, and cover, as well as biotic factors such as birds, other fish, an individual fish's migratory tendencies, and disease. However, near a dam or water diversion structure, the response of fish to hydrodynamics frequently supersedes their response to other stimuli (Popper & Carlson, 1998). It typically has been held that juvenile outmigrant salmon tend to follow the highest flow of water as they migrate to the sea. While this tends to hold true for bulk-flow regimes, as downstream migrating salmon approach a barrier to their migration there is an elevated likelihood for increased searching or milling, even when they are at an opening which provides passage across the blockage. This holding tendency may be alleviated, or increased, by improved design of fish passage or fish exclusion structures (Johnson & Moutsund, 2000).
To encourage fish to choose a specific route of passage through a water control structure, some basic principles of adjusting hydrology are established. First, in order to encourage schooling behavior, which has been associated with more direct passage habits, a route should be wide enough to accommodate the entire school of fish if fish passage is to be encouraged. Alternatively, a potential passage route may be designed to be narrower if the structure is to discourage fish passage (Johnson, et al., 2009). Secondly, competitive flow fields and turbulence should be minimized near the water control structure if fish passage is desired or increased if fish exclusion if preferential (Johnson, et al., 2009), (Faber, Weiland, Moursund, & Carlson, 2001). Finally, flows over 3 cfs tend to decrease the milling time at a water diversion structure, but sudden acceleration of the flow field tends to increase milling time (Faber, Weiland, Moursund, & Carlson, 2001).

At the Dalles Dam, studies have developed recommendations to encourage fish passage through enlarging the fish entrainment zone, defined here as the zone near a fish passage where, once in, fish pass through the fish passage at about a 95% rate. These recommendations included reducing turbulence, increasing water discharge, and mounting lights to the top deck above passage entrances (Adams & Hatton, 2012). Effectively, these recommendations summarize the basic approaches to encourage fish passage through a water control structure. In general, larger, wider openings parallel to the flow and located in the thalwag towards the surface will experience substantially more juvenile salmonid fish passage than smaller, skinnier openings perpendicular to river flow and located at inner banks of a waterway and deep in the water column. (NMFS, 2011).

A5.1. Attraction of Salmonids

Besides attraction flow there has been some documentation that salmonids are attracted to a constant light source during nocturnal downstream migration. In studies, promising results have shown that intermittent low wattage lighting can attract fish to the vicinity of the fish entrainment zone, then when the light is turned off the fish tend to continue through the passage (Larinier & Travade, 2002).

A5.2. Exclusion Barriers

The primary categories of exclusion barriers are physical and behavioral. Other types of barriers, such as visual, auditory, and electrical stimuli have all been used in a wide variety of experimental barriers. These include bubble screens, sound screens, attractive or repellent light screens, and electrical screens. Often, the deployment of these technologies have not matched the expectations as results obtained in field applications have been much less reliable than those obtained under controlled conditions (NMFS, 2011) (Larinier & Travade, 2002).

Design criteria for a variety of physical barriers which may be referred to as Positive-Exclusion Screen and Bypass Systems (PESBS), have been developed and have been demonstrated to minimize adverse impacts to fish at water diversion sites while reducing entrainment in irrigation canals. In general, these consist of screens with small openings and fish-tight seals which are positioned at a slight angle to flow. This orientation allows fish to be guided to safety at the downstream end of the screen where a bypass system begins. The bypass system ideally, minimizes fish exposure to screens and provides hydraulic conditions which safely return fish to the river downstream of a water diversion structure. The main detriment of PESBS is cost, low velocity requirement, structure complexity, and maintenance (NMFS, 2011).

An example of a PESBS barrier which has been found to reduce juvenile salmonid entrainment are drum screens, which have been widely used in irrigation channel intakes. These screens provide a very effective solution to the problem of fish entrainment in shallow irrigation channels. Drum screens are installed across a channel at a specified angle (around 26°) to guide fish into a bypass. The mesh screen is typically made either of stainless steel or galvanized wire. However, use of drum screens is limited to sites where water level variations are very limited since the screens must be 70 to 80% submerged to remain effective. Experience shows that drum screens can be highly effective in guiding salmon juveniles to bypasses with very little damage to the fish and are relatively effective at self-cleaning as long as the electric motor keeps the drum turning. (Larinier & Travade, 2002).

Another type of barrier which may be utilized in this system includes picket barriers. In general, picket barriers diffuse streamflow through pickets extending the entire width of the passable route. These pickets should be sufficiently spaced to provide a physical barrier to migrant fish. This category of exclusion barrier includes a fixed bar rack and a variety of hinged floating picket weir designs. While picket barriers work well under general conditions, they do have some down sides as they require removal for high flow events and must be continually monitored for debris accumulations (NMFS, 2011). Ideally, bar spacing should be equivalent to

about one tenth of the total length of the fish, although picket barriers have been found to have a behavioral repelling effect with wider bar spacing. However, with bigger spaces between the bars the repelling effect diminished rapidly, as with a spacing of about 6-7 cm, juvenile salmonids would easily pass through, unless there was a very strong velocity component tangential to the trash-rack (Larinier & Travade, 2002).

To deploy PESBS effectively, whatever the type of barrier utilized, one or more bypasses are needed. They are necessary to divert fish around the water control structure and return them safely downstream. A bypass can be employed in conjunction with barriers, or alone without a barrier if fish are naturally guided to the bypass by suitable flow conditions. (Larinier & Travade, 2002).

Considerable work has been conducted to develop less expensive behavioral devices as a substitute for the expense and maintenance required for conventional fish guidance systems such as PESBS (EPRI 1986). A behavioral device often requires volitional taxis on the part of the fish to avoid entrainment and these types of systems are referred to as “hydrodynamic”, additionally some devices have been investigated to elicit a “startle” response. Some types of behavioral devices were developed with the hope of attracting fish to a desired area while others were designed to repel fish (NMFS, 2011).

Deployment of startle-response devices report that their efficiencies are consistently much lower than for conventional screens. Experiments suggest there is significant behavioral variation in startle responses between individual fish of the same size and species. Therefore, it is difficult to predict if a fish will move toward or away from that device. It has been hypothesized that this variation in response is because fish likely have difficulty discerning where a signal is coming from and what constitutes a clear path to safety (NMFS, 2011).

Hydrodynamic devices aim to utilize documented fish response to hydrological conditions to guide fish passage. Two types of these systems described here are “Louver” screens, and “Guide Walls”. Louver screens essentially consist of vertical slats at right angles to the direction of the flow. They have been used at several sites since the 1950s, most notably at irrigation channel intakes on the West Coast of the USA. More recently there has been a move away from Louver screens installation due to their efficiency, which in the order of 60-90%, is considered to be inadequate for protecting juvenile salmonids because it is much lower than that of PESBS. Louvers function better at sites where river discharge and water velocities remain relatively constant during downstream migration periods because their efficiency is highly dependent on the flow pattern in the channel intake. Additionally, the louver screen system generally requires a trash-rack to protect the structure from debris which can seriously compromise the fish guidance efficiency (Larinier & Travade, 2002). Guide walls are similar to louver screens and are installed at an angle to the channel intake that can be used to deflect species which tend to preferably migrate in the surface layers, such as salmon. Such a device has been installed on the East Coast of the USA at the Bellow Falls power station. This guide wall extends vertically halfway down the water column (which is 9m deep), at an angle of 40° across the channel, and guides fish towards a sluice gate and a channel leading to the tailrace. An auxiliary bypass located near the trash-rack is intended to accommodate fish which have passed under the wall. The efficiency of

the guide wall is estimated at 84%, and with approximately 10% of the smolts passing through the secondary bypass, the total structure efficiency is estimated at over 90%. The efficiency of a guide wall is thought to be closely related to the angle of the wall with respect to the flow and above all to the depth at which the wall is submerged (Larinier & Travade, 2002).

A6. Relevant Modeling Studies

Several analytical tools have been developed, and used, to evaluate fish passage or exclusions barriers location and design. Typically based on fish habitat and movement choices in response to hydrological conditions the tools have a variety of complexity, and the model utilized is often a result of data available, computing power, and desired resolution of model output.
In most cases 2-D hydrodynamic models such as SRH-2D are not adequate to describe fish movements. The typical exception of this, is if the fish are known to be close to the water surface the majority of the time (Tompkins, et al., 2017).

As a result of 2-D models general inadequacy in describing fish movements, various 3-D hydrodynamic models have been developed to predict Juvenile Salmon Entrainment. Some of these include the Juvenile Entrainment Evaluation Tool (JEET), Eulerian-Lagrangian Agent Based Model (ELAM), the COMPASS model, and Critical Streak-line Analysis.

A6.1. A model to predict Juvenile Salmon Swim Paths

(Amado, 2012) presented a numerical model which is designed to simulate juvenile salmon swimming behavior. The model uses parameters obtained by analyzing swim paths combined with computational fluid dynamics flows. To calibrate the model swim paths, Chinook were monitored at Rocky Reach Dam, and Sockeye and Steelhead at Priest Rapids Dam. Chinook movement data was available at both dams but only swim paths measured at Rocky Reach were used to configure the model to test the concept of transferability of fish behavior between dams (Amado, 2012).

This model assumes that fish select swimming variables based on current flow conditions. A possible modification to the model may be to develop probability disruptions that encapsulate behavior given current and past flow and swimming conditions. The correlation between measured fish swim paths and flow field information can be represented by probability distributions. These distributions, together with a particle tracking algorithm, can be used to predict fish behavior under various flow conditions not only at the site where swim paths were measured, but also at other locations with similar hydraulics and populations (Amado, 2012).

A6.2. Juvenile Entrainment Evaluation Tool (JEET)

JEET is a modeling tool which was designed to analyze the influence of notch dimensions on juvenile salmon entrainment for fish migrations at different river stages. This tool assumes that the ratio of fish entrained is equal to the volume of water entrained, meaning that this model assumes that fish are evenly distributed within the flow.

As such it does not evaluate notch location, real fish distribution across the river, or impacts of changes in the hydrodynamic field on entrainment, but it may be useful in general notch design (Tompkins, et al., 2017).

A6.3. Critical Streakline Analysis

A simple model which may prove more useful than JEET includes the Critical Streakline Analysis in which entrainment potential is predicted through employing incremental distances which are defined by comparing the cross-channel fish distribution to the fish passage entrainment location or the "critical streakline" – defined as the location where the water entering the passage site begins. In this model, the fish distributed inside the critical streakline location immediately upstream of the passage location defines the entrainment potential of the passage. This model is particularly useful for defining potentially viable locations for a passage site but is not ideal for determining ideal passage design. In particular, the model is well suited for identifying weir locations where entrainment would be expected to be relatively low or high. (Tompkins, et al., 2017) This information may be especially valuable in better defining the weir arrival spatial distributions of fish for more advanced models.

A6.4. Markov-Chain Analysis of Movements of Fish

A more complex model which is based on Markov-Chain Analysis is defined by a stochastic process that specifies the probability of transitioning from one "state" to another. In this model a state is a distinct area across the face of a water control structure, which consist of 3-D volumes of water bound by water surface, river bottom, the dam face, and upstream a predefined distance. The probability that a fish will move from one state to another is assumed to be independent of the state the fish was in previously (Adams & Hatton, 2012).

The authors (Adams & Hatton, 2012) built upon the work of (Johnson, Hedgepeth, Skalski, & Giorgi, 2004) whom developed a new technique to map the fish entrainment zone. After Johnson et al. developed the technique it was applied using data on salmon smolts migrating at the Dalles Dam on the Columbia River. After this practical study Johnson et al. determined that the Markov chain analysis may be used in comparative studies which examine changes in fish entrainment zones caused by engineered structures.

(Adams & Hatton, 2012) were able to employ Markov chain analysis at McNary Dam to summarize the behavior of juvenile salmonids at the dam forebay. This allowed them to confirm what had previously been summarized using visualization software and refined understanding of how fish behavior and passage can be affected by dam operations. Additionally, the numerical data used to quantify fish behavior through Markov chain analysis may also be used to examine how a proposed structure may influence fish behavior (Adams & Hatton, 2012).
The advantages of Markov chain analysis include that no arbitrary subsets of the spatial zone of inference need to be specified, between cell movement is based on direct observations, a large amount of information can be extracted from the fish movement data, and fish movement data

can be analyzed in the original three dimensions without the need to collapse the data to lower dimensions. One disadvantage is that as data are needed for every volumetric cell, computational analysis may be intense (Adams & Hatton, 2012).

A6.5. COMPASS Model

Previous to the COMPASS model development Richard Zabel's dissertation developed some of the processes through the theory that a two-parameter travel time model may be effective at describing the arrival time distributions of run-of-the-river, yearling chinook. One parameter determines the rate of downstream migration while the other parameter determines the rate of population spreading. (Zabel, 1994). An additional contribution to the development of the COMPASS model is the downstream passage component of the COMPASS model which was derived from CRiSP, a previous salmon passage model composed of four sub-models: dam passage, reservoir survival, travel time, and hydrodynamics. The COMPASS model combined the two-parameter travel time model with CRiSP as well as some other minor modeling components. This process resulted in COMPASS, which was developed to predict the probability that fish pass through specific routes at a dam with route-specific survival probabilities based on monitoring data (Zabel, et al., 2008).

Because both distance traveled, and travel time are important factors, both form much of the basis of the model and appears in all four sub-models. Temperature appears in all four sub-models as well, and flow appears in three out of four. Spill was found in the model to be important for Chinook but not for Steelhead. In all cases, the model-predicts fish velocity is significantly influenced by water velocity (Zabel, et al., 2008). The model results suggest that salmon populations are responsive to river conditions and thus will respond to river manipulations. However, the results also suggest that different species will respond differentially, and thus multi-species approaches are desirable (Zabel, et al., 2008).

A6.6. Eulerian-Lagrangian-Agent method (ELAM)

Fine-scale fish movement modeling may be categorized as Lagrangian individual-based models, and Eulerian stochastic particle models. The individual-based Lagrangian analysis methods provide more information on individual tracks and behavioral classifications than the Eulerian approach which includes diffusion theory and population trends. In many cases, researchers of behavioral ecology have focused on the Eulerian population level approach simply because individual level data has not been available (Pitcher, 1993). However, with the development of better monitoring equipment and techniques, the ability to employ Lagrangian techniques has become more feasible because individual fish may be tracked in an appropriate spatial and temporal scale (Johnson & Moutsund, 2000).

The Eulerian-Lagrangian-Agent method (ELAM) couples Eulerian and Lagrangian methods within an agent reference framework. ELAM based models have been shown to be especially effective at simulating the motion dynamics of individual fish, using high fidelity computational fluid dynamic models to represent flow fields (Goodwin, Toney, Nestler, Anderson, & Kim, 2005).

In ELAM, the agent-based model simulates the movement decisions made by individual fish. A Eulerian computational fluid dynamic model is included that solves the Reynolds-averaged Navier-Stokes equations with a standard k-1 turbulence model with wall functions using a multi-block structured mesh that governs the physical and hydrodynamic domains of a water control structure. Additionally, Lagrangian particle-tracking is used to interpolate information from the Eulerian mesh to point locations needed by the agent model to track the predicted path of each modeled fish in 3-D (Weber, Goodwin, Li, Nestler, & Anderson, 2006).

The resulting ELAM framework has been successfully employed for describing large-scale patterns in hydrodynamics as well as the smaller scale at which fish make movement decisions. This ability to simultaneously predict dynamics at multiple scales allows ELAM methods to more realistically represent fish movements, as compared to many other modeling options (Goodwin, Nestler, Anderson, Weber, & Loucks, 2005).

However, while the ELAM model has been shown to provide enough output data to be appropriate in determining a fish passage location, to determine the basic notch configuration an ELAM model should include 3-D hydrodynamics and higher order fish responses (Tompkins, et al., 2017). In a previous study which employed SRH-2D hydrodynamic model to generate hydrodynamic inputs to ELAM, the authors found that ELAM tends to under-predict entrainment due to the inability of the 2-D model to capture secondary currents. In this study the model was able to characterize the general movement of juvenile salmonids through complex flow fields through resolving combined effects of flow field changes and the corresponding behavior change, but not able to optimize flow field design to elicit a particular response in fish populations. The authors note that if the calibration issues of the hydrodynamic and behavioral components are resolved that ELAM will likely be a more effective tool for passage design (Tompkins, et al., 2017).

A7. Conclusions

While many questions regarding the habits of downstream juvenile migration remain unanswered, and many of the answers that have been postulated are generalities, hypothesis, and theories, there is still a significant body of work which has helped to develop designs based on models which continue to function successfully. Hopefully, as the science continues to develop, less monitoring will be necessary to confidently develop a suitable design. However, for most models in their current form, significant amounts of monitoring is still often required to develop a suitable design for a downstream fish passage.

A8. References

Adams, N., & Evans, S. (2011). *Summary of Juvenile Salmonid Passage and Survival at McNary Dam - Acoustic survival studies, 2006-09.* US Geological Survey, Open-File Report 2011-1179, 144p.

Adams, S., & Hatton, T. (2012). *A Markov Chain Analysis of the Movement of Juvenile Salmonids, Including Sockeye Salmon, in the Forebay of McNary Dam, Washington and Oregon, 2006-09.* US Geological Survey, US Army Corps of Engineers, Open File Report 2012-1120.

Amado, A. (2012). *Development and Application of a Mechanistic Model to Predict Juvenile Salmon Swim Paths.* PhD thesis, University of Iowa.

Beeman, J., Stutzer, G., Juhnke, S., & Hetrick, N. (2006). *Survival and Migration Behavior of Juvenile Coho Salmon in the Klamath River Relative to Disharge at Iron Gate Dam.* US Geological Survey, Western Fisheries Research Center, US Fish and Wildlife Service, Arcata Fish and Wildlife Center.

Bevelhimer, M., & Adams, S. (1993). *A bioenergetics analysis of diel vertical migration by kokanee salmon.* Canadian Journal of Fishery Aquatic Science 50:2336-2349.

Biette, R., & Green, G. (1980). *Growth of underyearling sockeye salmon under constant and cyclic temperatures in relation to live zooplankton ration size.* Canadian Journal of Fisheries Aquatic Science 37:1759-1771.

Bjornn, T., & Reiser, D. (1991). *Habitat requirements of salmonids in streams.* Influences of forest and rangeland management on salmonid fishes and their habitats, American Fisheries Society Special Publication 19.

Brett, J. (1971). *Energetic response of salmon to temperature: A study of some thermal relations in the physiology and freshwater ecology of sockeye salmon.* American Zoology.

Clark, C., & Levy, D. (1988). *Diel vertical migrations by juvenile sockeye salmon and the antipredation window.* American Naturalist 131:271-290.

Faber, D., Weiland, M., Moursund, R., & Carlson, T. (2001). *Evaluation of the Fish Passage Effectiveness of the Bonneville I Prototype Surface Collector using Three-Dimensional Ultrasonic Fish Tracking.* US Army Corps of Enigineers, Pacific Northwest Laboratory.

Friesen, T., Vile, J., & Pribyl, A. (2007). *Outmigration of juvenile Chinook salmon in the lower Willamette River, Oregon.* Northwest Scientist 81:173-190.

Furey, N. (2016). *Migration Ecology of Juvenile Pacific Salmon Smolts: The Role of Fish Condition and Behavior Across Landscapes.* The University of British Columbia - Thesis for PhD .

Godin, J. (1982). *Migrations of salmonid fishes during early life history phases: Daily and annual timing.* Proceedings of the salmon and trou migratory behavior symposium. School of Fisheries, University of Washington, Seattle.

Goodwin, R., Nestler, J., Anderson, J., Weber, L., & Loucks, D. (2005). *Forecasting 3-D Fish Movement Behavior Using a Eulerian-Lagrangian-Agent Method (ELAM).* Ecological Modelling 192:197-223.

Goodwin, R., Toney, T., Nestler, J., Anderson, J., & Kim, J. (2005). *Evaluation of Wanapum Dam Bypass Configurations for Outmigrating Juvenile Salmon Using Virtual Fish:*

Numerical Fish Surrogate (NFS) Analysis. ERDC/EL TR-05-7, US Army Engineer Research and Development Center.

Healy, B., & Lonzarich, D. (2000). *Microhabitat use and behavior of overwintering juvenile coho salmon in a Lake Superior tributary.* Transactions of the Americans Fisheries Society.

Holtby, L. (1988). *Effects of logging on stream temperatures in Carnation Creek, British Columbia, and associated impacts on the coho salmon.* Canadian Journal of Fishery Aquatic Science 45:502-515.

Huusko, R. (2018). *Downstream Migration of Salmon Smolts in Regulated Rivers: Factors Affecting Survival and Behaviour.* University of Oulu, Thesis for PhD A-709.

Johnson, G., Hedgepeth, J., Skalski, J., & Giorgi, A. (2004). *A Markov Chain Analysis of Fish Monvements to Determine Entrainment Zones.* Fisheries Research 69:349-358.

Johnson, G., Khan, F., Hedgepath, J., Mueller, R., Rakowski, C., Richmond, M., . . . Skalski, J. (2006). *Hydroacoustic Evaluation of Juvenile Salmonid Passage at the Dalles Dam Sluiceway.* US Army Corps of Engineers, PNNL-15540.

Johnson, G., Richmond, M., Hedgepeth, J., Ploskey, G., Anderson, M., Deng, Z., . . . Steinbeck, J. (2009). *Smolt Responses to Hydrodynamic Conditions in Forebay Flow Nets of Surface Flow Outlets, 2007.* US Army Corps of Engineers, PNNL-17387.

Johnson, R., & Moutsund, R. (2000). *Evaluation of Juvenile Salmon Behavior at Bonneville Dam, Columbia River, using a multibeam technique.* Aquatic Living Resources 13:313-318.

Larinier, M., & Travade, F. (2002). *Downstream Migration: Problems and Facilities.* Bulletin Francias de la Penche et de la Pisciculture 364 Suppl:181-207 Ch.13.

Lonzarich, D., & Quinn, T. (1995). *Experimental evidence for the effect of depth and structure on the distribution, growth, and survival of stream fishes.* Canadian Journal of Zoology.

McMahon, T. (2011). *Behavior, Habitat Use, and Movements of Coho Salmon (Oncorhynchus kisuth) Smolte during Seaward Migration.* Montana State University.

Miller, J., Gray, A., & Merz, J. (2010). *Quantifying the contribution of juvenile migratory phenotypes in a population of Chinook Salmon Oncorhynchus tshawytcha.* Marine Ecology Progress Series 408: 227-240.

Morita, K., & Nagasawa, T. (2010). *Latitudinal variation in the growth and maturation of masu salmon.* Canadian Journal of FIshery Aquatic Science 67:955-965.

Morita, K., Tamate, M., Kuroki, M., & Nagasawa. (2014). *Temperature dependent variation in alternative migratory tactics and its implications for fitness and population dynamics in a salmonid fish.* Journal of Animal Ecology 83:1268-1278.

NMFS, (. M. (2011). *Anadromous Salmonid Passage Facility Design.* NOAA, NMFS, Northwest Region.

Pavlov, D., Kirillova, E., & Kirillov, P. (2008). *Patterns and Some Mechanisms of Downstream Migration of Juvenile Salmonids (with Reference to the Utkholok and Kalkaveyem Rivers in Northwestern Kamchatka).* Severtsov Institute of Ecology and Evolution, Journal of Ichthyology 11:937-980.

Pitcher, T. (1993). *Behavior of teleoset fishes.* Chapman & Hall.

Popper, A., & Carlson, T. (1998). *Application of sound and other stimuli to control fish behavior.* Transactions of the American Fisheries Society 127:673-707.

Quinn, T. (2018). *The Behavior and Ecology of Pacific Salmon and Trout.* 2nd ed. University of Washington Press.

Quinn, T., Sergeant, C., Beaudreau, A., & Beauchamp, D. (2012). *Spatial and temporal patterns of vertical distribution for three planktivorous fishes in Lake Washington.* Eology of Freshwater Fish 21:337-348.

Silva, A., Katopodis, C., Santos, J., Ferreira, M., & Pinheiro, A. (2012). *Cyprinid Swimming Behaviour in Response to Turbulent Flow.* Ecological Engineering 44:314-328.

Steinhart, G., & Wurtsbaugh, W. (1999). *Under-ice vertical migrations of Oncorhynchus nerka and their zooplankton prey.* Canadian Journal of Fishery Aquatic Science 56 (Suppl. 1): 152-161.

Taylor, S. (2008). *Climate warming causes phenological shift in pink salmon bahavior at Auke Creek.* Transactions of the American Fisheries Society.

Tompkins, M., Anderson, J., Goodwin, P., Ruggerone, G., Speir, C., & Viers, J. (2017). *Yolo Bypass Salmon Habitat Restoration and Fish Passage Analytical Tool Review.* Delta Science Program.

Turchin, P. (1998). *Quantitative analysis of movement.* Sinauer Associates.

Weber, L., Goodwin, R., Li, S., Nestler, J., & Anderson, J. (2006). *Application of an Eulerian-Lagrangian-Agent method (ELAM) to rank alternative designs of a juvenile fish passage facility.* Journal of Hydroinformatics.

Weiland, M., & Carlson, T. (2001). *Evaluation of the Fish Passage Effectiveness of the Bonneville I Prototype Surface Collector using Three-Dimensional Ultrasonic Fish Tracking.* US Army Corps of Enigineers, Pacific Northwest Laboratory.

Zabel, R. (1994). *Spatial and Temporal Models of Migrating Juvenile Salmon with Applications.* University of Washington.

Zabel, R., Falukner, J., Smith, S., Anderson, J., Holmes, C., Beer, N., . . . Giogi, A. (2008). *Comprehensive passage (COMPASS) model: a model of downstream migration and survival of juvenile salmonids through a hydropower system.* Hydrobiologia 609:289-300.